UNIVERSITY OF CALIFORNIA, SAN DIEGO

Signaling by PHLPP1 and PKC alpha: function and specificity

A dissertation submitted in partial satisfaction of the
requirements for the degree Doctor of Philosophy

in

Biomedical Sciences

by

Audrey Kathleen O'Neill

Committee in Charge:

Professor Alexandra C. Newton, Chair
Professor Joan Heller Brown
Professor Kun-Liang Guan
Professor Jerrold Olefsky
Professor Jing Yang

2012

The dissertation of Audrey Kathleen O'Neill is approved, and it is acceptable in quality and form for publication on microfilm and electronically:

_____

_____

_____

_____

_____

Chair

University of California, San Diego

2012

DEDICATION

Dedicated to my grandparents,

Thomas & Kathryn O'Neill

and

Jack and Nancy Reardan,

for their love and support.

TABLE OF CONTENTS

LIST OF FIGURES

LIST OF TABLES

ACKNOWLEDGMENTS

First, I would like to thank my mentor, Alexandra Newton, who has helped bring this dissertation to completion by supporting and guiding my research and by teaching me how to design, perform, and, most importantly, learn from experiments (even those producing negative results). She has been a wonderful leader and inspiration for me, and her relentless positivity and persistence have set an example that I will do my best to follow.

I would also like to acknowledge the critical contributions of past and present members of the Newton lab (Hilde Abrahamsen, Corina Antal, Laura Braughton, John Brognard, Lisa Gallegos, Christine Gould, Tianyan Gao, C.C. King, Maya Kunkel, Matt Niederst, Gloria (Ximena) Reyes, Cicely Schramm, Emma Sierecki, Shoana Sikorski, Irene Tobias, Noel Warfel, and Alyssa Wu-Zhang), who provided invaluable technical assistance and helpful discussions of data. I would particularly like to thank Lisa Gallegos, with whom I collaborated on the PKCα/DLG1 project and who was consistently reliable, helpful, and positive; Gloria Reyes, Tianyan Gao, and Shoana Sikorski, who gave me a great deal of assistance with the PHLPP1-null mouse project; and C.C. King and Maya Kunkel, who are inexhaustible sources of wisdom and kindness.

Many members of the scientific community in San Diego contributed their time and expertise to helping me learn new techniques and/or gain access to materials I needed for this work. I would like to thank members of the Brown lab, especially Nicole Purcell and Sunny Xiang, as well as Vincenzo Cirulli, Malik Keshwani, Manuela Quintavalle, and Sara Courtneidge, for their assistance. I would also like to acknowledge Jeffrey Morimune for his help in the lab. Finally and most importantly, I would like to note the contributions of my thesis committee, Drs. Joan Heller Brown, Kun-Liang Guan, Jerry Olefsky, and Jing Yang, for their excellent critiques of and suggestions for my research.

I would also like to thank my collaborators, who include Satoru Masubuchi and Paolo Sassone-Corsi at UC Irvine; Muhan Chen and Lloyd Trotman at Cold Spring Harbor; Erin Garcia and Randy Hall at Emory University; and Verline Justilien and Alan Fields at the Mayo Clinic, as

well as Lisa Gallegos and Matt Niederst. In particular, I would like to acknowledge the continuing contributions and critiques from Randy Hall, Verline Justilien, and Alan Fields, who were instrumental in bringing the PKCα/DLG1 project to completion.

My friends both in and outside of the Biomedical Sciences Graduate Program have helped me every step of the way through graduate school, both scientifically and personally. I would particularly like to thank Ohn Chow, Chris and Nichole Gregg, Mason Israel, Paris Mowlavi, and Ali Torkamani, as well as Sheila Rosenberg and my best friends Courtney Summers and Stephanie Lopez – I couldn't have done it without you. Two people who deserve to be singled out for thanks are Molly Bush and Eric Zamore, my wonderful roommate and boyfriend, respectively; their persistence, acuity, and kindness not only helped me survive graduate school but set an example I hope to one day live up to.

Finally, I would like to thank my family, particularly my grandparents, to whom this thesis is dedicated, and my mother Susan, father Tom, and sister Claire, for their continuous patience, support, and love throughout this process.

The text of Chapter 1 is, in part, a review article submitted to FEBS Journal by O'Neill AK, Niederst MJ, and Newton AC. I was the author of this literature review.

A version of Figure 2.2 was originally included in Masubuchi, S., Gao, T., O'Neill, A., Eckel-Mahan, K., Newton, A. C., and Sassone-Corsi, P. (2010) Proc Natl Acad Sci U S A 107, 1642-1647, as Figure 1. I was a secondary author who contributed to Figure 1 of this paper.

The text of Chapter 3 is, in part, a reprint of the material as it appears in the Journal of Biological Chemistry, 2011, by O'Neill AK, Gallegos LL, Justilien V, Garcia EL, Leitges M, Fields AP, Hall RA, and Newton AC. I was the co-primary author and researcher.

VITA

2004 Bachelor of Science, Brown University

2012 Doctor of Philosophy, University of California, San Diego

ABSTRACT OF THE DISSERTATION

Signaling by PHLPP1 and PKC alpha: function and specificity

by

Audrey Kathleen O'Neill

Doctor of Philosophy in Biomedical Sciences

University of California, San Diego, 2012

Professor Alexandra C. Newton, Chair

Signaling networks involve multiple layers of regulation. Determination of the essential components of such networks and the ways in which specificity of signaling is ensured is necessary for a full understanding of normal physiology and disease. The studies presented herein focus on signaling by protein kinase C and its negative regulator PHLPP, which are

important for cell motility and growth. Though PHLPP1 has previously been shown to directly dephosphorylate numerous kinases that are important for maintaining the balance between proliferation and apoptosis, PHLPP1-null mice did not display substantial changes in the phosphorylation of these factors. Furthermore, these mice developed normally and lacked the expected changes in growth and insulin signaling; this lack of phenotype may be due to compensation by the closely related phosphatase PHLPP2 or other negative regulators of growth. We also showed that PKCα's effects on cellular migration in a wound healing assay were dependent on a novel, PDZ ligand-based interaction with the scaffold DLG1. We determined that PKCα phosphorylates a previously unrecognized site on DLG1 and that PKCα activity at the scaffold correlates with invasive behavior in lung cancer cells. These data suggest that PKCα may promote metastasis in a DLG1-dependent manner and highlight the importance of scaffolding interactions for the proper regulation of signaling.

Chapter 1:

Regulation of signaling by PHLPP and PKC

Cell signaling relies heavily on post-translational modifications, which alter protein function in order to relay signals within the cell. Phosphorylation is a key modification in signaling and much of the work in the field has been devoted to studying the molecules, protein kinases, that supply these key modifications. However, spatiotemporal specificity of signaling requires much more than a global "ON" signal provided by kinases. Equally important is termination of signaling by cellular phosphatases, and there is accumulating evidence that these enzymes are finely regulated and can act to modify specific sites rather than acting as a general brake to cellular phosphorylation. In addition, scaffolding proteins play key roles in the spatiotemporal regulation of kinases and phosphatases, targeting these enzymes to specific cellular locales in response to specific stimuli to ensure that they modify the right substrates at the right time.

Work in our laboratory focuses on mechanisms of signaling by the protein kinase C (PKC) family of isozymes and by the phosphatase PHLPP, which dephosphorylates and downregulates PKC as well as the related kinase Akt (Figure 1.1). Both the "ON" switch (PKC) and the "OFF" switch (PHLPP) in this pathway are tightly regulated, as I will highlight below. In particular, I will discuss the ways in which both of these signaling enzymes are regulated by interactions with protein scaffolds such as receptor for activated C kinase (RACK1) for PKC and Na^+/H^+ exchanger regulatory factor (NHERF) 1 for PHLPP.

The PHLPP phosphatases: function and regulation

The recently discovered PH (pleckstrin homology) domain Leucine rich repeat Protein Phosphatase (PHLPP) family is emerging as a central component in suppressing cell survival pathways. Originally discovered in a rational search for a phosphatase that directly dephosphorylates and inactivates Akt, PHLPP is now known to potently suppress cell survival both by inhibiting oncogenic pathways and by promoting apoptotic pathways. In the first instance, PHLPP directly dephosphorylates a conserved regulatory site (termed the hydrophobic motif) on

Akt, protein kinase C (PKC), and S6 kinase, thereby terminating signaling by these pro-survival kinases. In the second instance, PHLPP dephosphorylates and thus activates the pro-apoptotic kinase Mst1, thereby promoting apoptosis. PHLPP is deleted in a large number of cancers and the genetic deletion of one isozyme in mouse models results in tumors of the prostate, underscoring PHLPP's role as a tumor suppressor. This review summarizes the targets and cellular actions of PHLPP, with emphasis on its role as a tumor suppressor in the oncogenic PI3K (phosphoinositide 3-kinase)/Akt signalling cascade.

Introduction

The PHLPP family of serine/threonine phosphatases contains three isozymes (Figure 1): the alternatively-spliced PHLPP1β (also known as suprachiasmatic nucleus oscillatory protein, SCOP (1)) and PHLPP1α (2), and PHLPP2 (3). PHLPP1α and PHLPP1β differ only in the first exon (see (4) for diagram), resulting in an approximately 50 kDa N-terminal extension to PHLPP1β.

PHLPP1 and PHLPP2 share a common architecture (Figure 1.2), including a phosphatase domain, which is 58% conserved between PHLPP1 and PHLPP2 (5). Sequence analysis reveals that the phosphatase domain belongs to the PP2C branch of the PPM family, whose members rely on Mg^{2+} or Mn^{2+} for activity and are insensitive to common phosphatase inhibitors such as okadaic acid (2,6).

Conserved regulatory domains in PHLPP include a pleckstrin homology (PH) domain, a leucine rich repeat segment (LRR), and a C-terminal PDZ (post synaptic density protein (PSD95), Drosophila disc large tumor suppressor (DLG), and zonula occludens-1 protein (zo-1)) ligand. (7). PHLPP1β and PHLPP2 also contain a putative Ras association (RA) domain near their N-termini, although the function of these RA domains is as yet unverified. The PH domain has a relatively low affinity for phosphoinositides (8), because it contains only the middle arginine of the R-X-R-S-F motif required for phosphoinositide binding (5). The full-length protein has been reported not to bind phosphatidylinotisol 3,4-bisphosphate or phosphatidylinotisol 3,4,5-trisphosphate (PIP_3) *in*

vitro (9); however, whether phosphoinositide binding occurs in cells remains to be established. The PH domain is, however, important for protein interactions and is essential for the regulation of one PHLPP substrate, PKC (10). The series of leucine-rich repeats have been reported to regulate signalling through the extracellular signal-regulated kinase (ERK) pathway (7). Finally, a PDZ ligand is present at the C-terminus of PHLPP1 (DTPL) and PHLPP2 (DTAL); the PDZ scaffold NHERF has recently been reported to bind both sequences (11). PHLPP is conserved in eukaryotes. Interestingly, the yeast homologue CYR1 contains an adenylate cyclase domain near the C-terminus but no PDZ ligand (6).

The PHLPP family was identified in a rational, systematic search for genes predicted to encode a phosphatase domain linked to a PH domain (2), criteria hypothesized to be important for a phosphatase that would dephosphorylate the lipid second messenger kinases Akt (itself controlled by a PH domain) and protein kinase C (also controlled by membrane-targeting modules). The mRNA of PHLPP1β had previously been identified in a screen for transcripts whose levels oscillate in a circadian fashion in the rat suprachiasmatic nucleus and had thus been termed SCOP (1). Biochemical and cellular studies validated PHLPP1 and PHLPP2 as functional phosphatases that dephosphorylate and inactivate Akt at its hydrophobic motif site, serine 473 (2,3). Since their identification, the PHLPP isozymes have been shown to be widely expressed in human and mouse tissues, with particularly high expression in brain (1,5,12); both PHLPP proteins appear be localized at the membrane and in the cytosol and nucleus of multiple cell types (5).

Molecular, cellular, and physiological functions of PHLPP

Targets of PHLPP

PHLPP was originally identified as the phosphatase for a conserved C-terminal phosphorylation site first identified on PKC (13,14) and S6 kinase (15) that is conserved in many members of the AGC family, including Akt (16). This segment is flanked by hydrophobic residues and is thus referred to as the hydrophobic motif (16).

Akt – The PHLPP isozymes bind to the oncogenic serine/threonine kinase Akt and dephosphorylate it under serum-starved, agonist-stimulated, and normal conditions (2,3). Upon recruitment to the plasma membrane, Akt is activated by sequential phosphorylations on its activation loop (at threonine 308 in Akt1) and hydrophobic motif (serine 473). Akt phosphorylated at T308 alone is only about 10% as active as the fully phosphorylated form but retains activity towards a group of substrates (17). Phosphorylation of S473 stabilizes the active conformation of the kinase, allowing for full activation and phosphorylation of all its known substrates (18-20). Thus, dephosphorylation of S473 by PHLPP is critical for regulation of Akt activity. PHLPP1 and PHLPP2 display a preference for S473 over T308 *in vivo* (2,3). Accordingly, PHLPP expression decreases Akt activity *in vitro* and the phosphorylation of numerous Akt substrates in cells, while depletion of either or both PHLPP isozymes results in increased Akt substrate phosphorylation (2,3,21-24). Further supporting the high degree of substrate specificity, knockdown of PHLPP1 versus PHLPP2 affects different subsets of Akt substrates: PHLPP1 knockdown results in increased phosphorylation of GSK (glycogen synthase kinase) 3α and β, HDM2 (human homolog to murine double minute 2), and TSC2 (tuberous sclerosis complex 2)/tuberin, whereas PHLPP2 knockdown increases the phosphorylation of GSK3β, FoxO (Forkhead Box O) 1, p27, and TSC2. This selectivity arises because PHLPP1 binds to and dephosphorylates Akt2 and Akt3 but not Akt1, while PHLPP2 binds and regulates Akt1 and Akt3 but not Akt2 (3,25). The mechanisms behind this specificity are unknown but could involve differential scaffolding of the isozymes: the PDZ ligand of PHLPP1 is necessary for its regulation of Akt (2), and the PDZ ligands of the two isozymes differ slightly. For instance, the PDZ ligand of PHLPP2 appears to bind many more recombinant PDZ domains on a PDZ domain array than that of PHLPP1 (M.T. Kunkel, E.L. Garcia, R.A. Hall, and A.C. Newton, unpublished data).

Protein kinase C – Both PHLPP1 and PHLPP2 dephosphorylate the hydrophobic motif of PKC (serine 657 in PKCα) *in vitro* and in cells (10). Dephosphorylation of this site in PKC does not acutely impair its activity; rather, it shunts the protein to the detergent-insoluble pellet, where it

is rapidly degraded (26). Thus, knockdown of PHLPP results in increased steady-state levels of PKC. Indeed, PKC levels correlate inversely with PHLPP levels in both cancer and normal cell lines (10). PHLPP1 binds PKC via the C1 domain of the kinase and the PP2C and PH domains of the phosphatase; notably, the PH domain of PHLPP is required for PHLPP to dephosphorylate PKC in cells, suggesting that this module may play a scaffolding role (10).

S6 kinase – PHLPP has recently been shown to directly dephosphorylate the hydrophobic motif of Akt's close relative S6K1 *in vitro;* Liu and colleagues elegantly demonstrated that PHLPP knockdown or deletion results in increased phosphorylation of S6K1 and its downstream substrate S6 even when Akt is not activated, or when S6K1 phosphorylation is uncoupled from Akt upon treatment with rapamycin (27). Interestingly, PHLPP repression of S6K1 leads to increased insulin-stimulated signaling via loss of feedback inhibition of insulin receptor substrate 1 (IRS-1; see Figure 2), with the apparently paradoxical result that PHLPP knockdown leads to *decreased* Akt phosphorylation at both the hydrophobic motif and activation loop in the colon cancer cells used in this study.

The ERK signaling pathway – There is some evidence that PHLPP plays a role in regulating the activation of ERK, although its direct target in this context is unknown. Overexpression of PHLPP1 represses phosphorylation of ERK induced by multiple agonists, including phorbol esters, cytokines, CpG oligonucleotides, and CD40 (7,24), and siRNA-mediated depletion of PHLPP1 increases the levels of phospho-ERK in neural and B-cell models (12,24,28). Interestingly, the LRR region of the yeast PHLPP ortholog CYR1 binds Ras, allowing Ras-dependent activation of the associated adenylate cyclase (29). This observation led Shimizu et al. (7) to propose that the LRR of PHLPP1β 1) competes with nucleotides for binding to Ras and 2) is necessary for PHLPP1β to repress phorbol ester-stimulated ERK phosphorylation. However, it is unclear if the regulation of ERK by PHLPP in this context results from dampening of PKC activation or from direct effects on Ras, and further investigation into possible mechanisms is warranted. Unpublished data from our lab suggests that depletion of PHLPP1 and/or PHLPP2

results in increased levels of growth factor receptors, resulting in the observed increases in ERK phosphorylation (M. Niederst, G. Reyes-Cava, M.T. Kunkel, J. Brognard, J. Enserink, and A.C. Newton, manuscript in preparation).

Mst1 – PHLPP has recently been shown to catalyze an activating dephosphorylation of the pro-apoptotic kinase Mst1, thus providing another mechanism to suppress cell survival. Specifically, Pardee and coworkers reported that in certain gastrointestinal cancer cells, overexpression of PHLPP significantly increased apoptosis in the absence of significant decreases in the phosphorylation of its known targets, Akt, ERK, or PKC, leading to a search for cell type-specific downstream partners of PHLPP. A mass spectrometry-based screen for PHLPP1-interacting proteins identified Mst1, which was then shown to be a direct substrate for PHLPP1 and PHLPP2. In certain pancreatic cancer cells, PHLPP dephosphorylates an inhibitory residue (threonine 387) on Mst1, resulting in activation of the kinase and increased downstream signalling through p38 and c-Jun N-terminal kinase (JNK), ultimately leading to apoptosis and growth arrest (30). Interestingly, another study showed that PHLPP1 and 2 do act to dephosphorylate Akt2 and 1, respectively, in a different pancreatic cancer cell line (25), indicating that even within a given cancer type, PHLPP can modulate different targets depending on the specific cell line. These data highlight the cell type-dependent actions of PHLPP and reveal the multiple ways in which PHLPP acts to oppose survival signaling.

Cellular and physiological functions of PHLPP

By both 1] terminating signaling by two survival kinases, Akt and PKC, and 2] activating signaling by a pro-apoptotic kinase, Mst1, PHLPP strongly opposes cell growth and survival; this has been shown in numerous cellular and xenograft models (2,3,22,24,25,30). In addition, PHLPP1 and PHLPP2 decrease protein synthesis and cell size by a mechanism dependent on downregulation of S6K (27). PHLPP1 and PHLPP2 also appear to repress cellular migration, and both isozymes are less highly expressed in metastatic breast cancer lines compared to primary

breast cancer or normal breast lines (30,31), suggesting that PHLPP may play a role in cancer cell motility.

In normal physiology, PHLPP1 depletion or deletion is cardioprotective: by increasing Akt activation, PHLPP1 knockdown blocks doxorubicin-induced apoptosis in neonatal rat ventricular myocytes, and ischemic injury is reduced in PHLPP1 knockout mouse hearts (23). Similarly, PHLPP1 depletion may be neuroprotective, as it has been shown to increase Akt signalling in hippocampal and striatal neurons (12,32). The effects of PHLPP1 on Akt are also important for regulatory T cells (Tregs), which require suppression of Akt signaling for their development and function and which have elevated expression of PHLPP1 and PHLPP2 compared to conventional T cells. Deletion of PHLPP1 inhibits the development of conventional T cells into Tregs positive for the marker protein Foxp3, and Tregs from PHLPP1 knockout mice are less able to suppress the proliferation of conventional T cells (33).

Given the high level of PHLPP expression in the brain, it is not surprising that PHLPP has been postulated to play roles in several neural functions, namely long-term memory and the regulation of circadian rhythms. Inducible overexpression of PHLPP1β in the murine forebrain blocks the formation of long-term novel object memory (28), while deletion of PHLPP1 interferes with light-induced resetting of the circadian clock (34). Interestingly, injection of a PKC inhibitor into the suprachiasmatic nucleus has been shown to affect the circadian response to a light pulse (35), raising the possibility that the regulation of PKC by PHLPP is essential for the proper function of the circadian clock.

PHLPP in cancer – Several lines of data support a role for PHLPP as a tumor suppressor *in vivo*. First, as previously mentioned, PHLPP overexpression in glioblastoma (GBM), breast, colon, and pancreatic cancer cell lines decreases colony formation and growth *in vitro* and in xenograft models (2,22,25,30,36). Second, PHLPP expression is lost or decreased in a variety of human cancers (as detailed in the regulation section below). Furthermore, the PHLPP1 knockout mouse displays an increased incidence of prostate intraepithelial neoplasia, which eventually

progresses to frank carcinoma when combined with partial loss of PTEN (phosphatase and tensin homolog located on chromosome 10) (37). Interestingly, it appears that PHLPP1 loss cooperates with PTEN loss and p53 mutation to promote prostate carcinogenesis. PHLPP1-/-, PTEN+/- mouse prostate cells initially undergo senescence; however, upon spontaneous inactivation of p53, this genetic combination results in increased proliferation in the prostate, carcinoma formation, and increased mortality. Moreover, PHLPP1-/-, PTEN+/-, p53-mutant mouse embryonic fibroblasts are dependent upon Akt activity for their increased abilities to proliferate, survive, and form colonies in soft agar, suggesting that in this context, at least, PHLPP blocks carcinogenesis through its actions on Akt. The idea that PHLPP1 and PTEN downregulation cooperate to increase carcinogenesis is supported by studies in humans: Kaplan-Meier analysis of relapse after radical prostatectomy revealed that a "PTEN/PHLPP1 low" status predicts relapse better than Gleason scoring (37). Finally, though few variations in the PHLPP protein sequences have been described, a single nucleotide polymorphism in PHLPP2 (L1016S, located in the phosphatase domain) has been shown to result in reduced inhibition of basal Akt phosphorylation. This polymorphism has relevance for human cancer, as grade III but not grade II breast tumours often display loss of heterozygosity at this locus, resulting in preferential loss of expression of only the more active leucine allele (38).

Regulation of PHLPP

Downregulation of PHLPP in cancer – The genetic locus for PHLPP1, which lies at 18q21.33, undergoes loss of heterozygosity in a high percentage of colon cancers (39,40); similarly, the PHLPP2 locus at 16q22.3-16q23.1, which contains a fragile site, is susceptible to loss of heterozygosity in breast and ovarian cancers, Wilms' tumours, and prostate and hepatocellular carcinomas (41-45).

Consistent with a role for PHLPP in the progression of prostate cancer, several studies have shown that PHLPP levels are decreased in this disease. Chen et al. (37) discovered that PHLPP1 and PHLPP2 protein expression is lost in 30% and 45%, respectively, of human prostate

cancer samples, while Hellwinkel et al. (46) found that PHLPP1 mRNA levels were frequently downregulated in high-grade but not low-grade prostate cancer samples, supporting the idea that PHLPP1 loss participates with other genetic abnormalities to promote prostate cancer progression. In fact, loss of both PHLPP1 and PHLPP2 is associated with PTEN and p53 loss in metastatic but not primary prostate cancer, which suggests that p53 loss is a late event that cooperates with PHLPP loss in this disease (37). The critical role of PHLPP in suppressing this disease may be explained by the strong dependence of prostate cancer on PI3K/Akt signaling; a survey of 218 prostate tumors found that the PI3K pathway is altered in almost half of the primary tumors and all metastatic samples. (Notably, this same study found downregulation of PHLPP1 or PHLPP2 in 11% of primary tumors and 37% of metastases (47).)

In addition to prostate cancer, PHLPP levels are decreased in a number of other malignancies (summarized in Table 1), particularly chronic lymphocytic leukemia (CLL), GBM, and colon cancer. However, the factors that regulate PHLPP expression in normal and cancer cells are incompletely characterized and deserve further attention.

Regulation of PHLPP expression – Transcriptional regulation of the PHLPP1 and PHLPP2 genes is still very much a black box, although there are several hints at possible regulators. SMAD3, a downstream effector of transforming growth factor-β, binds the PHLPP1 promoter, and this binding has been shown to correlate with increased PHLPP1 expression during the development of regulatory T cells (33). Interestingly, the SMAD3 binding partner SMAD4 acts as a tumor suppressor in PTEN-null prostate cancer and is often co-deleted with PHLPP1, with which it shares a genetic locus (37,48). Expression of Huntington's disease-associated alleles of *huntingtin* decreases the mRNA levels of PHLPP1, perhaps via nuclear transcription factor Y (NF-Y), which has putative binding sites located in the PHLPP1 promoter (32). PHLPP1 mRNA expression is also repressed by the microRNA miR-190, which is upregulated by exposure to the carcinogen arsenic and which is overexpressed in many cancers, including CLL (49). There may also be a connection between Akt signaling and PHLPP1 mRNA

expression, though the mechanism is unclear; one study found a slight elevation in PHLPP1 but not PHLPP2 mRNA in primary myotubes from type 2 diabetics, which displayed decreased Akt activation in response to insulin. Conversely, Warfel et al. (50) examined microarray data from the NCI-60 panel of cancer cell lines and found decreased levels of PHLPP1 mRNA in GBM lines compared to astrocytoma lines, correlating with increased Akt activation in GBM. However, effects on PHLPP1 protein synthesis and degradation downstream of Akt often complicate the interpretation of Akt-dependent changes in PHLPP protein levels, which may involve transcriptional, translational, and/or protein degradation-dependent mechanisms.

The post-translational regulation of PHLPP is better understood than its transcriptional regulation. To date, two mechanisms controlling the steady-state levels of PHLPP protein have been described. Both act downstream of Akt, implying the existence of at least two negative feedback loops involving PHLPP and Akt (see Figure 1.3). First, the rate of PHLPP translation is controlled by mTOR (mammalian target of rapamycin): treating cells with the mTOR inhibitor rapamycin or genetically interfering with the mTORC1 complex decreases PHLPP1 and PHLPP2 protein levels without affecting protein degradation or mRNA expression, suggesting that mTOR activation downstream of Akt results in increased translation of PHLPP1 and PHLPP2 (36). Consistent with this, PHLPP1 depletion in 3T3 fibroblasts and the subsequent increase in Akt signaling increase PHLPP2 protein but not mRNA levels in an mTOR-dependent fashion (37). Second, the rate of degradation of PHLPP is controlled by Akt activity, whose inhibitory phosphorylation of GSK3β results in stabilization of PHLPP1 protein (51). Specifically, casein kinase- and GSK3β-mediated phosphorylation of PHLPP1 at threonine 851 and serine 847, respectively, contributes to recognition of PHLPP1 by the E3 ligase β-TrCP (β-transducin repeats-containing protein) and subsequent ubiquitin-mediated degradation. Notably, this latter feedback loop is frequently lost in GBM (both in GBM cell lines and primary GBM neurospheres from human tumours); in these samples, β-TrCP is sequestered in the nucleus, away from its substrate PHLPP1, and the rate of PHLPP1 degradation becomes insensitive to Akt activation (50). Either

or both of these Akt-dependent mechanisms may explain the increase in PHLPP1 protein levels seen under conditions of Akt activation, including insulin stimulation of hepatoma cells (21), treatment of rat ventricular myocytes with leukaemia inhibitory factor, and transgenic overexpression of insulin-like growth factor 1 in the mouse heart (23). It should be noted that β-TrCP-dependent degradation of PHLPP1 is not the only mechanism by which PHLPP1 is degraded: the calcium-dependent protease calpain has also been shown to degrade PHLPP1β *in vitro* and *in vivo*, and inhibition of calpain in the hippocampus blocks long-term novel object memory formation, which is opposed by PHLPP1β expression (see "cellular and physiological functions of PHLPP", above) (28). Also, the deubiquitinase UCH-L1 (ubiquitin carboxy terminal-hydrolase L1), which acts as a tumor promoter in CLL, decreases PHLPP1β protein but not mRNA expression in a manner that depends upon its deubiquitinase activity (52).

Regulation of PHLPP by Protein Scaffolds – The key role of protein-protein interactions in achieving spatial and temporal specificity of signaling by enzymes has come to the forefront of the signal transduction field in recent years (53). PHLPP is no exception: a number of protein scaffolds for PHLPP have been proposed to be essential for the regulation of PHLPP targets.

First, NHERF1, which binds PHLPP1, PHLPP2, and PTEN via its two PDZ domains, has been reported to localize PHLPP1 to the membrane in GBM cells, an interaction that allows the phosphatase to exert anti-proliferative effects (11). Interestingly, samples from patients with high-grade GBM often display concomitant reductions in PHLPP1, PTEN, and NHERF1 protein levels, and upon PTEN depletion in LN229 cells, PHLPP1 becomes better able to reduce Akt activation, potentially because of increased scaffold availability. These data again highlight the cooperation between PHLPP1 loss and PTEN loss and suggest that in the absence of PTEN, PHLPP1 provides an additional layer of negative regulation of the PI3K pathway (11). The scaffold Scribble has been proposed to play a similar role in colon cancer cells, where it coordinates PHLPP1 (via Scribble's LRR region) and Akt at the membrane, allowing PHLPP1 to dephosphorylate Akt (54). Finally, the putative tumour suppressor FKBP51 (FK506 binding protein 51) has been reported to

scaffold PHLPP to Akt in pancreatic cancer cells (55). FKBP51 is essential for PHLPP to dephosphorylate Akt and exert its apoptotic effects in these cells; accordingly, overexpression of FKBP51 results in decreases in S473 phosphorylation of Akt and cell survival that are dependent on the presence of PHLPP (56). Other studies suggest that this interaction may play a role in suppressing Akt signaling in lung and prostate cancers. In non-small cell lung cancer cells, repression of insulin-stimulated Akt phosphorylation downstream of the P2X7 purinergic receptor requires both PHLPP and the activity of FKBP51, which scaffolds Akt in these cells and may recruit PHLPP, PTEN, and calcineurin to oppose Akt phosphorylation (57). In models of prostate cancer, castration or androgen receptor inhibition decreases PHLPP1 protein levels in a manner that depends upon FKBP51 depletion, suggesting that FKBP51 not only scaffolds PHLPP but also plays a role in maintaining its stability (58,59). In human prostate cancer tissue samples, PHLPP1 protein levels are correlated with the levels of PTEN, FKBP51, and the androgen receptor, raising the possibility that the androgen and PI3K pathways may interact via inhibition of PHLPP (59).

PHLPP has also been shown to interact with several other signaling factors, though the effects of these interactions are mainly unknown. PHLPP2 binds to adenylate cyclase in rat cardiomyocytes, and this interaction appears to contribute to forskolin-stimulated downregulation of Akt (60). (Interestingly, this interaction recapitulates the proximity between a PP2C phosphatase domain and adenylate cyclase seen in yeast, where these two domains are part of the same protein, CYR1.) In addition, a recent proteomic screen of the human deubiquitinases revealed ubiquitin-specific peptidases (USPs) 12 and 46 as binding partners for both PHLPP1 and PHLPP2 (61). These and other interactions remain to be further characterized and may offer hints to mechanisms of PHLPP regulation or the discovery of new PHLPP targets.

Phosphatase activity of PHLPP – Little is yet known about how the intrinsic catalytic activity of PHLPP is controlled in cells. However, a recent screen for specific inhibitors of PHLPP revealed insights into the structure of the phosphatase domain. Homology modeling of the

structure of the PP2C domain of PHLPP2 onto the known structure of PP2Cα (6), combined with knowledge about the structure of several validated PHLPP2 inhibitors, allowed Sierecki et al. to construct a set of models for the active site, all of which included one, two, or three manganese ions, and to determine key residues for the catalytic activity, which include aspartate 806, glutamate 989, and aspartate 1024 (62). Virtual screening using the best of these theoretical catalytic domain structures allowed the identification of numerous new predicted inhibitors, a few of which were experimentally tested and shown to inhibit PHLPP activity *in vitro* and *in vivo*. As expected, these inhibitors increase phosphorylation of Akt and its downstream substrates and attenuate etoposide-induced apoptosis in cell culture (62).

Endogenous regulators of PHLPP activity *per se* remain to be identified. Both isozymes have an abundance of predicted phosphorylation sites, and phosphorylation is a likely mechanism that controls the catalytic activity of the enzyme. Indeed, it has been suggested that factors downstream of the insulin receptor may modulate PHLPP activity (63), and serum stimulation or overexpression of Akt1, 2, or 3 was reported to decrease the activity of tagged, exogenously expressed PHLPP (9). Further study of the regulation of PHLPP activity *in vivo* in the coming years is likely to unveil mechanisms that control the catalytic activity of PHLPP.

Phosphatases in the PI3K pathway

The PI3K/Akt signaling cascade (see Figure 1.3) is a well-studied, complex pathway that promotes cell growth and survival. Attesting to the importance of precise control of Akt signaling for cellular homeostasis, signaling through this pathway is often increased in primary and metastatic tumors (47,64), and its activation, combined with that of other factors such as Ras (65), is crucial for driving the majority of human cancers (66). In fact, several inhibitors of the pathway targeted at PI3K, Akt, and/or mTOR are currently in clinical trials as cancer therapeutics (64). Though much attention has been focused on the mutation of factors that positively affect this pathway (e.g., growth factor receptors and PI3K), negative regulation is equally important and often involves dephosphorylation, which opposes signaling through this pathway via several

mechanisms. These include downregulation of PI3K signalling via removal of its product PIP_3 by the lipid phosphatase PTEN (67) and dephosphorylation of Akt at its activation loop and hydrophobic motif by protein phosphatase 2A (PP2A) and PHLPP, respectively (2,3,68). The importance of proper phosphatase regulation of this pathway is highlighted by several recent studies showing that depletion of both PHLPP and PTEN is necessary for full activation of Akt in GBM (11) and predicts metastasis and relapse in prostate cancer (37).

This exquisitely tuned pathway is subject to several layers of negative feedback regulation (Figure 1.3). One well-characterized loop involves S6K-mediated inhibitory phosphorylation of IRS-1, which dampens activation of PI3K in the face of excess mTOR activation (69). Also, Yu et al. (70) recently showed that mTORC1 phosphorylates and stabilizes the adaptor protein Grb10, which negatively regulates signaling through growth factor receptors. Recent studies (described in more detail above) have demonstrated the existence of three more feedback loops, these ones involving PHLPP. First, mTOR activation positively regulates the translation of PHLPP1 and PHLPP2 via activation of S6K and inhibition of 4EBP1, thereby resulting in inactivation of Akt by PHLPP-mediated dephosphorylation (36). Second, increased Akt activation results in phosphorylation and inhibition of GSK3β, resulting in decreased phosphorylation of PHLPP1 at serine 847. Dephosphorylated PHLPP1 protein cannot be recognized by its E3 ligase β-TrCP and is therefore stabilized, leading to increased levels of PHLPP and decreased activation of Akt (50,51). Notably, this feedback loop is lost in GBM because of sequestration of β-TrCP in the nucleus, away from its substrate PHLPP1 (50). Finally, PHLPP also dephosphorylates the activation loop of S6K1, thus activating PI3K/Akt signalling through upregulation of IRS-1 (27).

PHLPP: conclusions

Repression of signaling by protein phosphatases, originally conceived as a promiscuous, general “OFF” signal, has increasingly been recognized as an important layer of specific and dynamic regulation in mammalian cells. The PHLPP phosphatases, which dephosphorylate the

oncogenic kinase Akt (among other targets), provide good examples of specificity of signaling. First, they are highly selective for the hydrophobic motif of Akt over the activation loop; second, they display a remarkable isozyme specificity, with PHLPP1 binding and dephosphorylating Akt2 and 3 and PHLPP2 binding and dephosphorylating Akt1 and 3. Their localization and binding to Akt also appear to be tightly regulated by the scaffolding proteins NHERF1, Scribble, and FKBP51 in a cell type-dependent manner, and the requirement for various protein-protein interaction domains for binding to these factors and to PHLPP substrates highlights the additional layer of regulation provided by such non-catalytic domains. Finally, the existence of several feedback loops involving upregulation of PHLPP protein levels downstream of Akt activation suggest that precise regulation of this phosphatase is essential for the modulation of signaling through the PI3K/Akt pathway.

The rise in studies concerning PHLPP since its characterization in 2005 is beginning to unveil the targets and upstream regulators of this phosphatase. With recent evidence demonstrating a tumor suppressor role of PHLPP, future studies of the regulation of this enzyme in normal and cancer cells is likely to provide major insights into this enzyme as a therapeutic target and/or biomarker in human cancer.

Protein kinase C signaling: control by scaffolding proteins

Introduction to the PKC isozymes

Though PKC was initially isolated and biochemically characterized by Nishizuka and colleagues in 1977 (71), interest in the enzyme increased dramatically upon the discovery (in 1982) that it acts as a receptor for the tumor-promoting compounds phorbol esters (72). These compounds are analogs of diacylglycerol (DAG), which, along with Ca^{2+}, activates PKC downstream of phospholipase C (73,74).

Classification of PKC family members – The 10 mammalian PKC isozymes are classified into subfamilies based on their upstream activators (Figure 1.4; reviewed in (75,76)). All PKCs have a conserved C-terminal catalytic domain and an N-terminal regulatory domain that includes

an autoinhibitory pseudosubstrate region. The conventional PKC (cPKC) isozymes PKCα, PKCβI and -βII (which are splice variants of the same gene), and PKCγ, are activated by DAG, which binds their tandem C1 domains, and Ca^{2+}, via the C2 domain. The novel PKC isozymes (PKCδ, -ε, -η, and -θ) are Ca^{2+} insensitive but bind DAG with two orders of magnitude higher affinity than the cPKCs (77), rendering them able to be activated by DAG alone. Interestingly, evolutionary analysis of the novel subfamily reveals segregation into two subfamilies: one "δ-like" group that includes human PKCδ and –θ and can be activated by binding of tyrosine kinases to the C2 domain and subsequent tyrosine phosphorylation, and one "ε-like" group that includes human PKCε and -η (76). Finally, the atypical family members PKCζ and -ι/λ (human and mouse, respectively) are regulated by neither DAG nor Ca^{2+} but instead are activated by protein-protein interaction mediated by their PB1 (Phox and Bem1p) domains, among other regions. In addition to differences among their upstream regulators, these subfamilies also have subtly different consensus phosphorylation motifs, with cPKCs preferring basic residues at -6, -4, -2, +2, and +3 and novel PKCs preferring hydrophobic amino acids at +2 and +3. However, there is a high degree of overlap among the substrate requirements of the various PKC isozymes, with the result that all family members are capable of phosphorylating certain sites (78).

PKC's life cycle – For proper maturation and activity, PKC isozymes require an ordered series of phosphorylations in their catalytic domains (reviewed in (75)). These phosphorylation sites, which are conserved in most AGC kinases, are the activation loop (threonine 500 in PKCβII), which is phosphorylated by phosphoinositide-dependent kinase 1 (PDK-1), and the turn (threonine 641 in PKCβII) and hydrophobic motifs (serine 660 in PKCβII; Figure 1.4, which are phosphorylated in a manner that depends on the mammalian target of rapamycin complex 2 (mTORC2) and PKC's own catalytic activity. (Note, however, that atypical PKC isozymes have a negatively charged glutamic acid residue at their hydrophobic motif and thus do not require phosphorylation at this site.) Fully phosphorylated PKC is catalytically competent but not yet activated; for conventional and novel isozymes, the phosphorylations are constitutive and confer

increased protein stability rather than increased catalytic activity. Acute activation of PKC instead requires binding by upstream activators (DAG, phospatidylinositol-4,5-bisphosphate (PIP_2), and/or Ca^{2+}). Upon agonist stimulation, increased levels of these signaling factors at the membrane result in PKC translocation to the membrane, followed by a conformational change that results in ejection of the pseudosubstrate from the active site and full catalytic activity of the enzyme. Catalytically active PKC is highly sensitive to dephosphorylation by cellular phosphatases including PHLPP, and unphosphorylated PKC is shunted to the detergent-insoluble fraction of the cell and rapidly degraded. Thus, chronic stimulation with phorbol esters or other PKC agonists results in decreased protein levels of PKC.

Functions of PKC – PKC has many cellular and organismal functions, as might be expected for a large and varied kinase family. Notably, several isozymes play opposing roles in processes such as tumorigenesis. Though enzymes activated by the tumor promoters phorbol esters might be expected to act as oncogenes, the overall effect of PKC activation depends on the isozyme and cellular context. For example, conventional and atypical PKCs tend to protect cells against apoptosis, while PKCδ activity is required for caspase activation and apoptosis (79). Even the effect of a single PKC isoform can depend on the cellular context. PKCα, for example, is overexpressed in prostate cancer but downregulated in colon cancer (among other malignancies; reviewed in (80)), and deletion of PKCα impairs the proliferation and survival of GBM cells (81) but increases tumorigenesis in an intestinal cancer model (82). (The context-dependent effects of PKCα signaling may be partially responsible for the lack of PKC-based cancer therapeutics; though an antisense inhibitor of PKCα showed promise in pre-clinical testing (83), it failed to meet efficacy standards in the clinic (80).) PKC isozymes also play roles in the response to ischemic insult, cellular proliferation and mitosis (84,85), immune responses, nociceptive signaling, and synaptic plasticity (reviewed in (76,79)). Of all the effects of PKC activation, the best-studied area is that of cytoskeletal dynamics; PKC isozymes have been particularly implicated in the control of cell polarity and migration (86-91). Given the need for precise spatiotemporal control of

cytoskeletal changes during the establishment of cell polarity and during migration, it is unsurprising that multiple PKC-binding proteins have been implicated in these processes (see below).

Localized control of PKC signaling

The idea that PKC activity is controlled in different ways in different cellular regions is not a new one; a set of PKC activity reporters targeted to various organelles revealed differences in phosphatase-suppressed, basal, and phorbol ester-stimulated PKC activity among these regions (92). Also, levels of PKC's upstream regulators also affect PKC activity at various regions; for example, in response to UTP, DAG levels spike at the plasma membrane but demonstrate a slow, persistent rise at the Golgi; this phenomenon is reflected by acute UTP-stimulated PKC activation at the plasma membrane and chronic activation at the Golgi (92). By extension, therefore, PKC stability, activity, and substrate selectivity can be controlled in even more specific ways by scaffolding proteins, which position PKC isozymes in microenvironments that favor certain changes in PKC behavior.

The importance of cellular scaffolds for PKC signaling was originally recognized by Mochly-Rosen and co-workers (93). The key role of scaffolds is highlighted by studies involving the *Drosophila* eye protein inaD, which contains several PDZ domains and scaffolds light-activated channels, phospholipase β, and the eye-specific cPKC. Interaction among these proteins is necessary for light-induced signaling, and *inaD* mutant flies have impaired responses to light (93). Also, experiments in PKCα-null mouse cerebellar neuron cultures demonstrate the requirement for PKC scaffolding in long-term depression (LTD). The impaired LTD observed in PKCα-null neurons can be rescued by full-length PKCα but not PKCα with the last four amino acids (encoding a PDZ ligand) mutated, suggesting that a PDZ-based interaction is critical for PKCα to mediate LTD (94).

Despite the elegance of these genetic studies, they fail to address the exact mechanisms by which PKC scaffolds affect signaling. In recent years, a host of biochemical and cell biological

studies have arisen to address this very question, with a resulting explosion in our understanding of regulation by scaffolding proteins. Perhaps unsurprisingly, the mechanisms of such regulation are almost as numerous as the scaffolds themselves (reviewed in (95)) and include stabilization of the active form of the kinase (96,97), positioning of PKC near particular substrates (98-100) or at particular regions (101), decreasing PKC's association with negative regulators (102), inhibiting PKC in response to extracellular cues (103), and changing PKC's sensitivity to pharmacological inhibitors (104). In addition, several PKC substrates appear to use direct scaffolding interactions with PKC to increase their own phosphorylation (105,106). It is not my intention to provide an exhaustive list of proteins that interact with PKC; instead, I will use the following sections to highlight a few examples of the myriad ways in which scaffolds can alter PKC's functions.

1. Scaffolds target PKC to specific intracellular locales: pericentrin and PKCβII – The centrosome (also known as the microtubule organizing center) is composed of centrioles along with pericentriolar material, which contains numerous proteins that are essential for microtubule organization and cell division (107). Pericentrin is one such protein; it contains a central α-helical domain flanked by non-helical domains and is hypothesized to form a dynamic lattice composed of helices with protruding N- and C-terminal domains. In this way, it could act to stabilize the centrosome during mitosis while also binding a number of signaling and structural proteins (108). Pericentrin is known to bind a host of such proteins, including γ-tubulin (109,110), dynein light intermediate chain (111), chromatin remodeling proteins (112), Chk1 (113), and protein kinase A (114). Given pericentrin's structural role as a multifunctional scaffold, it is hardly surprising that it is involved in a number of centrosomal processes, including cell cycle progression, spindle organization, and asymmetric division, nor that it is essential for embryonic development (107). Alterations in pericentrin are also associated with certain human disorders, including diabetes and certain forms of dwarfism, in which pericentrin is mutated and depleted from the centrosome (115,116); mental disorders, in which it is mutated and/or upregulated (107); and solid tumors, in

which pericentrin levels are upregulated in association with centrosomal defects and chromosomal abnormalities (117,118).

One key role of pericentrin involves binding to PKCβII (Figure 1.5A). This conventional isozyme translocates to the centrosome in a manner that depends on pericentrin, which binds via PKCβII's C1a domain (84,119). Specific disruption of this interaction results in microtubule disorganization and failure of cytokinesis. The involvement of PKC in microtubule organization appears to be isozyme-specific, because overexpression of PKCβII (or its C1a domain alone) but not of PKCε or ζ blocks cytokinesis and results in the formation of binucleate cells (84). Taken together, these data support a model in which pericentrin localizes endogenous PKCβII to the centrosome in a regulated fashion, allowing PKCβII to facilitate microtubule organization and cytokinesis via an unknown mechanism. Clearly, PKC isozymes can play varying roles at different cellular locales, and scaffolding interactions can be critical for bringing PKCs to these specific locations.

2. Scaffolds stabilize and activate PKC: syndecan-4 and PKCα – Syndecan-4 is a transmembrane proteoglycan that binds the extracellular matrix and is a component of focal adhesions (120,121). The cytoplasmic tails of syndecans contain a variable domain that differs among family members; syndecan-4's variable region (referred to as "4V") is thought to mediate its adhesive role, which is unique among the syndecans (122). Several lines of evidence support the idea that syndecan-4 exerts its adhesive effects by scaffolding PKCα. (The 4V region of the protein binds PKCα but not PKCδ or PKCε (Figure 1.5B) (122).) First, overexpression of wild type syndecan-4 but not a syndecan-4 mutant lacking the cytoplasmic domain increases the levels of PKCα at the membrane and stabilizes PKCα, perhaps by sequestering it away from cytosolic proteases (120); syndecan-4 overexpression also results in increased PKCα activity and increased adhesion (121,123). Interestingly, syndecan-4 binding appears to increase PKCα's catalytic activity as well as its stability: a peptide corresponding to the 4V region interacts with PKCα's catalytic domain and increases PKCα activity *in vitro* (124,125). Though the mechanisms

of activation are still incompletely understood, syndecan-4 appears to activate PKC at least partially through binding to the upstream activator phosphoinositide 4,5-bisphosphate (PIP_2). PIP_2 binding to syndecan-4 induces syndecan-4 oligomerization (126), which is required for PKCα activation (124). *In vitro*, PIP_2 and the 4V peptide synergistically activate PKCα, removing PKCα's dependence on Ca^{2+} for activation (124,126). In summary, syndecan-4 appears to increase PKC signaling by positioning PKCα at the membrane, rendering it resistant to degradation, and increasing PKCα's activity both directly and by increasing the local concentration of PIP_2. The PKCα-syndecan-4 interaction appears to play roles in fibroblast growth factor (FGF) signaling: treatment with FGF increases this interaction (120), and a PIP_2 binding-defective mutant of syndecan-4 fails to activate PKCα or promote wound healing in response to FGF (126). This scaffolding interaction suggests that scaffold proteins do not only passively regulate PKC; rather, they can increase PKC's activity in addition to positioning it at locations that favor its stability and downstream signaling.

3. Scaffolds position activated PKC near its substrates: RACK-1 and PKCα – RACK-1 (receptor for activated C kinase 1), one of the best characterized PKC-binding proteins, is a multifunctional scaffold that binds many signaling molecules, including PP2A, Src, and many members of the cAMP/protein kinase A pathway, leading to roles in proliferation, adhesion, and migration (96). RACK-1 binds the activated forms of several PKC isozymes, notably PKCα, -βII, and ε, and can influence PKC's activity via multiple mechanisms, including positioning PKC near its upstream regulator phospholipase Cγ, acting as a "raft" to transport PKC from one intracellular locale to another, and placing PKC in close proximity to certain substrates (127-129). One such substrate is myelin protein zero (MPZ), a single transmembrane domain protein that is the major protein component of myelin in the peripheral nervous system (Figure 1.5C) (130). The proper regulation of MPZ is critical for myelin compaction and adhesion and for normal nerve function; mutations in the human form of this protein result in the demyelinating neuropathy Charcot-Marie-Tooth disease (131,132). Recent studies suggest a critical role for PKCα-dependent

phosphorylation of MPZ in cell adhesion. Deleting portions of the intracellular domain of MPZ revealed that a region containing a putative PKC phosphorylation site is required for cell-cell adhesion, and more precise mutational studies revealed that alteration of the phospho-acceptor serine or its surrounding residues or treatment with the PKC inhibitor calphostin C blocks adhesion. Notably, although several PKC isozymes are expressed in the sciatic nerve, only PKCα binds MPZ (131). Phosphorylation of the PKC consensus site appears to be dependent on binding of MPZ to RACK-1 and its binding partner p65, suggesting that the RACK-1/p65 complex forms a bridge between MPZ and active PKCα, allowing phosphorylation of MPZ. This hypothesis is supported by the finding that mutation of a single residue that is critical for RACK-1 binding (G184 in the intracellular domain) or of the p65 binding site on MPZ results in decreased adhesion but that this effect can be rescued by replacing the PKC phospho-acceptor with a phospho-mimic (130). Notably, human mutations in G184 or the PKC consensus motif result in late-onset forms of Charcot-Marie-Tooth, highlighting the critical role of scaffolding interactions in maintaining normal nervous system function (133,134).

4. Inducing PKC's dissociation from its substrates: 14-3-3ε and PKCα – PKC signaling has long been hypothesized to decrease insulin action in insulin-responsive tissues (135,136) and may play roles in diabetes in humans; the protein expression levels of PKCα, β, ε, and ζ are increased in the livers of type 2 diabetic patients compared to healthy controls (137). One possible mechanism underlying PKC's negative regulation of insulin signaling is serine phosphorylation of IRS-1 by PKCα (Figure 1.5D). In response to insulin stimulation, PKCα translocates to the membrane and binds to IRS-1, serine phosphorylating it at several residues (138-141); this represents a means of signal termination, because serine phosphorylation impairs tyrosine phosphorylation of IRS-1 and its binding to PI3K (139). The scaffolding protein 14-3-3ε, which acts by binding several phosphorylated residues on each target protein (142), is known to bind IRS-1 (143), and it has recently been proposed that 14-3-3 binding sites match well with PKC consensus phosphorylation sites (144). Therefore, it is likely that 14-3-3ε binds to sites in

IRS-1 that have been previously phosphorylated by PKCα; this hypothesis is supported by the finding that inhibition of PKC activity blocks the insulin-stimulated association of IRS-1 with 14-3-3ε. IRS-1, PKCα, and 14-3-3ε form a complex in response to insulin, but it appears that this complex is short-lived, because 14-3-3ε binding to IRS-1 decreases the PKCα-IRS-1 interaction, de-repressing the tyrosine phosphorylation of IRS-1 and increasing insulin signaling (141). In this case, then, the scaffold 14-3-3ε acts to move PKCα *away* from its substrate IRS-1, facilitating precise temporal control of IRS-1 signaling in response to insulin.

PKC scaffolding: conclusions

I have summarized a few of the ways that scaffolding proteins can affect PKC's activity and choice of targets. Interestingly, binding of PKC by different scaffolds can lead to different cellular effects of PKC activation, including cell division, adhesion, and a decrease in insulin signaling. Consistent with this, alterations in PKC or its scaffolds are associated with a wide spectrum of human pathologies, including dwarfism, peripheral neuropathy, and diabetes, depending in part on which PKC-scaffold interaction is altered. Indeed, cell type-specific scaffolding interactions may play a role in the differential effects of PKC isozymes in various cells, e.g., pro-oncogenic effects of PKCα in prostate cancer versus downregulation of PKCα in colon cancer (80,145).

In this chapter I have provided a brief introduction to the signaling enzymes PHLPP and PKC and highlighted various mechanisms by which interacting proteins regulate their levels, activity, and substrate specificity. As the signal transduction field matures, it has become increasingly apparent that spatiotemporal organization of signaling factors is critical for the proper regulation of dynamic processes such as proliferation and migration (53). However, it is also clear that the biological systems necessary for such effects involve a fair degree of redundancy and resistance to perturbation; thus, alteration or deletion of one component may not be enough to confer long-term changes. In this thesis I will discuss data showing that deletion of PHLPP1 alone is insufficient to confer major changes in growth, proliferation, or insulin sensitivity and reflect on

perturbations allowing loss of PHLPP1 to lead to phenotypes such as cancer and circadian rhythm defects. I will also demonstrate the regulation of PKCα by a novel binding partner, DLG1, and show that this specific interaction leads to changes in cellular migration.

Acknowledgments

The text of Chapter 1 is, in part, a review article submitted to FEBS Journal by O'Neill AK, Niederst MJ, and Newton AC. I was the author of this literature review.

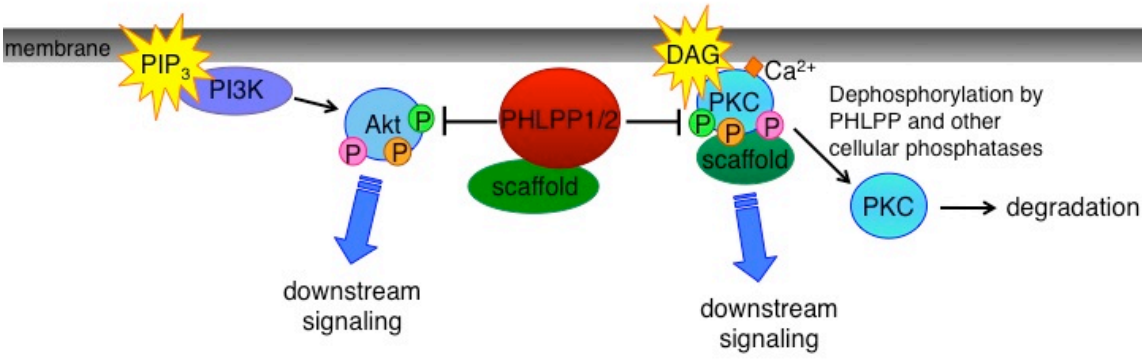

Figure 1.1: Signaling by PHLPP and PKC.
Both PKC and Akt are activated by lipid second messengers generated at cellular membranes (PIP_3 for PI3K/Akt and DAG, in concert with Ca^{2+}, for PKC). PHLPP1 and 2 act to oppose signaling by these kinases by directly dephosphorylating them at the hydrophobic motif (shown in green). In the case of Akt, this dephosphorylation event results in acute downregulation of its activity; in the case of PKC, dephosphorylation destabilizes the enzyme, resulting in its degradation. Both PKC and PHLPP are assisted by binding to scaffolding proteins such as RACK1 (for PKC) and NHERF1 (for PHLPP).

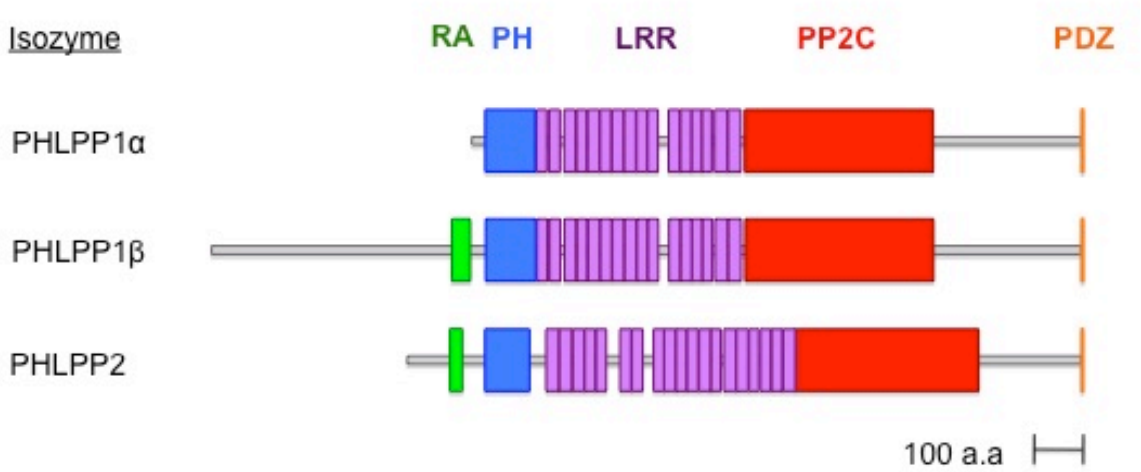

Figure 1.2: Domain structure of the human PHLPP isozymes.
All PHLPP family members contain a pleckstrin homology (PH) domain, a series of leucine-rich repeats (LRR), a PP2C phosphatase domain, and a C-terminal PDZ ligand. In addition, PHLPP1β and PHLPP2 contain a putative Ras association (RA) domain near their N-termini.

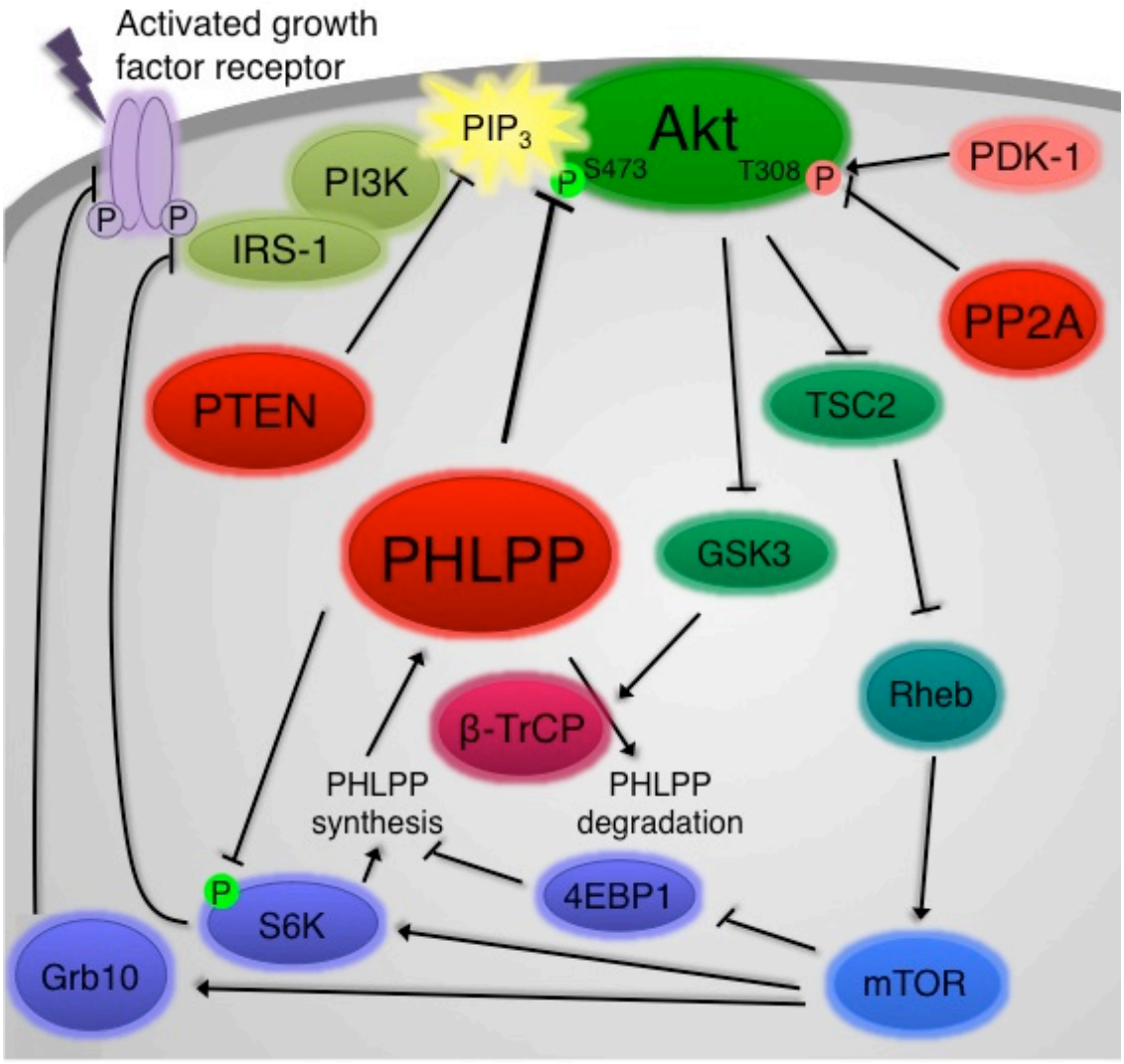

Figure 1.3: PHLPP suppresses the PI3K/Akt signaling pathway.
Upon activation of growth factor receptors, PI3K is recruited by IRS-1 and other proteins to the receptors, where it is activated by phosphorylation, resulting in production of the second messenger PIP_3 at the plasma membrane. Upon this stimulus, Akt translocates to the plasma membrane, where it is activated by phosphorylation at the activation loop (T308) and hydrophobic motif (S473). Fully phosphorylated, active Akt phosphorylates a range of downstream substrates, including TSC2, which indirectly regulates mTOR, and GSK3β. Several phosphatases (bright red) act to restrain PI3K/Akt pathway activation, including the lipid phosphatase PTEN, which dephosphorylates PIP_3, removing the upstream signal for Akt activation, and the protein phosphatases PP2A and PHLPP, which dephosphorylate Akt at T308 (the activation loop) and S473 (the hydrophobic motif), respectively. Note that PHLPP also dephosphorylates S6K1 at its hydrophobic motif, repressing protein synthesis and activating the S6K/IRS-1 feedback loop. PHLPP expression is tightly regulated downstream of Akt, resulting in negative feedback via two mechanisms. First, mTORC1 activation increases PHLPP1 and PHLPP2 protein translation via activation of S6K and inhibition of 4EBP1; second, GSK3β-mediated phosphorylation of PHLPP1 results in increased PHLPP degradation mediated by the E3 ligase β-TrCP. Thus, repression of GSK3β by Akt prevents PHLPP degradation and increases PHLPP protein levels.

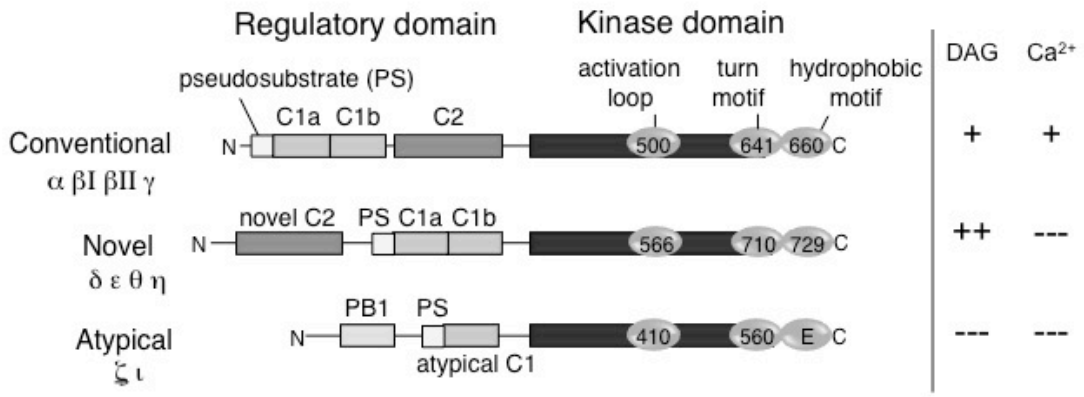

Figure 1.4: Domain structure and activator sensitivity of the three classes of PKC isozymes.
All PKC isozymes contain a N-terminal regulatory domain and a C-terminal catalytic domain. The regulatory domain contains an inhibitory pseudosubstrate (PS) sequence, along with one or more of the following regions: C1 domains, which bind DAG or its analogues phorbol esters; a C2 domain, which binds calcium; and a PB1 domain, which mediates protein-protein interactions. Note that novel PKCs possess a C2 domain that does not bind calcium; however, their C1 domains have a higher affinity for DAG than the conventional isozymes. Also, atypical PKCs respond to neither DAG nor calcium. The kinase domain of PKCs contains three important phosphorylation sites, indicated here by ovals: the activation loop, the turn motif, and the hydrophobic motif. In the atypical PKC isozymes, the hydrophobic motif is replaced by a glutamate.

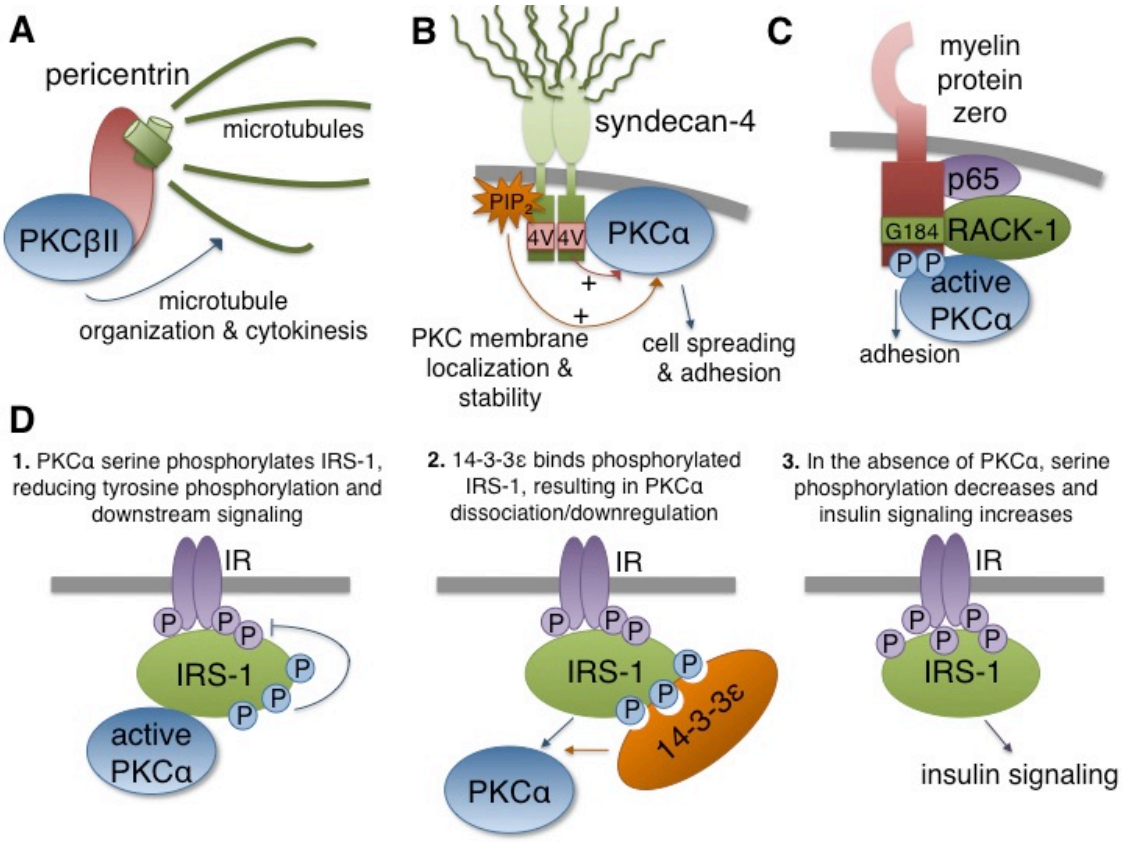

Figure 1.5: Mechanisms by which scaffolding proteins regulate cPKC signaling.

A. Pericentrin binds PKCβII and targets it to the centrosome, where it mediates microtubule organization and cytokinesis. B. The proteoglycan syndecan-4 binds to PKCα via the variable ("4V") region of its intracellular domain, promoting PKCα membrane localization and protein stability. The 4V region and $PI(4,5)P_2$, which also binds syndecan-4, synergistically increase PKCα activity; put together, these effects result in increased cell spreading and adhesion mediated by PKCα and syndecan-4. C. The scaffold RACK-1 binds active PKCα; along with its binding partner p65, RACK-1 promotes PKCα's phosphorylation of myelin protein zero, allowing cell adhesion and proper myelination. Mutations in the RACK1 binding site, G184, result in forms of the demyelinating disease Charcot-Marie-Tooth. D. The scaffold 14-3-3ε binds the serine-phosphorylated, inhibited form of IRS-1, prompting PKCα dissociation from the complex. This, in turn, results in dephosphorylation of the serine residues and increased insulin signaling through IRS-1. Phosphorylated serines are shown in blue and phosphorylated tyrosines in purple.

Table 1.1: Alterations in PHLPP levels in human cancer.

Tumor Type	PHLPP expression	Detection	Reference
Breast	PHLPP1 mRNA is 2.0 fold lower in invasive ductal breast carcinoma	mRNA – Array	(146)
Breast	PHLPP1 mRNA is 2.3 fold lower in ductal breast carcinoma	mRNA – Array	(147)
CLL	PHLPP1 mRNA is 12.4 fold lower in CLL	mRNA – Array	(148)
CLL	PHLPP1 mRNA is 5.5 fold lower in CLL	mRNA – Array	(149)
CLL with 13q14 deletion	PHLPP1 mRNA is absent in >50% of cases with 13q14 deletion	mRNA – qPCR	(150)
Colon	PHLPP2 mRNA is 5 fold lower in colon cancer	mRNA – Array	(151)
Colon	PHLPP2 mRNA is 6.1 fold lower in rectal adenoma	mRNA – Array	(151)
Colon	PHLPP2 mRNA is 3.5-3.9 fold lower in several types of colon adenoma	mRNA – Array	(152)
Colon	PHLPP2 mRNA is 2 fold lower in colorectal adenoma	mRNA – Array	(153)
Colon	PHLPP1 and PHLPP2 expression is lost or reduced in >95% of tumor tissue samples	Protein – IHC	(22)
Esophageal	PHLPP1 mRNA is 5.0 fold lower in esophageal adenocarcinoma	mRNA – Array	(154)
Esophageal	PHLPP2 mRNA is 3.8 fold lower in esophageal adenocarcinoma	mRNA – Array	(154)
GBM	PHLPP1 mRNA is 2.1 fold lower in GBM	mRNA – Array	(155)
Liver, Pancreas, Stomach	PHLPP1 expression is significantly decreased in liver, pancreas, and stomach tumor samples	Protein – IHC	(30)
Mantle Cell Lymphoma	PHLPP1 mRNA is 4.3 fold lower in mantle cell lymphoma	mRNA – Array	(148)
Melanoma	PHLPP2 mRNA is 2.3 fold lower in benign melanocytic skin novus	mRNA – Array	(156)
Pancreatic ductal adenocarcinoma	Low PHLPP1 but not PHLPP2 expression is negatively correlated with survival	Protein – IHC	(25)
Prostate	PHLPP1 mRNA is significantly reduced in high Gleason Score tumors	mRNA – qPCR	(46)
Prostate	PHLPP1 and PHLPP2 mRNAs are absent in 30% and 50% of prostate tumors, respectively	mRNA – Array	(37)
Prostate	PHLPP1 expression is 4 fold lower in PTEN-null, AR-null prostate cancer compared to benign lesions	Protein – IHC	(59)

References

1. Shimizu, K., Okada, M., Takano, A., and Nagai, K. (1999) *FEBS Lett* **458**, 363-369

2. Gao, T., Furnari, F., and Newton, A. C. (2005) *Mol Cell* **18**, 13-24

3. Brognard, J., Sierecki, E., Gao, T., and Newton, A. C. (2007) *Mol Cell* **25**, 917-931

4. O'Neill, A., and Newton, A. C. (2009) *Atlas Genet Cytogenet Oncol Haematol*, URL: http://AtlasGeneticsOncology.org/Genes/PHLPP1ID44544ch44518q44521.html

5. Brognard, J., and Newton, A. C. (2008) *Trends Endocrinol Metab* **19**, 223-230

6. Barford, D., Das, A. K., and Egloff, M. P. (1998) *Annu Rev Biophys Biomol Struct* **27**, 133-164

7. Shimizu, K., Okada, M., Nagai, K., and Fukada, Y. (2003) *J Biol Chem* **278**, 14920-14925

8. Park, W. S., Heo, W. D., Whalen, J. H., O'Rourke, N. A., Bryan, H. M., Meyer, T., and Teruel, M. N. (2008) *Mol Cell* **30**, 381-392

9. Kanan, Y., Matsumoto, H., Song, H., Sokolov, M., Anderson, R. E., and Rajala, R. V. (2010) *J Neurochem* **113**, 477-488

10. Gao, T., Brognard, J., and Newton, A. C. (2008) *J Biol Chem* **283**, 6300-6311

11. Molina, J. R., Agarwal, N. K., Morales, F. C., Hayashi, Y., Aldape, K. D., Cote, G., and Georgescu, M. M. (2011) *Oncogene*

12. Jackson, T. C., Verrier, J. D., Semple-Rowland, S., Kumar, A., and Foster, T. C. (2010) *J Neurochem* **115**, 941-955

13. Keranen, L. M., Dutil, E. M., and Newton, A. C. (1995) *Current biology : CB* **5**, 1394-1403

14. Tsutakawa, S. E., Medzihradszky, K. F., Flint, A. J., Burlingame, A. L., and Koshland, D. E., Jr. (1995) *J Biol Chem* **270**, 26807-26812

15. Pearson, R. B., Dennis, P. B., Han, J. W., Williamson, N. A., Kozma, S. C., Wettenhall, R. E., and Thomas, G. (1995) *The EMBO journal* **14**, 5279-5287

16. Newton, A. C. (2003) *The Biochemical journal* **370**, 361-371

17. Fayard, E., Tintignac, L. A., Baudry, A., and Hemmings, B. A. (2005) *J Cell Sci* **118**, 5675-5678

18. Guertin, D. A., Stevens, D. M., Thoreen, C. C., Burds, A. A., Kalaany, N. Y., Moffat, J., Brown, M., Fitzgerald, K. J., and Sabatini, D. M. (2006) *Dev Cell* **11**, 859-871

19. Jacinto, E., Facchinetti, V., Liu, D., Soto, N., Wei, S., Jung, S. Y., Huang, Q., Qin, J., and Su, B. (2006) *Cell* **127**, 125-137

20. Yang, Z. Z., Tschopp, O., Hemmings-Mieszczak, M., Feng, J., Brodbeck, D., Perentes, E., and Hemmings, B. A. (2003) *J Biol Chem* **278**, 32124-32131

21. Andreozzi, F., Procopio, C., Greco, A., Mannino, G. C., Miele, C., Raciti, G. A., Iadicicco, C., Beguinot, F., Pontiroli, A. E., Hribal, M. L., Folli, F., and Sesti, G. (2011) *Diabetologia* **54**, 1879-1887

22. Liu, J., Weiss, H. L., Rychahou, P., Jackson, L. N., Evers, B. M., and Gao, T. (2009) *Oncogene* **28**, 994-1004

23. Miyamoto, S., Purcell, N. H., Smith, J. M., Gao, T., Whittaker, R., Huang, K., Castillo, R., Glembotski, C. C., Sussman, M. A., Newton, A. C., and Brown, J. H. (2010) *Circ Res* **107**, 476-484

24. Suljagic, M., Laurenti, L., Tarnani, M., Alam, M., Malek, S. N., and Efremov, D. G. (2010) *Leukemia* **24**, 2063-2071

25. Nitsche, C., Edderkaoui, M., Moore, R. M., Eibl, G., Kasahara, N., Treger, J., Grippo, P. J., Mayerle, J., Lerch, M. M., and Gukovskaya, A. S. (2011) *Gastroenterology*

26. Gysin, S., and Imber, R. (1997) *Eur J Biochem* **249**, 156-160

27. Liu, J., Stevens, P. D., Li, X., Schmidt, M. D., and Gao, T. (2011) *Mol Cell Biol*

28. Shimizu, K., Phan, T., Mansuy, I. M., and Storm, D. R. (2007) *Cell* **128**, 1219-1229

29. Field, J., Xu, H. P., Michaeli, T., Ballester, R., Sass, P., Wigler, M., and Colicelli, J. (1990) *Science* **247**, 464-467

30. Qiao, M., Wang, Y., Xu, X., Lu, J., Dong, Y., Tao, W., Stein, J., Stein, G. S., Iglehart, J. D., Shi, Q., and Pardee, A. B. (2010) *Mol Cell* **38**, 512-523

31. Qiao, M., Iglehart, J. D., and Pardee, A. B. (2007) *Cancer Res* **67**, 5293-5299

32. Saavedra, A., Garcia-Martinez, J. M., Xifro, X., Giralt, A., Torres-Peraza, J. F., Canals, J. M., Diaz-Hernandez, M., Lucas, J. J., Alberch, J., and Perez-Navarro, E. (2009) *Cell Death Differ* **17**, 324-335

33. Patterson, S. J., Han, J. M., Garcia, R., Assi, K., Gao, T., O'Neill, A., Newton, A. C., and Levings, M. K. (2011) *J Immunol* **186**, 5533-5537

34. Masubuchi, S., Gao, T., O'Neill, A., Eckel-Mahan, K., Newton, A. C., and Sassone-Corsi, P. (2010) *Proc Natl Acad Sci U S A* **107**, 1642-1647

35. Lee, B., Almad, A., Butcher, G. Q., and Obrietan, K. (2007) *Eur J Neurosci* **26**, 451-462

36. Liu, J., Stevens, P. D., and Gao, T. (2010) *J Biol Chem* **286**, 6510-6520

37. Chen, M., Pratt, C. P., Zeeman, M. E., Schultz, N., Taylor, B. S., O'Neill, A., Castillo-Martin, M., Nowak, D. G., Naguib, A., Grace, D. M., Murn, J., Navin, N., Atwal, G. S., Sander, C., Gerald, W. L., Cordon-Cardo, C., Newton, A. C., Carver, B. S., and Trotman, L. C. (2011) *Cancer Cell* **20**, 173-186

38. Brognard, J., Niederst, M., Reyes, G., Warfel, N., and Newton, A. C. (2009) *J Biol Chem* **284**, 15215-15223

39. Goel, A., Arnold, C. N., Niedzwiecki, D., Chang, D. K., Ricciardiello, L., Carethers, J. M., Dowell, J. M., Wasserman, L., Compton, C., Mayer, R. J., Bertagnolli, M. M., and Boland, C. R. (2003) *Cancer Res* **63**, 1608-1614

40. Johnson-Pais, T. L., Nellissery, M. J., Ammerman, D. G., Pathmanathan, D., Bhatia, P., Buller, C. L., Leach, R. J., and Hansen, M. F. (2003) *Int J Cancer* **105**, 285-288

41. Patael-Karasik, Y., Daniely, M., Gotlieb, W. H., Ben-Baruch, G., Schiby, J., Barakai, G., Goldman, B., Aviram, A., and Friedman, E. (2000) *Cancer Genet Cytogenet* **121**, 26-32

42. Rakha, E. A., Green, A. R., Powe, D. G., Roylance, R., and Ellis, I. O. (2006) *Genes Chromosomes Cancer* **45**, 527-535

43. Safford, S. D., Goyeau, D., Freemerman, A. J., Bentley, R., Everett, M. L., Grundy, P. E., and Skinner, M. A. (2003) *Ann Surg Oncol* **10**, 136-143

44. Torring, N., Borre, M., Sorensen, K. D., Andersen, C. L., Wiuf, C., and Orntoft, T. F. (2007) *Br J Cancer* **96**, 499-506

45. Tsuda, H., Zhang, W. D., Shimosato, Y., Yokota, J., Terada, M., Sugimura, T., Miyamura, T., and Hirohashi, S. (1990) *Proc Natl Acad Sci U S A* **87**, 6791-6794

46. Hellwinkel, O. J., Rogmann, J. P., Asong, L. E., Luebke, A. M., Eichelberg, C., Ahyai, S., Isbarn, H., Graefen, M., Huland, H., and Schlomm, T. (2008) *BJU Int* **101**, 1454-1460

47. Taylor, B. S., Schultz, N., Hieronymus, H., Gopalan, A., Xiao, Y., Carver, B. S., Arora, V. K., Kaushik, P., Cerami, E., Reva, B., Antipin, Y., Mitsiades, N., Landers, T., Dolgalev, I., Major, J. E., Wilson, M., Socci, N. D., Lash, A. E., Heguy, A., Eastham, J. A., Scher, H. I., Reuter, V. E., Scardino, P. T., Sander, C., Sawyers, C. L., and Gerald, W. L. (2010) *Cancer Cell* **18**, 11-22

48. Ding, Z., Wu, C. J., Chu, G. C., Xiao, Y., Ho, D., Zhang, J., Perry, S. R., Labrot, E. S., Wu, X., Lis, R., Hoshida, Y., Hiller, D., Hu, B., Jiang, S., Zheng, H., Stegh, A. H., Scott, K. L., Signoretti, S., Bardeesy, N., Wang, Y. A., Hill, D. E., Golub, T. R., Stampfer, M. J., Wong, W. H., Loda, M., Mucci, L., Chin, L., and DePinho, R. A. (2011) *Nature* **470**, 269-273

49. Beezhold, K., Liu, J., Kan, H., Meighan, T., Castranova, V., Shi, X., and Chen, F. (2011) *Toxicol Sci*

50. Warfel, N. A., Niederst, M., Stevens, M. W., Brennan, P. M., Frame, M. C., and Newton, A. C. (2011) *J Biol Chem* **286**, 19777-19788

51. Li, X., Liu, J., and Gao, T. (2009) *Mol Cell Biol* **29**, 6192-6205

52. Hussain, S., Foreman, O., Perkins, S. L., Witzig, T. E., Miles, R. R., van Deursen, J., and Galardy, P. J. (2010) *Leukemia* **24**, 1641-1655

53. Pawson, C. T., and Scott, J. D. (2010) *Nature structural & molecular biology* **17**, 653-658

54. Li, X., Yang, H., Liu, J., Schmidt, M. D., and Gao, T. (2011) *EMBO Rep* **12**, 818-824

55. Teti, A., Colucci, S., Grano, M., Argentino, L., and Zambonin Zallone, A. (1992) *The American journal of physiology* **263**, C130-139

56. Pei, H., Li, L., Fridley, B. L., Jenkins, G. D., Kalari, K. R., Lingle, W., Petersen, G., Lou, Z., and Wang, L. (2009) *Cancer Cell* **16**, 259-266

57. Mistafa, O., Ghalali, A., Kadekar, S., Hogberg, J., and Stenius, U. (2010) *J Biol Chem* **285**, 27900-27910

58. Carver, B. S., Chapinski, C., Wongvipat, J., Hieronymus, H., Chen, Y., Chandarlapaty, S., Arora, V. K., Le, C., Koutcher, J., Scher, H., Scardino, P. T., Rosen, N., and Sawyers, C. L. (2011) *Cancer Cell* **19**, 575-586

59. Mulholland, D. J., Tran, L. M., Li, Y., Cai, H., Morim, A., Wang, S., Plaisier, S., Garraway, I. P., Huang, J., Graeber, T. G., and Wu, H. (2011) *Cancer Cell* **19**, 792-804

60. Gao, M. H., Miyanohara, A., Feramisco, J. R., and Tang, T. (2009) *Biochem Biophys Res Commun* **384**, 193-198

61. Sowa, M. E., Bennett, E. J., Gygi, S. P., and Harper, J. W. (2009) *Cell* **138**, 389-403

62. Sierecki, E., Sinko, W., McCammon, J. A., and Newton, A. C. (2010) *J Med Chem* **53**, 6899-6911

63. Zhang, M., and Riedel, H. (2009) *J Cell Biochem* **107**, 65-75

64. Courtney, K. D., Corcoran, R. B., and Engelman, J. A. (2010) *J Clin Oncol* **28**, 1075-1083

65. Wong, K. K., Engelman, J. A., and Cantley, L. C. (2010) *Curr Opin Genet Dev* **20**, 87-90

66. Brognard, J., and Hunter, T. (2011) *Curr Opin Genet Dev* **21**, 4-11

67. Maehama, T., and Dixon, J. E. (1998) *J Biol Chem* **273**, 13375-13378

68. Beaulieu, J. M., Sotnikova, T. D., Marion, S., Lefkowitz, R. J., Gainetdinov, R. R., and Caron, M. G. (2005) *Cell* **122**, 261-273

69. Wullschleger, S., Loewith, R., and Hall, M. N. (2006) *Cell* **124**, 471-484

70. Yu, Y., Yoon, S.-O., Poulogiannis, G., Yang, Q., Ma, X. M., Villen, J., Kubica, N., Hoffman, G. R., Cantley, L. C., Gygi, S. P., and Blenis, J. (2011) *Science* **332**, 1322-1326

71. Inoue, M., Kishimoto, A., Takai, Y., and Nishizuka, Y. (1977) *The Journal of biological chemistry* **252**, 7610-7616

72. Castagna, M., Takai, Y., Kaibuchi, K., Sano, K., Kikkawa, U., and Nishizuka, Y. (1982) *J Biol Chem* **257**, 7847-7851

73. Takai, Y., Kishimoto, A., Kikkawa, U., Mori, T., and Nishizuka, Y. (1979) *Biochemical and biophysical research communications* **91**, 1218-1224

74. Creba, J. A., Downes, C. P., Hawkins, P. T., Brewster, G., Michell, R. H., and Kirk, C. J. (1983) *The Biochemical journal* **212**, 733-747

75. Newton, A. C. (2010) *Am J Physiol Endocrinol Metab* **298**, E395-402

76. Sossin, W. S. (2007) *Learn Mem* **14**, 236-246

77. Giorgione, J. R., Lin, J. H., McCammon, J. A., and Newton, A. C. (2006) *The Journal of biological chemistry* **281**, 1660-1669

78. Nishikawa, K., Toker, A., Johannes, F. J., Songyang, Z., and Cantley, L. C. (1997) *The Journal of biological chemistry* **272**, 952-960

79. Dempsey, E. C., Newton, A. C., Mochly-Rosen, D., Fields, A. P., Reyland, M. E., Insel, P. A., and Messing, R. O. (2000) *Am J Physiol Lung Cell Mol Physiol* **279**, L429-438

80. Konopatskaya, O., and Poole, A. W. (2010) *Trends Pharmacol Sci* **31**, 8-14

81. Cameron, A. J., Procyk, K. J., Leitges, M., and Parker, P. J. (2008) *International journal of cancer. Journal international du cancer* **123**, 769-779

82. Oster, H., and Leitges, M. (2006) *Cancer research* **66**, 6955-6963

83. Dean, N., McKay, R., Miraglia, L., Howard, R., Cooper, S., Giddings, J., Nicklin, P., Meister, L., Ziel, R., Geiger, T., Muller, M., and Fabbro, D. (1996) *Cancer Res* **56**, 3499-3507

84. Chen, D., Purohit, A., Halilovic, E., Doxsey, S. J., and Newton, A. C. (2004) *The Journal of biological chemistry* **279**, 4829-4839

85. Unno, K., Hanada, T., and Chishti, A. H. (2008) *Experimental cell research* **314**, 3118-3129

86. Etienne-Manneville, S., Manneville, J. B., Nicholls, S., Ferenczi, M. A., and Hall, A. (2005) *J Cell Biol* **170**, 895-901

87. Holinstat, M., Mehta, D., Kozasa, T., Minshall, R. D., and Malik, A. B. (2003) *J Biol Chem* **278**, 28793-28798

88. Kermorgant, S., Zicha, D., and Parker, P. J. (2003) *J Biol Chem* **278**, 28921-28929

89. Kermorgant, S., Zicha, D., and Parker, P. J. (2004) *EMBO J* **23**, 3721-3734

90. Larsson, C. (2006) *Cell Signal* **18**, 276-284

91. Rosse, C., Linch, M., Kermorgant, S., Cameron, A. J., Boeckeler, K., and Parker, P. J. (2010) *Nat Rev Mol Cell Biol* **11**, 103-112

92. Gallegos, L. L., Kunkel, M. T., and Newton, A. C. (2006) *J Biol Chem* **281**, 30947-30956

93. Tsunoda, S., Sierralta, J., Sun, Y., Bodner, R., Suzuki, E., Becker, A., Socolich, M., and Zuker, C. S. (1997) *Nature* **388**, 243-249

94. Leitges, M., Kovac, J., Plomann, M., and Linden, D. J. (2004) *Neuron* **44**, 585-594

95. Poole, A. W., Pula, G., Hers, I., Crosby, D., and Jones, M. L. (2004) *Trends Pharmacol Sci* **25**, 528-535

96. Adams, D. R., Ron, D., and Kiely, P. A. (2011) *Cell communication and signaling : CCS* **9**, 22

97. Saurin, A. T., Brownlow, N., and Parker, P. J. (2009) *Cell Cycle* **8**, 549-555

98. Bass-Zubek, A. E., Hobbs, R. P., Amargo, E. V., Garcia, N. J., Hsieh, S. N., Chen, X., Wahl, J. K., 3rd, Denning, M. F., and Green, K. J. (2008) *The Journal of cell biology* **181**, 605-613

99. Faisal, A., Saurin, A., Gregory, B., Foxwell, B., and Parker, P. J. (2008) *The Journal of biological chemistry* **283**, 18591-18600

100. Tavalin, S. J. (2008) *The Journal of biological chemistry* **283**, 11445-11452

101. Numaga, T., Nishida, M., Kiyonaka, S., Kato, K., Katano, M., Mori, E., Kurosaki, T., Inoue, R., Hikida, M., Putney, J. W., Jr., and Mori, Y. (2010) *Journal of cell science* **123**, 927-938

102. Garcia-Hoz, C., Sanchez-Fernandez, G., Diaz-Meco, M. T., Moscat, J., Mayor, F., and Ribas, C. (2010) *The Journal of biological chemistry* **285**, 13480-13489

103. Guo, L. W., Gao, L., Rothschild, J., Su, B., and Gelman, I. H. (2011) *The Journal of biological chemistry* **286**, 38356-38366

104. Hoshi, N., Langeberg, L. K., Gould, C. M., Newton, A. C., and Scott, J. D. (2010) *Molecular cell* **37**, 541-550

105. Tigges, U., Koch, B., Wissing, J., Jockusch, B. M., and Ziegler, W. H. (2003) *The Journal of biological chemistry* **278**, 23561-23569

106. Lin, D., Edwards, A. S., Fawcett, J. P., Mbamalu, G., Scott, J. D., and Pawson, T. (2000) *Nature cell biology* **2**, 540-547

107. Delaval, B., and Doxsey, S. J. (2010) *The Journal of cell biology* **188**, 181-190

108. Rempel, N. E. (2001) *Einstein Quart J Biol and Med* **18**, 54-58

109. Zimmerman, W. C., Sillibourne, J., Rosa, J., and Doxsey, S. J. (2004) *Molecular biology of the cell* **15**, 3642-3657

110. Knop, M., and Schiebel, E. (1997) *The EMBO journal* **16**, 6985-6995

111. Purohit, A., Tynan, S. H., Vallee, R., and Doxsey, S. J. (1999) *The Journal of cell biology* **147**, 481-492

112. Sillibourne, J. E., Delaval, B., Redick, S., Sinha, M., and Doxsey, S. J. (2007) *Molecular biology of the cell* **18**, 3667-3680

113. Tibelius, A., Marhold, J., Zentgraf, H., Heilig, C. E., Neitzel, H., Ducommun, B., Rauch, A., Ho, A. D., Bartek, J., and Kramer, A. (2009) *The Journal of cell biology* **185**, 1149-1157

114. Diviani, D., Langeberg, L. K., Doxsey, S. J., and Scott, J. D. (2000) *Current biology : CB* **10**, 417-420

115. Huang-Doran, I., Bicknell, L. S., Finucane, F. M., Rocha, N., Porter, K. M., Tung, Y. C., Szekeres, F., Krook, A., Nolan, J. J., O'Driscoll, M., Bober, M., O'Rahilly, S., Jackson, A. P., and Semple, R. K. (2011) *Diabetes* **60**, 925-935

116. Griffith, E., Walker, S., Martin, C. A., Vagnarelli, P., Stiff, T., Vernay, B., Al Sanna, N., Saggar, A., Hamel, B., Earnshaw, W. C., Jeggo, P. A., Jackson, A. P., and O'Driscoll, M. (2008) *Nature genetics* **40**, 232-236

117. Pihan, G. A., Purohit, A., Wallace, J., Knecht, H., Woda, B., Quesenberry, P., and Doxsey, S. J. (1998) *Cancer research* **58**, 3974-3985

118. Kim, J., Choi, Y. L., Vallentin, A., Hunrichs, B. S., Hellerstein, M. K., Peehl, D. M., and Mochly-Rosen, D. (2008) *Cancer research* **68**, 6831-6839

119. Alvi, F., Idkowiak-Baldys, J., Baldys, A., Raymond, J. R., and Hannun, Y. A. (2007) *Cellular and molecular life sciences : CMLS* **64**, 263-270

120. Keum, E., Kim, Y., Kim, J., Kwon, S., Lim, Y., Han, I., and Oh, E. S. (2004) *The Biochemical journal* **378**, 1007-1014

121. Thodeti, C. K., Albrechtsen, R., Grauslund, M., Asmar, M., Larsson, C., Takada, Y., Mercurio, A. M., Couchman, J. R., and Wewer, U. M. (2003) *The Journal of biological chemistry* **278**, 9576-9584

122. Lim, S. T., Longley, R. L., Couchman, J. R., and Woods, A. (2003) *The Journal of biological chemistry* **278**, 13795-13802

123. Chaudhuri, P., Colles, S. M., Fox, P. L., and Graham, L. M. (2005) *Circulation research* **97**, 674-681

124. Oh, E. S., Woods, A., Lim, S. T., Theibert, A. W., and Couchman, J. R. (1998) *The Journal of biological chemistry* **273**, 10624-10629

125. Woods, A., Oh, E. S., and Couchman, J. R. (1998) *Matrix biology : journal of the International Society for Matrix Biology* **17**, 477-483

126. Horowitz, A., Tkachenko, E., and Simons, M. (2002) *J Cell Biol* **157**, 715-725

127. Nilsson, J., Sengupta, J., Frank, J., and Nissen, P. (2004) *EMBO reports* **5**, 1137-1141

128. Rigas, A. C., Ozanne, D. M., Neal, D. E., and Robson, C. N. (2003) *The Journal of biological chemistry* **278**, 46087-46093

129. Schechtman, D., and Mochly-Rosen, D. (2001) *Oncogene* **20**, 6339-6347

130. Gaboreanu, A. M., Hrstka, R., Xu, W., Shy, M., Kamholz, J., Lilien, J., and Balsamo, J. (2007) *The Journal of cell biology* **177**, 707-716

131. Xu, W., Shy, M., Kamholz, J., Elferink, L., Xu, G., Lilien, J., and Balsamo, J. (2001) *The Journal of cell biology* **155**, 439-446

132. Shy, M. E., Jani, A., Krajewski, K., Grandis, M., Lewis, R. A., Li, J., Shy, R. R., Balsamo, J., Lilien, J., Garbern, J. Y., and Kamholz, J. (2004) *Brain : a journal of neurology* **127**, 371-384

133. Shimizu, H., Oka, N., Kawarai, T., Taniguchi, K., Saji, N., Tadano, M., Bernardi, G., Orlacchio, A., and Kita, Y. (2010) *Clinical neurology and neurosurgery* **112**, 798-800

134. Street, V. A., Meekins, G., Lipe, H. P., Seltzer, W. K., Carter, G. T., Kraft, G. H., and Bird, T. D. (2002) *Neuromuscular disorders : NMD* **12**, 643-650

135. Draznin, B. (2006) *Diabetes* **55**, 2392-2397

136. Leitges, M., Plomann, M., Standaert, M. L., Bandyopadhyay, G., Sajan, M. P., Kanoh, Y., and Farese, R. V. (2002) *Mol Endocrinol* **16**, 847-858

137. Considine, R. V., Nyce, M. R., Allen, L. E., Morales, L. M., Triester, S., Serrano, J., Colberg, J., Lanza-Jacoby, S., and Caro, J. F. (1995) *The Journal of clinical investigation* **95**, 2938-2944

138. Nawaratne, R., Gray, A., Jorgensen, C. H., Downes, C. P., Siddle, K., and Sethi, J. K. (2006) *Mol Endocrinol* **20**, 1838-1852

139. Miele, C., Riboulet, A., Maitan, M. A., Oriente, F., Romano, C., Formisano, P., Giudicelli, J., Beguinot, F., and Van Obberghen, E. (2003) *The Journal of biological chemistry* **278**, 47376-47387

140. Cipok, M., Aga-Mizrachi, S., Bak, A., Feurstein, T., Steinhart, R., Brodie, C., and Sampson, S. R. (2006) *Biochemical and biophysical research communications* **345**, 817-824

141. Oriente, F., Andreozzi, F., Romano, C., Perruolo, G., Perfetti, A., Fiory, F., Miele, C., Beguinot, F., and Formisano, P. (2005) *The Journal of biological chemistry* **280**, 40642-40649

142. Tzivion, G., Shen, Y. H., and Zhu, J. (2001) *Oncogene* **20**, 6331-6338

143. Craparo, A., Freund, R., and Gustafson, T. A. (1997) *The Journal of biological chemistry* **272**, 11663-11669

144. Chan, P. M., Ng, Y. W., and Manser, E. (2011) *Molecular & cellular proteomics : MCP* **10**, M110 005157

145. Fields, A. P., and Murray, N. R. (2008) *Adv Enzyme Regul* **48**, 166-178

146. Karnoub, A. E., Dash, A. B., Vo, A. P., Sullivan, A., Brooks, M. W., Bell, G. W., Richardson, A. L., Polyak, K., Tubo, R., and Weinberg, R. A. (2007) *Nature* **449**, 557-563

147. Richardson, A. L., Wang, Z. C., De Nicolo, A., Lu, X., Brown, M., Miron, A., Liao, X., Iglehart, J. D., Livingston, D. M., and Ganesan, S. (2006) *Cancer Cell* **9**, 121-132

148. Basso, K., Margolin, A. A., Stolovitzky, G., Klein, U., Dalla-Favera, R., and Califano, A. (2005) *Nat Genet* **37**, 382-390

149. Haslinger, C., Schweifer, N., Stilgenbauer, S., Dohner, H., Lichter, P., Kraut, N., Stratowa, C., and Abseher, R. (2004) *J Clin Oncol* **22**, 3937-3949

150. Ouillette, P., Erba, H., Kujawski, L., Kaminski, M., Shedden, K., and Malek, S. N. (2008) *Cancer Res* **68**, 1012-1021

151. Sabates-Bellver, J., Van der Flier, L. G., de Palo, M., Cattaneo, E., Maake, C., Rehrauer, H., Laczko, E., Kurowski, M. A., Bujnicki, J. M., Menigatti, M., Luz, J., Ranalli, T. V.,

Gomes, V., Pastorelli, A., Faggiani, R., Anti, M., Jiricny, J., Clevers, H., and Marra, G. (2007) *Mol Cancer Res* **5**, 1263-1275

152. Kaiser, S., Park, Y. K., Franklin, J. L., Halberg, R. B., Yu, M., Jessen, W. J., Freudenberg, J., Chen, X., Haigis, K., Jegga, A. G., Kong, S., Sakthivel, B., Xu, H., Reichling, T., Azhar, M., Boivin, G. P., Roberts, R. B., Bissahoyo, A. C., Gonzales, F., Bloom, G. C., Eschrich, S., Carter, S. L., Aronow, J. E., Kleimeyer, J., Kleimeyer, M., Ramaswamy, V., Settle, S. H., Boone, B., Levy, S., Graff, J. M., Doetschman, T., Groden, J., Dove, W. F., Threadgill, D. W., Yeatman, T. J., Coffey, R. J., Jr., and Aronow, B. J. (2007) *Genome Biol* **8**, R131

153. Gaspar, C., Cardoso, J., Franken, P., Molenaar, L., Morreau, H., Moslein, G., Sampson, J., Boer, J. M., de Menezes, R. X., and Fodde, R. (2008) *Am J Pathol* **172**, 1363-1380

154. Hao, Y., Triadafilopoulos, G., Sahbaie, P., Young, H. S., Omary, M. B., and Lowe, A. W. (2006) *Gastroenterology* **131**, 925-933

155. Bredel, M., Bredel, C., Juric, D., Harsh, G. R., Vogel, H., Recht, L. D., and Sikic, B. I. (2005) *Cancer Res* **65**, 4088-4096

156. Talantov, D., Mazumder, A., Yu, J. X., Briggs, T., Jiang, Y., Backus, J., Atkins, D., and Wang, Y. (2005) *Clin Cancer Res* **11**, 7234-7242

Chapter 2:

Characterization of PHLPP1-null mice

Abstract

Given that PHLPP is known to repress Akt and PKC signaling in immortalized cell lines, the question of what functions the PHLPP isozymes perform *in vivo* naturally arises. Studies of mice deficient in PTEN, which also negatively regulates the Akt pathway, suggest that loss of PHLPP might result in increased oncogenesis, hypertrophy, and/or increased insulin sensitivity. To test this hypothesis, we generated a whole-body knockout of PHLPP1. PHLPP1-null mice were generated at the expected Mendelian ratios and appeared grossly normal. In addition, characterization of Akt and PKC activation in several tissues revealed no dramatic changes, arguing for the existence of compensatory mechanisms. Contrary to expectations, these mice did not display hypertrophy in most tissues but were slightly smaller than wild type controls. We found no evidence of changes in insulin signaling or glucose tolerance. Additionally, we generated primary and immortalized mouse embryonic fibroblasts (MEFs) and primary astrocytes from these mice; the primary cells did not show changes in Akt activation, though they were slightly more resistant to apoptosis than cells derived from wild type mice. Curiously, immortalized MEFs displayed the expected biochemical changes (increased Akt and ERK signaling, increased levels of PKC), suggesting that additional genetic alterations are necessary for deletion of PHLPP1 to have a dramatic effect. These data and data from other studies of PHLPP1-null mice support the conclusion that PHLPP1 expression is not necessary under most physiological conditions but becomes important only when additional stressors (whether genetic or environmental) are introduced.

Introduction

As discussed in Chapter 1, the best characterized targets of the PHLPP phosphatases (Akt, PKC, and S6K) act mostly to promote proliferation and oppose apoptosis (1-5). Consistent with the molecular function of PHLPP in dephosphorylating and downregulating these enzymes,

overexpression of PHLPP1 or 2 in cancer cell lines results in increased apoptosis and decreased growth, proliferation, and colony formation, while siRNA-mediated depletion of PHLPP has the opposite effect (1-8). Thus, results in cell lines support the hypothesis that PHLPP1 and 2 act as tumor suppressors and negative regulators of growth.

Most studies show similar effects of depleting PHLPP1 or PHLPP2, arguing that the two isozymes have redundant effects. However, Brognard and colleagues elegantly showed that in breast cancer cells, PHLPP1 shows a preference for Akt2 over Akt1, acting to repress signaling through Akt1-specific targets, while PHLPP2 shows the opposite preference (1); similar results were recently obtained in a pancreatic cancer cell line (9). These results argue that the two PHLPP proteins might not have totally overlapping functions and, furthermore, that PHLPP1 might be more important for repressing Akt signaling in tissue types that express higher levels of Akt2 than Akt1, including the insulin-responsive tissues (white adipose tissue, skeletal muscle, and liver) (10). The hypothesis that PHLPP1 might play roles in insulin signaling and glucose homeostasis is supported by studies showing that mice lacking Akt2 but not Akt1 develop insulin resistance and hyperglycemia; in fact, Akt1-null mice have improved insulin sensitivity (11,12). Interestingly, these two Akt isozymes can also play opposing roles in carcinogenesis: in mice overexpressing ErbB2 or polyoma middle T in the mammary gland, Akt1 deletion slows tumor development, whereas Akt2 deletion accelerates it (13). These results suggest that the effects of deleting or downregulating PHLPP expression in an intact mouse might be more complex than those observed in cell culture and might vary according to the expression and roles of the various Akt isozymes in various tissues.

Several previous studies have provided clues to the roles of the PHLPP isozymes in normal physiology. First, the initial observation that the mRNA expression of PHLPP1β (also known as “suprachiasmatic nucleus oscillatory protein” or SCOP) varies in a circadian manner in the suprachiasmatic nucleus, the hypothalamic center that controls circadian rhythms, raises the possibility that PHLPP1 might play a role in the proper regulation of circadian behavior (14).

Second, PHLPP1 is expressed at high levels in the hippocampus, where it appears to play roles in the regulation of ERK signaling and learning and memory (15,16). Also, as previously noted, PHLPP suppresses cell growth in culture (4,5); this effect is analogous to that of PTEN, whose growth-inhibitory effects have been extensively characterized (17,18). Examination of the effects of deleting or mutating PTEN in the mouse might, therefore, yield hints as to the possible effects of deleting PHLPP.

Complete inactivation of PTEN in the mouse results in prenatal lethality at embryonic day 6.5 (19,20), but PTEN heterozygotes have been generated and are viable. These mice develop hyperplasia and neoplasia in various tissues, including the gastrointestinal tract, thyroid, prostate, colon, and skin (17). Mouse models in which PTEN is conditionally deleted under the control of tissue-specific promoters have also been shown to be susceptible to tumors, including T-cell lymphomas and lung adenocarcinomas (17). Even in tissues where PTEN deletion does not result in frank tumor formation, such as pancreatic β cells and hepatocytes, it tends to predispose cells towards increased growth and proliferation (21,22). Unsurprisingly, PTEN deletion in insulin-responsive tissues including liver, adipose tissue, and skeletal muscle leads to increases in insulin signaling and, importantly, Akt activation (23-25). Given the known roles of PHLPP in the brain, the decrease in PHLPP1 mRNA levels observed in GBM (26), and the importance of PI3K/Akt signaling for GBM (27), mice lacking PTEN in glial cells could be a useful model for changes that might occur with deletion of PHLPP1. Conditional inactivation of PTEN under the glial fibrillary acidic protein (GFAP) promoter results in loss of PTEN protein in both neurons and glia, with corresponding increases in cell size and number. This results in overall brain enlargement and dysplasia in several regions, including the cerebellum and hippocampus. These mice develop seizures and ataxia, and many of them die before reaching 50 days of age (28,29). However, these changes do not appear to progress to carcinoma, suggesting either that complete deletion of PTEN produces a senescence response that limits cell proliferation and survival (30)

or that other factors (such as PHLPP) are able to restrain PI3K/Akt-mediated carcinogenesis in the absence of PTEN, as hypothesized by Molina and colleagues (7).

The goal of the current study was to generate PHLPP1-null mice (using a Cre-LoxP system that allows conditional deletion of the PHLPP1 gene) and to characterize changes in Akt, PKC, and ERK signaling as well as any physiological changes. I hypothesized that tissues from these mice would display increases in Akt phosphorylation at serine 473 as well as increases in PKC levels and that insulin-responsive tissues would be more insulin-sensitive as a result. I also theorized that the mice might display hypertrophy and would be prone to developing tumors in various tissues, including the brain. However, studies of mice lacking PHLPP1 and primary cells isolated from them mostly failed to support these conclusions: PHLPP1-null mice were smaller compared to their wild type littermates and showed no significant changes in Akt phosphorylation, PKC levels, or growth factor signaling. However, immortalized mouse embryonic fibroblasts derived from these mice did display upregulation of Akt signaling, as does PHLPP1-null, PTEN +/- prostate tissue, which is more prone to developing prostate intraepithelial neoplasia than PTEN +/- tissue with intact PHLPP (31). Taken together, these data support the conclusion that PHLPP1 loss can be compensated for by other mechanisms in most physiological situations; upon the development of other genetic abnormalities, however, PHLPP1 signaling becomes essential for reining in tumorigenesis.

Materials and Methods

Generation and validation of PHLPP1-null mice – The targeted exon (exon 4) of PHLPP1 was subcloned in between two LoxP sites on the pFlox-FRT vector. A SacI restriction site was introduced into the targeting vector for detection of homologous recombination events by Southern blot analysis. For negative selection, sequences encoding diphtheria toxin (DT) were amplified using PCR and subcloned into the vector. The neomycin selection cassette (Neo) is flanked by two FRT sites, which allow deletion of the Neo gene via Flp-mediated recombination in mice. The targeting vector was electroporated into 129/Sv ES cells and the cells were subjected

to positive and negative selection on the basis of neomycin and DT sensitivity (Figure 2.1A). Genomic DNA was isolated from the ES cells and digested with SacI, and relevant products were detected by Southern blot using the probe as marked on the diagram. The wild type allele generates an 11-kb fragment whereas the targeted knockout allele gives a 7-kb fragment. ES cells with a recombinant allele were injected into C57BL/6 blastocysts and transplanted into pseudopregnant C57BL/6 mice to generate chimeric pups. PHLPP1 fl/+ chimeras were bred with Protamine-Cre mice (129 background; 129-Tg(Prm-cre)58Og/J; Jackson) to generate fl/+, Protamine-Cre/+ males (Figure 2.1B). Breeding of these mice to wild type mice resulted in recombination of the LoxP sites and deletion of exon 4 in the male gametes, yielding PHLPP1+/Δ mice. Excision of the Neo cassette was performed by breeding PHLPP1 Δ/Δ mice to mice expressing Flp recombinase (129S4/SvJaeSor-Gt(ROSA)26Sor$^{tm1(FLP1)Dym}$/J; Jackson), resulting in the generation of PHLPP1 +/- mice. Unless otherwise stated, mice were on a 129 background. For certain experiments, mice were backcrossed into the C57BL/6 background for four generations. Mice were housed in cages containing four or fewer animals and weighed weekly from weaning (at approximately three weeks of age) onwards. Blood chemistry phenotyping was performed on 6-week-old mice (four males and four females) by the Murine Hematology and Coagulation Core at the University of California, San Diego. All animal protocols used were approved by the Institutional Animal Care and Use Committee of the University of California, San Diego. Genotyping PCR was performed using the following primers: FP43 (forward primer): 5′-TAG GAG AGA CTA GTG ACA TC-3′, RP44 (reverse primer 1): 5′-TGA GCT TAT ACG CTG TGA TGC-3′, RP56 (reverse primer 2): 5′-AGC CGA TTG TCT GTT GTG C-3′, and RP64 (reverse primer 3): 5′- TCA AAG TGG GAA AGG AAG GA-3′ (Figure 2.1A). Primer pair FP43/RP44 generates a 264-bp product from the wild type allele and a 336-bp product from the floxed allele. Primer pair FP43/RP56 generates a 486-bp product from the deleted (Δ) allele, and primer pair FP43/RP64 generates a 524-bp product from the deleted (-) allele (Figure 2.1C).

Validation of PHLPP1 deletion by RT-PCR and Western blotting was performed as described below.

Materials and antibodies – Phorbol 12,13-dibutyrate (PdBu) and etoposide were purchased from Calbiochem and dissolved in dimethyl sulfoxide (DMSO). Epidermal growth factor (EGF) was purchased from Peprotech and dissolved in PBS. Antibodies to PHLPP1 and PHLPP2 were from Bethyl Laboratories. The following antibodies were purchased from Cell Signaling: phospho-antibodies for T308 (p308) and S473 (p473) of Akt, phospho-p44/42 MAPK (Thr202/Tyr204; pERK), phospho-c-Jun (Ser73), phospho-GSK-3 α/β (Ser21/9), phospho-pan PKC (p660), phospho-Ser PKC substrate, PKCζ, EGFR, insulin receptor (InsR), and total Akt antibodies. A total ERK antibody was purchased from BD; γ-tubulin and β-actin antibodies were from Sigma. The following antibodies were from Santa Cruz: PKCα (C-20), PKCβII (C-18), PKCδ (C-20), PKCε (C-15), and PDGFR-β (M-20). Primary antibodies used for immunofluorescence staining were from Dako (rabbit anti-GFAP and glucagon) and The Binding Site (sheep anti-insulin (1:300)); secondary antibodies were from Jackson Immunoresearch (rhodamine donkey anti-sheep and anti-rabbit). Electrophoresis reagents were obtained from Bio-Rad. All other materials and chemicals were reagent-grade.

RT-PCR analysis of PHLPP1 and 2 expression – For analysis of PHLPP1 and 2 mRNA levels at various circadian times, male C57BL/6 mice (Jackson) were sacrificed by CO_2 overdose followed by cervical dislocation at clock time 0 ("lights on") and clock time 12 ("lights off"); for validation of PHLPP1 deletion, male PHLPP1 +/+ and Δ/Δ mice were sacrificed at clock time 6. All tissues were snap-frozen in liquid nitrogen and homogenized using a rotor-stator homogenizer (Omnitech). RNA was isolated using a Qiagen RNEasy lipid tissue kit (for brain, white adipose tissue, and mammary gland) or a standard Qiagen RNEasy kit (for all other tissues). For PHLPP1 deletion validation, RT-PCR was performed using a Qiagen OneStep RT-PCR kit and the following primers: (forward) 5′-TCT GTC GAA ATG GGA AGC CAC TGT C-3′ and (reverse) 5′-TGT ACC ACC ACA GCA CTG ATG C-3′ (in exons 16 and 17, respectively). For quantification of

mRNA levels across the circadian day, the same PHLPP1 primers were used, along with the following PHLPP2 primers: (forward) 5′-ACG CAC ATG GAT TTG CGG GAC AAT C-3′ and (reverse) 5′-TCA CTT CTT TGG AGC TCT CCC AAA-3′. The hypoxanthine-guanine phosphoribosyltransferase (HPRT) gene was used as a loading control; primers were the following: (forward) 5′-TGA AGG AGA TGG GAG GCC ATC ACA-3′ and (reverse) 5′-TTT GGG GCT GTA CTG CTT AAC CA-3′. Quantitative RT-PCR was performed using a Taqman RT kit (Applied Biosystems cat. no. N808-0234), SYBR Green PCR Master Mix (Applied Biosystems cat. no. 4367659), and an Applied Biosystems 7500 Real-Time PCR System according to the manufacturer's instructions. PHLPP1 and PHLPP2 mRNA values were normalized to HPRT mRNA values.

Lysis and Western blotting – Snap-frozen tissue samples were homogenized in RIPA buffer (50 mM Tris, pH 7.4, 150 mM NaCl, 1% Triton, 30 mM $Na_4P_2O_7$, 0.5% sodium deoxycholate, 0.1 mM Na_3VO_4, 50 µg/mL leupeptin, 2 mM benzamidine, and 0.1 mM phenylmethanesulfonylfluoride) using a rotor-stator homogenizer (Omnitech) and then centrifuged for 15 min at 130,000 x *g* at 4 °C; the supernatants were subjected to Western blotting. Cells were lysed in RIPA buffer, and whole cell lysates were used for Western blotting. The protein concentrations of both cell and tissue lysates were measured using a BCA protein assay kit (Thermo). Equal amounts of protein were loaded onto 7.5% or 10% SDS-PAGE gels and blotted with the indicated antibodies.

High fat diet study – PHLPP1 +/+ and -/- mice were backcrossed into the C57BL6 background for four generations; male backcrossed mice were placed into the following four groups (n=9 per group): normal chow (NC) PHLPP1 +/+, NC PHLPP1 -/-, high fat diet (HFD) PHLPP1 +/+, and HFD PHLPP1 -/-. At weaning, littermates were genotyped and re-housed according to genotype (n=3 mice of the same genotype per cage). At 8 weeks of age, mice were weighed and placed on a high fat diet (Research Diets cat. no. D12492; 60 kcal% fat) or kept on a standard chow diet. For the following 6 weeks, mice and food were weighed weekly. At 14 weeks

of age (after 6 weeks on HFD), glucose tolerance tests were performed; insulin tolerance tests were performed at week 16. One week after the insulin tolerance tests, the *in vivo* insulin stimulation procedure was performed, and mice were euthanized.

Glucose tolerance tests (GTTs) – Mice were fasted for 6 hours, weighed, and injected with 1 g/kg glucose (i.p.). Blood was collected via cheek or tail bleeding at 30 min before injection, at the time of injection (0 min), and 5, 20, 40, 60, and 120 min after glucose injection. Blood glucose was tested using a glucometer (Bayer Ascensia Elite XL). For insulin testing, blood was allowed to clot for 10 min at room temperature (RT), centrifuged for 10 min at 2000 x *g* at 4 °C. The serum was taken and tested by insulin ELISA (Crystal Chem).

Insulin tolerance tests (ITTs) – Randomly fed mice were weighed and given insulin (0.5 U/mL i.p., Lilly). Blood was collected via cheek or tail bleeding at 30 min before injection, at the time of injection (0 min), and 10, 20, and 40 min after injection and was tested using a glucometer.

In vivo insulin stimulation – At approximately 17 weeks of age, mice were fasted for 6 hours, weighed, and deeply anesthetized with pentobarbital (Nembutal, Lundbeck, 100 mg/kg i.p.). The peritoneal cavity was opened and visceral white adipose tissue and quadriceps muscle removed from the left side of the body (unstimulated condition). Insulin (5 U/kg, Lilly) was then injected into the posterior vena cava; 5 min later, white adipose and muscle were taken from the right side of the body (insulin-stimulated condition). Tissue samples were snap frozen and prepared for Western blotting as described above.

Staining and characterization of pancreatic islets – Pancreases were isolated from male PHLPP1 +/+ (n=6) and Δ/Δ (n=5) mice, embedded in paraffin, sectioned, and stained with hematoxylin and eosin. Representative pictures were taken and islet sizes quantified by a blinded observer using ImageJ (NIH). At least 36 islets were scored per mouse. For immunofluorescence staining, pancreases were frozen in O.C.T. (VWR), sectioned into 10-μm slices, fixed in 2% paraformaldehyde for 5 min at RT, permeabilized in 0.1% Triton for 10 min at RT, blocked, and

stained with primary and secondary antibodies. Nuclei were stained with Hoescht (10 μg/mL, Invitrogen) for 20 min at RT before mounting. At least two islets from 6 PHLPP1 +/+ and three PHLPP1 Δ/Δ mice were scored (in a blinded fashion) for the number of insulin-positive and glucagon-positive cells and for total islet area.

Mouse embryonic fibroblast (MEF) isolation, immortalization, and culture – MEFs were isolated and immortalized as described in (32). Briefly, pregnant mice were sacrificed by cervical dislocation. The decidua containing individual embryos (12.5 dpc) was isolated, washed, and transferred into a small plate containing PBS. The Reichert's membrane was removed by separation with forceps from its junction with the placenta. Next, the yolk sac and amnion were removed, and the placenta was separated from the embryo. Head, liver and attached internal organs were discarded; as much blood as possible was removed by washing the carcasses at least two times in PBS in a 50 ml Falcon tube. Approximately 5 mL of standard culture medium (DMEM (Cellgro) with 10% fetal bovine serum (FBS, Hyclone) and 1% penicillin/streptomycin) was added to the tube containing the embryos, and bodies were homogenized by passing them through a 21-gauge needle twice using a 5 ml syringe. This primary culture was considered passage 0 and was cultured until confluence was reached (typically three to 7 days). Thereafter, cells were harvested by trypsinization using three mL of trypsin-EDTA (Invitrogen) per 15 cm plate; trypsinization was stopped by the addition of 14 mL of medium. Cells were resuspended and the suspension was incubated in a 50 mL Falcon tube for 10 min. The top 15 mL, which contained primarily single cells, was then transferred to a fresh tube (sedimented clumps were discarded), pelleted (5 min, 1500 rpm), and split to four 15 cm plates. Cells were immortalized using the 3T3 protocol, which involves seeding 3 X 10^5 cells every three days.

PHLPP1 Δ/Δ MEFs were stably infected with HA-tagged human PHLPP1β (33) using retroviral infection. 293T cells were transiently transfected with the puromycin resistance construct pBABE or pBABE-HA-PHLPP1β and the packaging plasmid pCL10A. Conditioned medium from the transfected 293T cells was used to infect the PHLPP1 Δ/Δ MEFs as follows.

The day before infection, the MEFs were split to be 40-50% confluent. Conditioned medium from the 293T cells containing packaged plasmids (viral soup) was collected 12 h, 24 h, and 36 h after transfection. The viral soup was filtered using a 0.45 μm filter and used to infect the PHLPP1 Δ/Δ MEFs. After selection, individual clones stably expressing PHLPP1β were chosen and used for further experiments.

All cells were cultured in standard culture medium. Experiments in primary MEFs were performed at a passage number of 5 or fewer. For EGF stimulation, cells were serum-starved for four hours and then treated with EGF (10 ng/mL) for two to 60 min. Cells were then lysed and subjected to Western blotting as described above.

Primary astrocyte isolation and culture – PHLPP1 +/+ and Δ/Δ astrocytes were isolated as described in (27). Adherent astrocytes were then washed twice with PBS, trypsinized, and plated at approximately 3 X 10^5 cells per mL in DMEM with 10% FBS and P/S on lysine-coated six-well dishes. All astrocyte preparations that were subjected to wound healing analysis had at least 80% GFAP-positive cells by immunofluorescence, and experiments were performed on cells derived from three different preparations.

Apoptosis assay – Cells cultured under normal (MEFs) or 0.1% (astrocytes) serum conditions were treated for 24 hours with etoposide (50 μM) or DMSO and subjected to propidium iodine staining and fluorescence-assisted cell sorting as described in (34). The percentage of cells undergoing apoptosis (i.e., with sub-2n DNA content) was determined in triplicate for each of three separate experiments.

Proliferation assay – Astrocytes were plated at 12,500 per mL in 12-well plates in duplicate, and one set of duplicates was fixed in 4% formaldehyde at days 1-5 following the split. When all cells had been harvested, the samples and a standard curve consisting of wells with known numbers of cells were washed twice with ddH_2O and stained with 0.1% crystal violet for 30 min. Following staining, cells were washed 5 times with ddH_2O and lysed in 10% acetic acid. The

absorbance at 590 nm was then measured. At least three experiments were performed in duplicate.

Wound healing assay – Primary murine astrocytes were plated on lysine-coated six-well dishes at consistent cell densities. Approximately 48 h after plating, confluent monolayers were treated with mitomycin C (10 μg/mL in PBS, Calbiochem) in serum-free DMEM for one hour to inhibit cell proliferation and then washed twice with PBS. Fresh DMEM was added to the cells, and monolayers were scratched once with a 10-μL pipet tip. Pictures of the central region of the scratch were taken immediately and at various time points after scratch with a 5X objective lens. During the assay, cells were maintained at 37 °C/5% CO2. The wound area at the various time points was quantified using ImageJ.

Results

PHLPP1 and 2 are expressed ubiquitously in murine tissues – To determine where the PHLPP isozymes are expressed, we isolated tissues from male C57BL/6 mice and examined the mRNA levels of PHLPP1 and 2 by quantitative RT-PCR (Figure 2.1). Because PHLPP1 levels oscillate in a circadian fashion in the murine suprachiasmatic nucleus (14), we sampled the mice at two different circadian time points, clock time 0 (corresponding to lights on) and clock time 12 (lights off). This analysis revealed that the PHLPP isozymes are expressed at detectable levels in all tissues sampled, though there is a wide range of expression levels; for example, PHLPP1 and 2 levels are high in brain and lung but very low in liver. Also, PHLPP1 levels vary according to circadian time in many tissues, including kidney and lung, and tend to be lower at clock time 12 than at clock time 0. This pattern is consistent with that displayed in the suprachiasmatic nucleus (14), though the determinants of expression may differ. PHLPP2 levels also vary across the circadian day in the spleen, lung, and white adipose tissue (WAT), but in general these changes are less dramatic than those displayed by PHLPP1.

PHLPP1-null mice lack obvious biochemical changes in brain, WAT, or heart – Mice lacking the gene for PHLPP1 were generated using a Cre-LoxP system, in which LoxP sites were

inserted around the fourth exon of PHLPP1 (Figure 2.2A). The targeting vector also included a neomycin resistance cassette to allow embryonic stem cell selection. Embryonic stem cells expressing the correctly targeted floxed (fl) allele were identified by Southern blotting (Figure 2.1B), and the resulting chimeric mice and their offspring were genotyped using PCR with primers 43 and 44 (see Figure 2.1A). Fl/+ mice were bred to Protamine-Cre mice to generate fl/+, Cre/+ mice. Males of this genotype express Cre recombinase in their spermatids, allowing for hemizygous recombination of the LoxP sites in the gametes and the generation of offspring expressing one copy of the deleted (Δ) allele. (For convenience, the deleted allele containing the neomycin resistance cassette will be referred to as the "Δ" allele, and that in which the neo cassette has been excised by breeding to mice expressing Flp recombinase will be referred to as the "-" allele. No obvious differences were observed between PHLPP1 Δ/Δ and PHLPP1 -/- mice (data not shown).) The presence of the deleted alleles was confirmed by genotyping PCR (Figure 2.2C, data not shown), and the absence of PHLPP1 mRNA and protein was confirmed by RT-PCR (Figure 2.2D) and Western blotting (Figure 2.2E), respectively. PHLPP1 -/- and Δ/Δ mice were born at the expected Mendelian ratios and were grossly normal in appearance (data not shown).

Examination of the levels and phosphorylation states of various proteins in tissues from PHLPP1-null mice revealed a high degree of variability but no consistent changes. Figure 2.3 shows results from a representative experiment sampling the brain, heart, and WAT of 6-week-old male PHLPP1 -/- mice and their wild type littermates. Given that PHLPP1 dephosphorylates Akt and PKC, leading to decreased phosphorylation of Akt at serine 473 and decreased PKC stability, I expected to see increases in phospho-serine 473 (p473) and the levels of conventional and novel PKC isozymes. (PKCζ, an atypical PKC, was included for comparison; it lacks a phospho-acceptor at the hydrophobic motif and thus is not regulated by PHLPP (2).) There is some evidence that PHLPP negatively regulates the levels of various growth factor receptors and thus ERK signaling in immortalized cells (M. Niederst, G. Reyes-Cava, M.T. Kunkel, J. Brognard,

J. Enserink, and A.C. Newton, manuscript in preparation; see Figure 2.7E); therefore, I also examined the levels of the epidermal growth factor receptor (EGFR), the plasma-derived growth factor receptor (PDGFR), and the insulin receptor (IR), as well as phospho-ERK (pERK). With the exception of EGFR in brain, none of these parameters were increased in the PHLPP1-null tissues; in fact, phosphorylation of serine 473 of Akt, a direct target of PHLPP, was slightly decreased in WAT and heart (Figure 2.3B).

PHLPP1-null mice are slightly smaller than their wild type littermates – Both male and female PHLPP1-null mice were approximately 9% smaller than their wild type littermates at weaning, and this difference persisted through adulthood (Figure 2.4A). This change appeared to result from a global defect in growth rather than a change in body composition, because the femur length of the PHLPP1-null mice is also slightly less than that of wild type controls (N.H. Purcell and J.H. Brown, unpublished observations). Interestingly, female PHLPP1 heterozygotes were also smaller than their wild type counterparts, while male PHLPP1 heterozygotes tended to resemble wild type mice. No dramatic hypertrophic changes were observed in PHLPP1-null tissues (data not shown). Blood chemistry profiling revealed no dramatic changes in the PHLPP1-null mice, though total bilirubin and triglyceride levels were slightly elevated (Figure 2.4B, C, and D).

PHLPP1-null and wild type mice develop similar phenotypes when placed on a high fat diet – Because deletion of PHLPP1 is expected to increase Akt2 phosphorylation, which is important for insulin signaling in fat, muscle, and liver, I hypothesized that PHLPP1-null mice would display increased insulin sensitivity, leading to increased glucose tolerance. However, glucose and insulin tolerance tests performed on mice fed normal chow showed no overall differences between PHLPP1-null mice and their wild type littermates (data not shown). To uncover possible differences in insulin sensitivity, I decided to subject mice to an intervention that would cause them to develop insulin resistance and determine whether PHLPP1 deletion interferes with this process. High fat diet feeding results in rapid weight gain and failure to

efficiently clear glucose in C57BL/6 mice (35); therefore, I backcrossed PHLPP1 +/- mice onto the C57BL/6 background for four generations before crossing them to yield PHLPP1 -/- and +/+ littermates. Nine male mice of each genotype were placed on a high fat (HFD) or normal chow (NC) diet at 8 weeks of age, and those on a high fat diet rapidly gained weight compared to the NC-fed mice (Figure 2.5A; note that values are plotted relative to each mouse's weight at week 8 and do not reflect basal differences between PHLPP1 +/+ and -/- mice). Curiously, PHLPP1-null mice gained more weight on HFD than their wild type littermates despite consuming the same amount of food (Figure 2.5B). Glucose tolerance tests performed after 8 weeks on HFD revealed an inability to efficiently clear glucose, consistent with the expected defect in insulin signaling; however, there were no significant differences between PHLPP1-null and wild type mice (Figure 2.5C). Insulin tolerance tests also showed elevated basal glucose levels and slightly impaired glucose clearance in response to insulin in HFD-fed mice; in this experiment, there was a slight decrease in the ability of the HFD-fed PHLPP1-null mice to clear glucose relative to their wild type counterparts (Figure 2.5D). Overall, these data conclusively show that there is no increase in insulin sensitivity in the PHLPP1-null mice; put another way, deletion of PHLPP1 does not appear to protect mice from the effects of HFD. Studies involving *in vivo* insulin stimulation revealed that in white adipose tissue (WAT; Figure 2.5E and G) and skeletal muscle (Figure 2.5F and H), HFD feeding resulted in a loss of Akt activation (read out by serine 473 phosphorylation) in the wild type mice. The PHLPP1-null mice, however, were deficient in Akt activation in WAT in the NC- and HFD-fed conditions but displayed unimpaired Akt activation in skeletal muscle under both conditions.

The pancreatic islets of PHLPP1-null mice resemble those of wild type mice – Based on an initial observation that pancreatic islets from PHLPP1-null mice were smaller and abnormal in histological appearance compared to those of wild type mice (Figure 2.6A), I evaluated the size of numerous pancreatic islets comprehensively and in a blinded fashion. Neither the average islet size nor the size distribution was significantly altered in PHLPP1-null mouse pancreases (Figure

2.6B and C). I also stained the islets of PHLPP1-null and wild type mice with antibodies to insulin and glucagon to analyze the number and organization of insulin-producing β cells and glucagon-producing α cells (Figure 2.6D). PHLPP1-null islets were indistinguishable from wild type and displayed a normal islet structure, with a layer of glucagon-producing cells surrounding a core of insulin-producing cells. Co-staining with Hoescht (Figure 2.6D, right panels) enabled me to quantify the numbers of glucagon- and insulin-producing cells and the cell size (calculated as the total number of cells divided by the islet area); neither of these parameters was altered in the PHLPP1-null islets (Figure 2.6E and F).

Primary and immortalized cells lacking PHLPP1 display differences in their biochemical profiles and resistance to apoptosis – As previously discussed, cell lines depleted of PHLPP1 and/or 2 have increased levels of PKC isozymes, growth factor receptors, and signaling through ERK ((2); M. Niederst, G. Reyes-Cava, M.T. Kunkel, J. Brognard, J. Enserink, and A.C. Newton, manuscript in preparation) as well as increases in Akt phosphorylation under both basal (10% serum) and growth-factor stimulated conditions (1). Therefore, I determined whether mouse embryonic fibroblasts (MEFs) isolated from PHLPP1-null mice also displayed these changes. Primary (passage number ≤ 5) PHLPP1 Δ/Δ MEFs cultured in 10% serum or that were serum-starved for four hours and stimulated with EGF, as shown in Figure 2.7A, had no significant changes in Akt or ERK phosphorylation compared to PHLPP1 +/+ MEFs. Similar results were observed with insulin and PDGF stimulation (data not shown). Notably, though there was a slight upregulation of PHLPP2 protein levels in PHLPP1-null MEFs, the levels of several PKC isozymes and EGFR remained unaffected (Figure 2.7B). Finally, PHLPP1 deletion yielded only slight protection against basal and etoposide-induced apoptosis in these primary cells (Figure 2.7C). However, PHLPP1 Δ/Δ MEFs that had undergone the 3T3 immortalization process displayed a dramatic alteration in phenotype: they displayed increased Akt and ERK phosphorylation in response to EGF, consistent with a substantial increase in the levels of the EGFR, as well as increased levels of PKCα and βII (Figure 2.7D and E). These cells were also extremely resistant

to basal and etoposide-induced apoptosis; puzzlingly, however, stable overexpression of human PHLPP1β did not reverse this phenotype (Figure 2.7F). Taken together, these experiments indicate that immortalized MEFs lacking PHLPP1 much more strongly resemble the PHLPP1-depleted cancer cell lines previously studied by our lab and others (1,2,6) than do primary MEFs lacking PHLPP1.

Primary astrocytes lacking PHLPP1 display increased PKC signaling and decreased apoptosis – Given PHLPP1's known tumor suppressor role in GBM (3,7,26,33), I decided to examine the effects of PHLPP1 deletion in primary astrocytes, the precursor cells for GBM. PHLPP1 is expressed at the mRNA levels in all three glial cell types, with the highest level of expression in astrocytes (data not shown). Primary astrocytes isolated from PHLPP1-null mice, though their growth factor signaling was unchanged (data not shown), displayed increases in PKC signaling and phosphorylation but not PKC levels (Figure 2.8A-D; data not shown). Further characterization of these cells revealed unchanged cellular migration (in a wound healing assay) and proliferation (Figure 2.8E and F); PHLPP1-null astrocytes did display decreases in apoptosis under low serum conditions, however (Figure 2.8G).

Discussion

Contrary to my expectations, mice lacking PHLPP1 showed few if any dramatic biochemical or physiological changes when maintained under normal conditions. Similarly, primary cells from these mice lacked obvious changes in Akt signaling, though PHLPP1-null astrocytes displayed increased PKC signaling. However, these mice were not completely without phenotypes: studies performed by our collaborators (described below) revealed effects of PHLPP1 ablation that only became apparent upon genetic or physiological perturbations. Also, immortalized MEFs from these mice displayed the expected dramatic changes in Akt, PKC, and ERK activation, suggesting that additional genetic events might be required for these cells to display these changes.

Profiling of PHLPP1 and 2 mRNA levels in various mouse tissues revealed ubiquitous expression in all tissues examined. PHLPP1 and 2 levels were high in brain, consistent with a report showing abundant PHLPP1 and 2 expression in the mouse cerebellum, frontal cortex, and hippocampus (15), and consistent with the previously characterized effects of PHLPP1 in learning and memory (16), GBM (3,7), and Huntington's disease (36). Circadian profiling of PHLPP expression showed that PHLPP1 and 2 levels cycle in certain tissues (Figure 2.1); this may indicate a role for the PHLPPs in the maintenance of peripheral clocks. However, it should be noted that up to 10% of the transcriptome may oscillate in a circadian fashion, and the genes that cycle often differ from tissue to tissue, making it hard to pin down a general role for any circadian oscillatory transcript (37,38).

A surprising result is that PHLPP1 deletion does not cause consistent upregulation of Akt phosphorylation at serine 473 in any tissue I examined, notably brain, heart, and WAT (Figure 2.3). This effect cannot be explained by PHLPP1's preference for Akt2, because Akt2 is the most highly expressed Akt isozyme in WAT and heart (10), the very tissues in which PHLPP1 deletion actually decreases Akt phosphorylation slightly. PHLPP1 deletion also left the levels of various growth factor receptors and PKC isozymes unaffected, which contrasts sharply with the effects of deleting or depleting PHLPP1 in transformed cells. It is possible that the loss of PHLPP1 could be compensated for by upregulation of PHLPP2 activity; such upregulation would have to be at a post-translational level, because the levels of PHLPP2 do not increase in PHLPP1-null tissues (Figure 2.3, data not shown).

I expected that PHLPP1 deletion might cause increased growth and/or hypertrophy of certain organs, but, contrary to my expectations, the PHLPP1 mice were actually slightly smaller than their littermate controls (Figure 2.4A). Interestingly, there were gender-based differences in the size of the PHLPP1 heterozygotes, with the females resembling PHLPP1 knockouts and the males resembling wild type controls. This result suggests that PHLPP1 deletion may interact with gender-specific signaling, and it has been shown that the androgen-regulated gene product

FKBP5 regulates PHLPP1 expression and scaffolding to Akt (39-41). It is possible, therefore, that under low androgen conditions in female mice, PHLPP1 is not maximally expressed or maximally bound to Akt and thus is haploinsufficient with respect to growth effects (though why deletion of a negative regulator of Akt *reduces* growth is still a mystery). Though I did not systematically examine the size of PHLPP1-null organs, preliminary histopathological characterization of various tissues from PHLPP +/+ and Δ/Δ revealed no evidence of hypertrophy (data not shown). In the pancreatic islets, where preliminary results suggested that PHLPP1 deletion might lead to abnormalities (Figure 2.6A), rigorous examination revealed that there was no effect of PHLPP1 deletion on islet or cell size or morphology (Figure 2.6B-F), though Akt signaling is known to be required for promoting islet growth, and PTEN deletion results in dramatic islet hypertrophy (21,42,43).

Another expected effect of PHLPP1 deletion/Akt upregulation is increased insulin sensitivity. However, neither chow-fed mice nor mice on a high fat diet displayed increased insulin sensitivity or glucose tolerance when PHLPP1 was deleted (Figure 2.5C-D). These results may be partially explained by what appear to be opposing effects of PHLPP1 in WAT and skeletal muscle: Akt activation in response to insulin is lower in the WAT of PHLPP1-null mice fed a normal diet but higher in PHLPP1-null skeletal muscle under HFD conditions compared to controls (Figure2.5E-H). Thus, PHLPP1 deletion in both of these tissues may balance out to explain the lack of phenotype in the whole mouse.

The discrepancies between the primary and immortalized PHLPP1-null MEFs are puzzling: the former display little phenotype beyond a slight decrease in apoptosis (Figure 2.7A-C), while the latter display the expected increases in growth factor signaling and PKC levels (Figure 2.7D-E). This suggests that additional alterations acquired during the 3T3 immortalization process may be required for PHLPP1-null cells to develop these characteristics, a conclusion supported by experiments showing that re-expression of PHLPP1β in PHLPP1-null cells does not rescue their resistance to apoptosis (Figure 2.7F). Such alterations may inactivate redundant

pathways restraining growth factor receptor and PKC expression. Though 3T3 immortalization is obviously a poor model for cancer progression, insights from the oncogenesis field may apply here. The idea that genetic “hits” in multiple pathways are required for transformation and oncogenesis is not new, and it is now thought that non-hereditary cancers require four or more distinct mutation events to progress to full-blown tumors (44). However, in the current context, it is difficult to predict what such mutations might be: primary fibroblasts can escape the crisis phase of the immortalization process by up- or downregulating a number of genes, which vary from clone to clone and do not appear to fall into any one category (45,46). Also, immortalized mouse cells are frequently heteroploid (47), which complicates the analysis of upregulated genes enormously.

Certain clues to the possible changes in PHLPP1-null MEFs are provided by studies by our collaborators showing that primary PHLPP1-null MEFs proliferate more slowly than wild type MEFs and have increased levels of p53. When p53 is depleted by shRNA, these cells can escape senescence and arrest and grow much faster than the controls. Similar effects were observed *in vivo*: at four months of age, PHLPP1 -/-, PTEN +/- prostates include senescent areas that are negative for Akt phosphorylation at serine 473 and for the proliferation marker Ki67, consistent with PHLPP1 deletion resulting in a senescence response. However, by 8 months of age, the PHLPP1 -/-, PTEN +/- prostates have developed mutations in p53 and display dramatically upregulated Akt phosphorylation (31). These data support a model in which 1) p53 upregulation suppresses proliferation and increased Akt signaling in primary PHLPP1-null MEFs and 2) once p53 is lost or mutated, PHLPP1-null MEFs display unrestrained Akt signaling and proliferation.

This report, in which PHLPP1-/- and PHLPP1-/-, PTEN+/- were examined with respect to a prostate cancer phenotype, highlights a common theme in the PHLPP1 knockouts: an extra perturbation, whether genetic or environmental, appears to be required for the PHLPP1-null mice to exhibit a dramatic phenotype. For example, the circadian rhythms of PHLPP1 knockouts appear normal under standard light/dark conditions and even in complete darkness (i.e., under

free-running conditions). However, when given a short or long light pulse to reset the circadian clock, PHLPP1-null mice display a drastically impaired ability to stabilize their circadian period (48). Studies by Patterson and colleagues in regulatory T cells (Tregs) illustrate a linked concept, namely that PHLPP1 loss may have consequences only in cells where extremely tight control of Akt signaling is required. Tregs, which act to suppress the immune response, have a reduced capacity to downregulate Akt, and low Akt activation in response to T cell receptor stimulation is necessary for their development and function. This repression of Akt appears to rely on a high level of PHLPP1 and 2 expression relative to conventional T cells, and deletion of PHLPP1 results in impairment of Treg development and their ability to suppress the proliferation of conventional T cells. However, the effects of this improperly restrained immune system are not observed in the intact mice until they are subjected to another experimental perturbation, namely the i.p. injection of excess conventional T cells, which causes colitis. In this case, PHLPP1-null Tregs were less able to block the colitis phenotype (49). Finally, returning to the prostate cancer study, it was observed that while only 25% of PHLPP1 knockout mice developed high-grade prostate intraepithelial neoplasia by 18 months of age, additional deletion of one allele of PTEN resulted in complete penetrance of this phenotype by 12 months of age. This resulted in a dramatic shortening of lifespan in PTEN +/-, PHLPP1 -/- mice relative to those lacking PHLPP1 alone (31).

Overall, the data presented here support the idea that PHLPP1 supplies a layer of suppression of the PI3K/Akt and PKC pathways but that suppression is inessential in most cases, because loss of PHLPP1 expression can be compensated for by other mechanisms. However, in certain cells (e.g., Tregs, prostate epithelial cells) or under certain stresses, PHLPP1 expression may be required for efficient signal termination. The mechanisms that compensate for PHLPP1 loss are unclear and probably vary based on cell type. PHLPP2 protein levels are increased in PHLPP1-null MEFs and prostate tissue in a manner that seems to depend on mTOR signaling

(Figure 2.7, (31)), but not in tissues such as brain, WAT, and heart (Figure 2.3). It is likely, therefore, that other alterations can compensate for PHLPP1 loss in these tissues.

Acknowledgments

I thank Dr. Tianyan Gao (University of Kentucky) and the UCSD Transgenic Core for producing the PHLPP1 fl/+ chimeras, Dr. David Ditto in the Murine Hematology and Coagulation Lab at UCSD for performing the blood chemistry analyses, Dr. Gloria Reyes for isolating and immortalizing the mouse embryonic fibroblasts and stably infecting them with PHLPP1β, and Drs. Nicole Purcell and Joan Heller Brown for determining the femur length of the PHLPP1 Δ/Δ mice. A version of Figure 2.2 was originally included in Masubuchi, S., Gao, T., O'Neill, A., Eckel-Mahan, K., Newton, A. C., and Sassone-Corsi, P. (2010) Proc Natl Acad Sci U S A 107, 1642-1647, as Figure 1. I was a secondary author who contributed to Figure 1 of this paper.

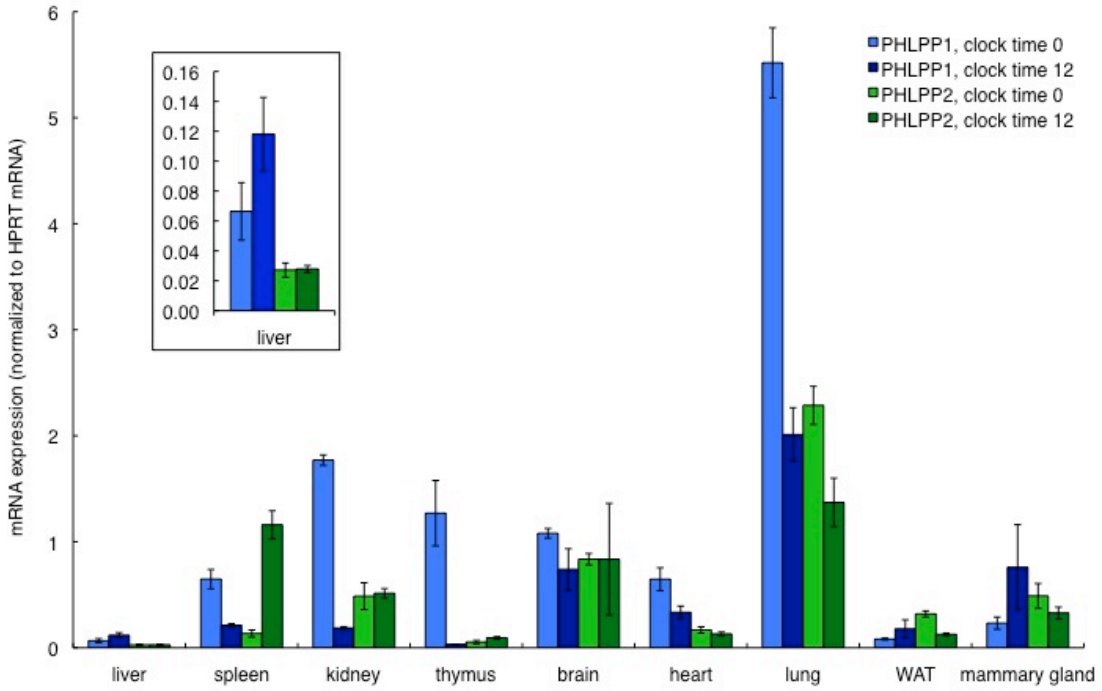

Figure 2.1: Expression of PHLPP1 and 2 mRNA in various mouse tissues.
Light blue and light green bars represent relative PHLPP1 and 2 expression at clock time 0 (lights on); darker bars represent expression at clock time 12 (lights off). Inset: expansion of liver mRNA expression graph. WAT, white adipose tissue.

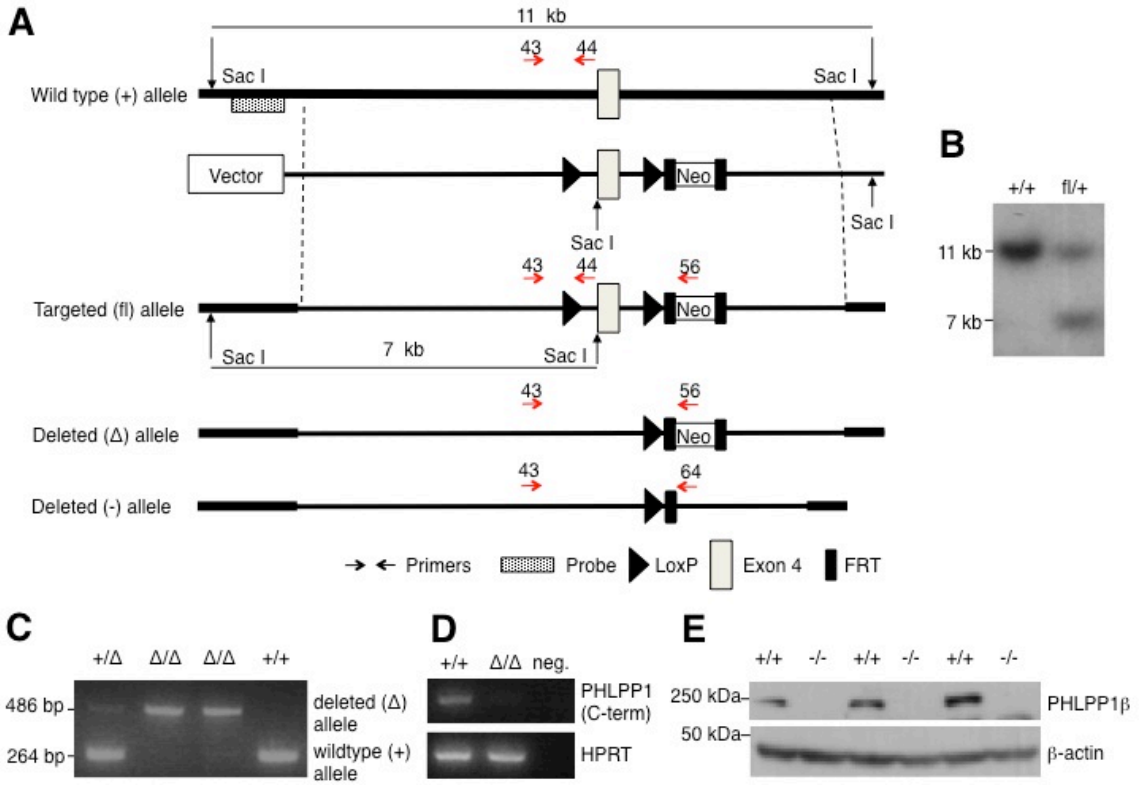

Figure 2.2: Generation of PHLPP1-null mice.
A. Targeting strategy used to disrupt the PHLPP1 gene. Shown are the wild type allele, the targeting vector, the targeted (floxed) allele, the deleted allele (Δ) generated by Cre-mediated recombination of the floxed (fl) allele, and the deleted (-) allele after excision of the neo cassette. The DNA probe used for screening the Southern blots is marked by a dotted box, and the PCR primers used for genotyping are indicated by small red arrows. B. Southern blot analysis of Sac I-digested DNA from embryonic stem cells used to generate chimeric mice. The probe labels an 11 kb fragment in the wild type cells and a 7 kb fragment in cells in which homologous recombination has occurred. C. Genotyping results from PHLPP1 +/Δ X +/Δ crosses. PHLPP1 fl/+ chimeras were bred with Protamine-Cre mice to generate fl/+, Protamine-Cre/+ males. Breeding of these mice to wild type mice resulted in recombination of the LoxP sites and deletion of exon 4 in the male gametes, yielding PHLPP1 +/Δ mice. D. RT-PCR for PHLPP1 transcript from RNA isolated from the brains of PHLPP1 +/+ and Δ/Δ mice. Forward and reverse primers were located in exons 16 and 17 respectively. Hypoxanthine phosphoribosyltransferase 1 (HPRT) primers were used in a control reaction, and the negative control ("neg.") represents a lane with no cDNA template. E. Western blot for PHLPP1 protein in brain lysates derived from PHLPP1 +/+ and -/- mice. β-actin serves as a loading control.

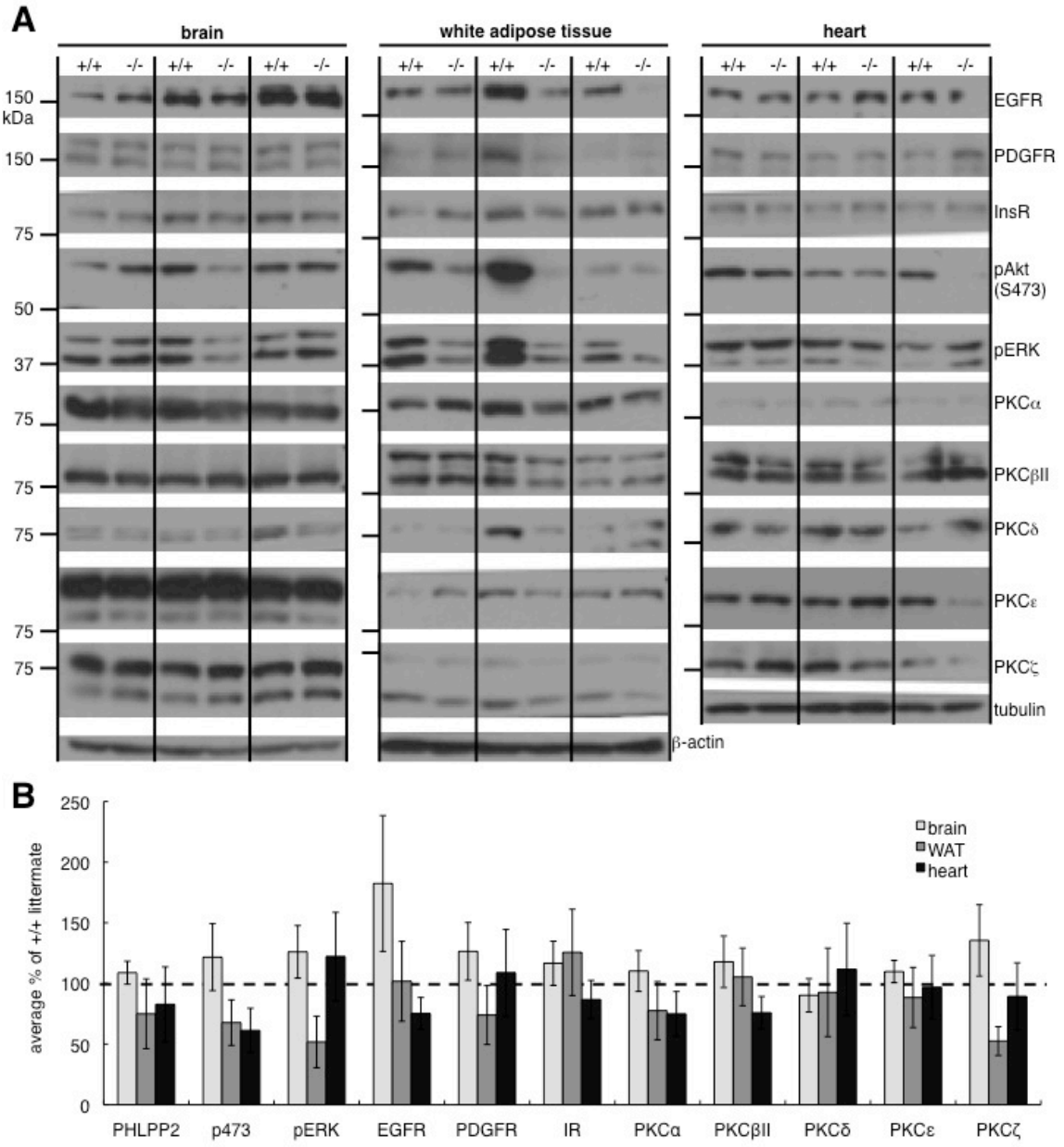

Figure 2.3: Expression and phosphorylation of various signaling factors in PHLPP1-null mouse tissues.

A. Representative Western blots depicting the expression of several growth factor receptors and PKC isozymes and the phosphorylation of Akt and ERK in brain, white adipose tissue (WAT), and heart samples from male 6 week-old PHLPP1-null 129 mice and wild type littermates. β-actin was used as a loading control for the brain and white adipose tissue samples, and γ-tubulin was used as a loading control for the heart samples. B. Quantification of protein expression and phosphorylation in 5-11 PHLPP1-null mice compared to their wild type littermates. Expression was normalized to β-actin (for brain and WAT) or γ-tubulin (for heart samples) and plotted relative to the corresponding expression level in the wild type controls (set as 100% and marked by dashed line).

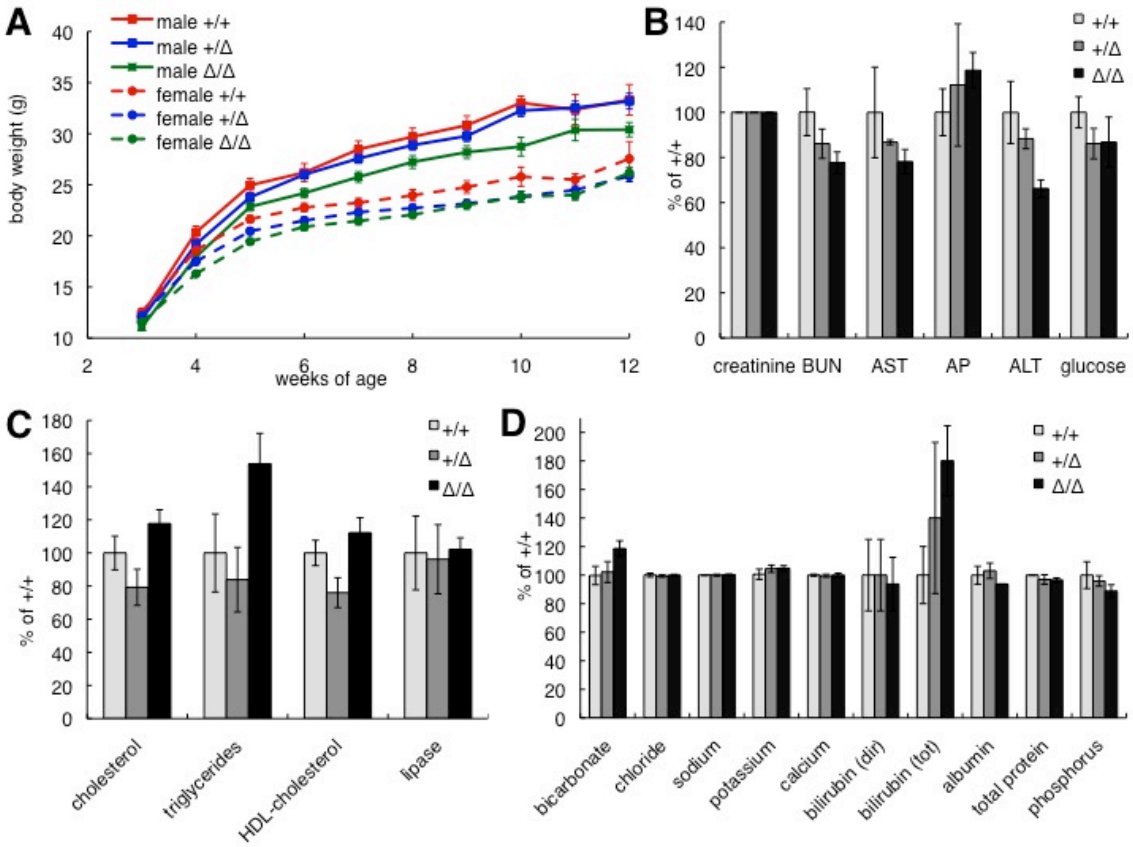

Figure 2.4: Body weights and blood parameters of PHLPP1-null and heterozygous mice.
A. Weights of male and female PHLPP1 +/+, +/Δ, and Δ/Δ mice from weaning to twelve weeks of age. At least 9 mice of each genotype and sex were weighed per week. B, C, and D. Levels of various factors in the blood of male 16-24-week-old mice (fed *ad libitum*).

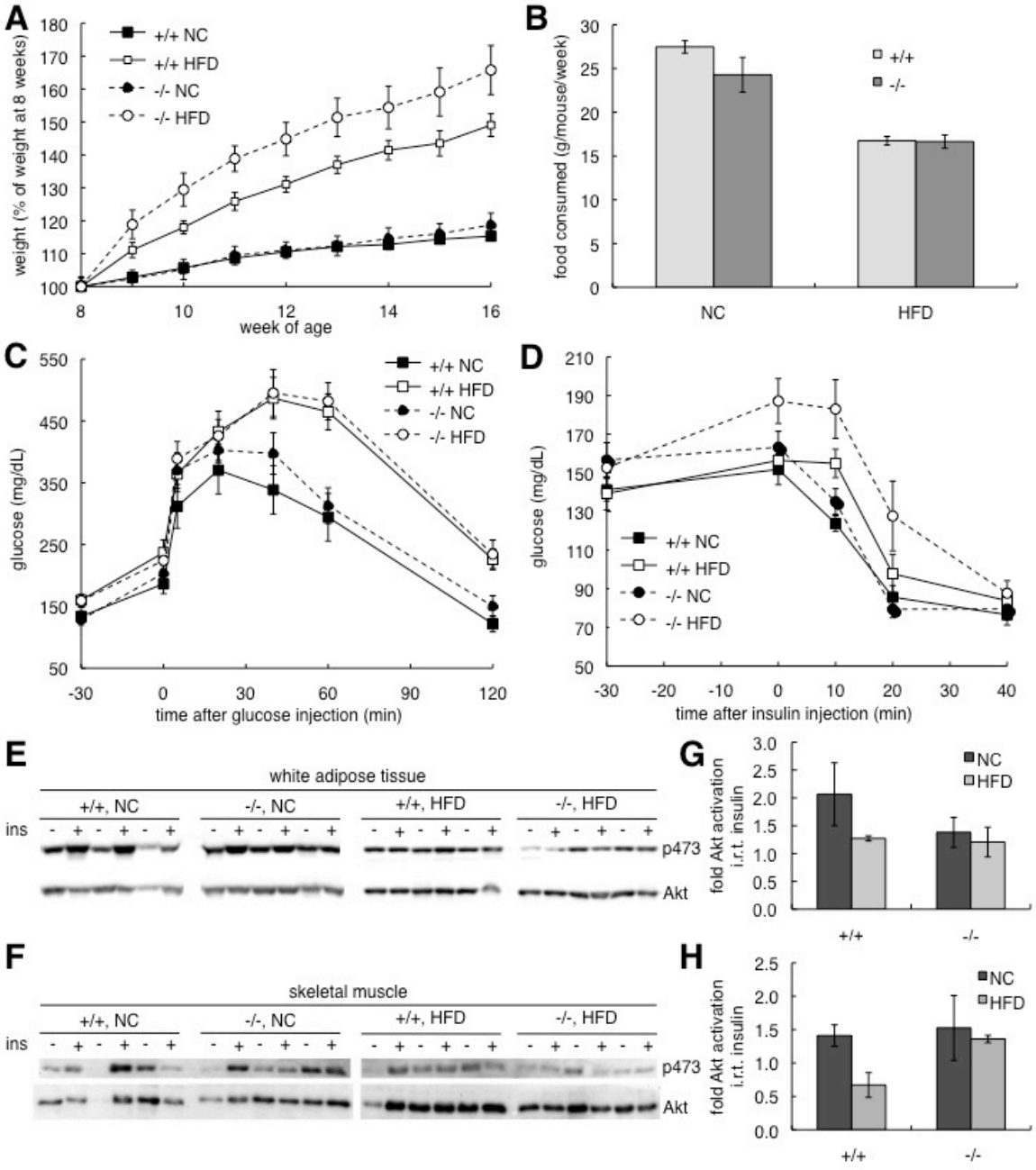

Figure 2.5: Responses of PHLPP-null mice and their wild type littermates to a high fat diet.
A. Body weights of PHLPP1-null (-/-) or wild type (+/+) C57BL/6 mice fed normal chow (NC) or a high fat diet (HFD) starting at week 8, plotted relative to each mouse's starting weight. B. Food consumption by PHLPP1 +/+ and -/- mice on NC or HFD, averaged across the course of the study (weeks 8-16). C and D. Intraperitoneal glucose tolerance tests (C) and insulin tolerance tests (D) performed in PHLPP1 +/+ and -/- mice on NC or HFD at week 16 (after 8 weeks on a HFD). E and F. Western blots depicting changes in Akt phosphorylation at serine 473 in response to *in vivo* insulin stimulation in the white adipose tissue (E) and skeletal muscle (F) of PHLPP1 +/+ and -/- mice on NC or HFD (n=3 mice per group). Insulin stimulation was performed and tissue extracted after 9 weeks on HFD. G and H. Quantification of Akt phosphorylation derived from the data in E (G, white adipose tissue) and F (H, skeletal muscle).

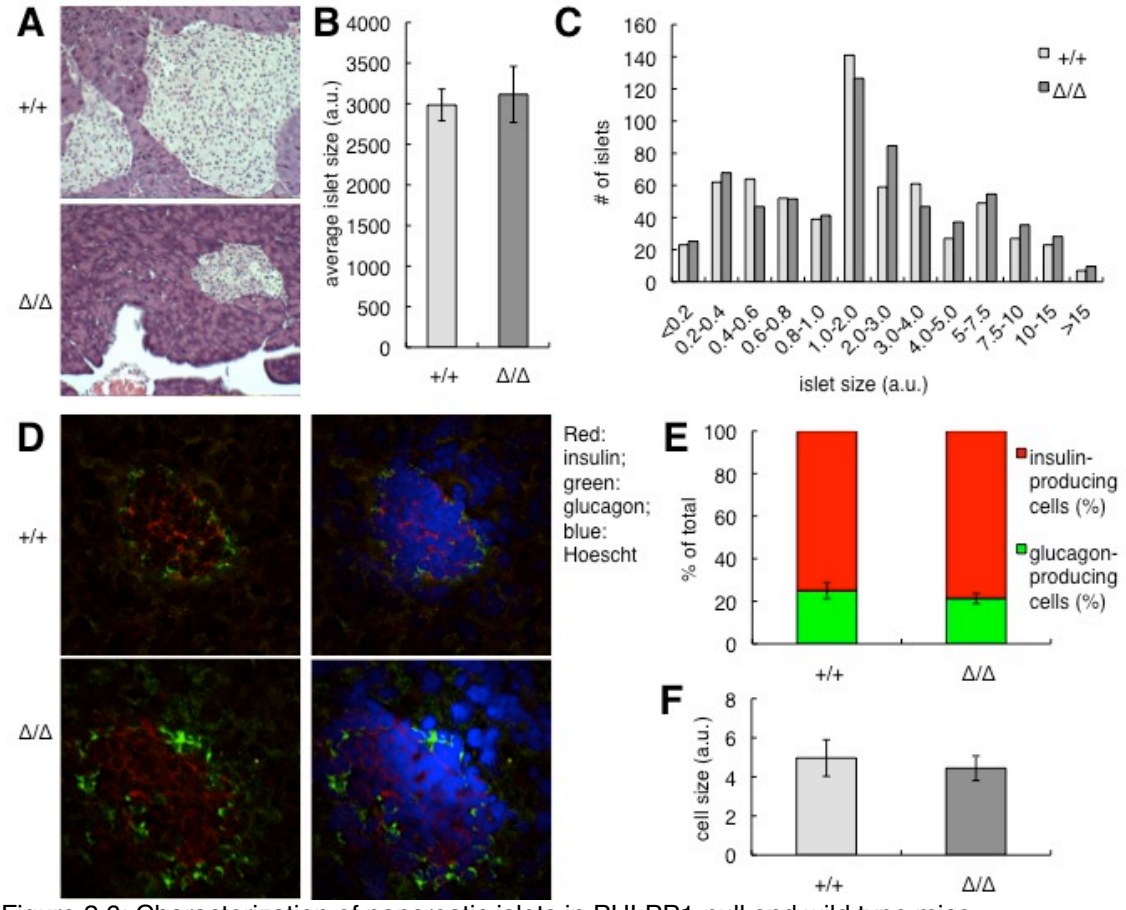

Figure 2.6: Characterization of pancreatic islets in PHLPP1-null and wild type mice.
A. Representative hematoxylin and eosin-stained pancreatic sections from PHLPP1 +/+ and Δ/Δ mice. B and C. Quantification of the average islet size (B) and islet size distribution (C) in three pancreatic sections from each of 6 wild type and 5 PHLPP1-null mice. D. Insulin (red) and glucagon (green) staining of pancreatic islets from wild type and PHLPP1-null mice (images on left) combined with Hoescht (blue) staining to show cell number and size (images on right). E and F. Distribution of insulin- and glucagon-producing cells (E) and average cell size (F) across two pancreatic sections from each of 6 wild type and three PHLPP1-null mice.

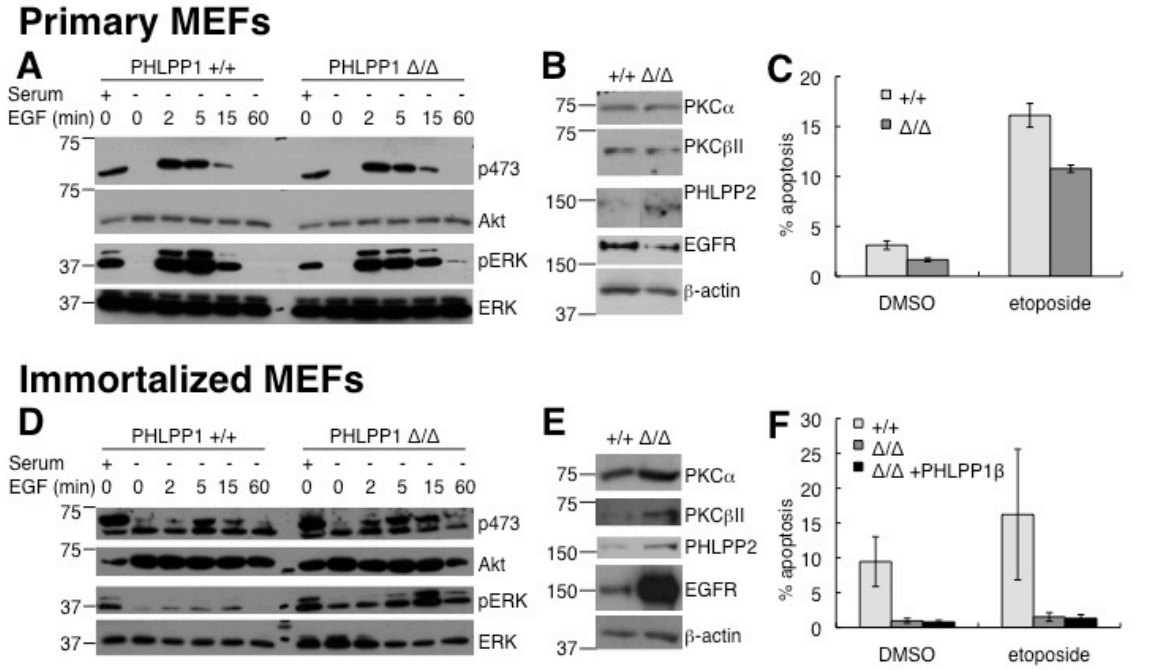

Figure 2.7: Characterization of biochemical changes and apoptosis in primary and immortalized mouse embryonic fibroblasts (MEFs) lacking PHLPP1.
A and D. Representative Western blots depicting Akt (serine 473) and ERK phosphorylation in response to EGF stimulation in primary (A) and immortalized (D) MEFs wild type for (+/+) or lacking (Δ/Δ) PHLPP1. B and E. Levels of PKC isozymes, growth factor receptors, and PHLPP2 under normal serum conditions in primary (B) and immortalized (E) PHLPP1 +/+ and Δ/Δ MEFs. C and F. Basal and etoposide-stimulated apoptosis in primary (C) and immortalized (F) PHLPP1 +/+ and Δ/Δ MEFs. "+PHLPP1β" indicates Δ/Δ MEFs stably reconstituted with human PHLPP1β.

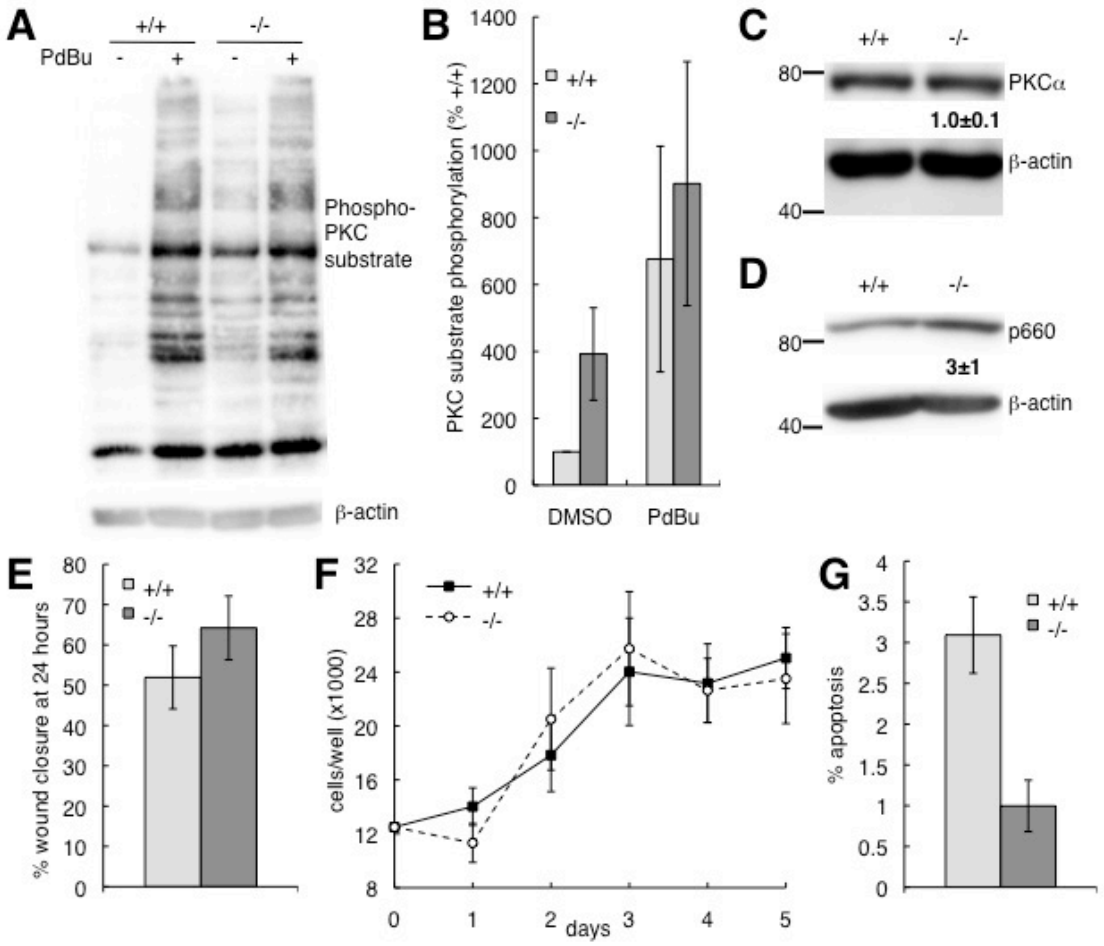

Figure 2.8: Increased PKC signaling and decreased apoptosis in primary astrocytes isolated from PHLPP1-null mice.

A. Western blot depicting PKC substrate phosphorylation in response to PdBu in wild type (+/+) or PHLPP1-null (-/-) astrocytes. B. Quantification of 5 experiments as in (A). C and D. Western blots depicting the levels of PKCα (C) and PKC phosphorylation at the hydrophobic motif, corresponding to serine 660 in PKCβII (D) in wild type and PHLPP1-null astrocytes. The numbers below the blots indicate the fold elevation in protein level or phosphorylation in the PHLPP1-null astrocytes compared to the controls and represent the means±SEM of 10 and 9 experiments, respectively. E, F, and G. Wound healing behavior in a scratch assay (E), proliferation (F), and apoptosis in low (0.1%) serum conditions (G). The data points represent the means±SEM of 5, three, and two experiments for (E), (F), and (G), respectively.

References

1. Brognard, J., Sierecki, E., Gao, T., and Newton, A. C. (2007) *Mol Cell* **25**, 917-931

2. Gao, T., Brognard, J., and Newton, A. C. (2008) *J Biol Chem* **283**, 6300-6311

3. Gao, T., Furnari, F., and Newton, A. C. (2005) *Mol Cell* **18**, 13-24

4. Liu, J., Stevens, P. D., Li, X., Schmidt, M. D., and Gao, T. (2011) *Mol Cell Biol*

5. Qiao, M., Wang, Y., Xu, X., Lu, J., Dong, Y., Tao, W., Stein, J., Stein, G. S., Iglehart, J. D., Shi, Q., and Pardee, A. B. (2010) *Mol Cell* **38**, 512-523

6. Liu, J., Weiss, H. L., Rychahou, P., Jackson, L. N., Evers, B. M., and Gao, T. (2009) *Oncogene* **28**, 994-1004

7. Molina, J. R., Agarwal, N. K., Morales, F. C., Hayashi, Y., Aldape, K. D., Cote, G., and Georgescu, M. M. (2011) *Oncogene*

8. Suljagic, M., Laurenti, L., Tarnani, M., Alam, M., Malek, S. N., and Efremov, D. G. (2010) *Leukemia* **24**, 2063-2071

9. Nitsche, C., Edderkaoui, M., Moore, R. M., Eibl, G., Kasahara, N., Treger, J., Grippo, P. J., Mayerle, J., Lerch, M. M., and Gukovskaya, A. S. (2011) *Gastroenterology*

10. Yang, Z. Z., Tschopp, O., Hemmings-Mieszczak, M., Feng, J., Brodbeck, D., Perentes, E., and Hemmings, B. A. (2003) *J Biol Chem* **278**, 32124-32131

11. Buzzi, F., Xu, L., Zuellig, R. A., Boller, S. B., Spinas, G. A., Hynx, D., Chang, Z., Yang, Z., Hemmings, B. A., Tschopp, O., and Niessen, M. (2010) *Mol Cell Biol* **30**, 601-612

12. Cho, H., Mu, J., Kim, J. K., Thorvaldsen, J. L., Chu, Q., Crenshaw, E. B., 3rd, Kaestner, K. H., Bartolomei, M. S., Shulman, G. I., and Birnbaum, M. J. (2001) *Science* **292**, 1728-1731

13. Maroulakou, I. G., Oemler, W., Naber, S. P., and Tsichlis, P. N. (2007) *Cancer Res* **67**, 167-177

14. Shimizu, K., Okada, M., Takano, A., and Nagai, K. (1999) *FEBS Lett* **458**, 363-369

15. Jackson, T. C., Verrier, J. D., Semple-Rowland, S., Kumar, A., and Foster, T. C. (2010) *J Neurochem* **115**, 941-955

16. Shimizu, K., Phan, T., Mansuy, I. M., and Storm, D. R. (2007) *Cell* **128**, 1219-1229

17. Suzuki, A., Nakano, T., Mak, T. W., and Sasaki, T. (2008) *Cancer science* **99**, 209-213

18. Chalhoub, N., and Baker, S. J. (2009) *Annual review of pathology* **4**, 127-150

19. Kim, R. H., and Mak, T. W. (2006) *Br J Cancer* **94**, 620-624

20. Di Cristofano, A., Pesce, B., Cordon-Cardo, C., and Pandolfi, P. P. (1998) *Nat Genet* **19**, 348-355

21. Stiles, B. L., Kuralwalla-Martinez, C., Guo, W., Gregorian, C., Wang, Y., Tian, J., Magnuson, M. A., and Wu, H. (2006) *Mol Cell Biol* **26**, 2772-2781

22. Tsuruta, H., Kishimoto, H., Sasaki, T., Horie, Y., Natsui, M., Shibata, Y., Hamada, K., Yajima, N., Kawahara, K., Sasaki, M., Tsuchiya, N., Enomoto, K., Mak, T. W., Nakano, T., Habuchi, T., and Suzuki, A. (2006) *Cancer Res* **66**, 8389-8396

23. Horie, Y., Suzuki, A., Kataoka, E., Sasaki, T., Hamada, K., Sasaki, J., Mizuno, K., Hasegawa, G., Kishimoto, H., Iizuka, M., Naito, M., Enomoto, K., Watanabe, S., Mak, T. W., and Nakano, T. (2004) *The Journal of clinical investigation* **113**, 1774-1783

24. Wijesekara, N., Konrad, D., Eweida, M., Jefferies, C., Liadis, N., Giacca, A., Crackower, M., Suzuki, A., Mak, T. W., Kahn, C. R., Klip, A., and Woo, M. (2005) *Mol Cell Biol* **25**, 1135-1145

25. Kurlawalla-Martinez, C., Stiles, B., Wang, Y., Devaskar, S. U., Kahn, B. B., and Wu, H. (2005) *Mol Cell Biol* **25**, 2498-2510

26. Bredel, M., Bredel, C., Juric, D., Harsh, G. R., Vogel, H., Recht, L. D., and Sikic, B. I. (2005) *Cancer Res* **65**, 4088-4096

27. TCGA. (2008) *Nature* **455**, 1061-1068

28. Backman, S. A., Stambolic, V., Suzuki, A., Haight, J., Elia, A., Pretorius, J., Tsao, M. S., Shannon, P., Bolon, B., Ivy, G. O., and Mak, T. W. (2001) *Nat Genet* **29**, 396-403

29. Fraser, M. M., Zhu, X., Kwon, C. H., Uhlmann, E. J., Gutmann, D. H., and Baker, S. J. (2004) *Cancer Res* **64**, 7773-7779

30. Chen, Z., Trotman, L. C., Shaffer, D., Lin, H. K., Dotan, Z. A., Niki, M., Koutcher, J. A., Scher, H. I., Ludwig, T., Gerald, W., Cordon-Cardo, C., and Pandolfi, P. P. (2005) *Nature* **436**, 725-730

31. Chen, M., Pratt, C. P., Zeeman, M. E., Schultz, N., Taylor, B. S., O'Neill, A., Castillo-Martin, M., Nowak, D. G., Naguib, A., Grace, D. M., Murn, J., Navin, N., Atwal, G. S., Sander, C., Gerald, W. L., Cordon-Cardo, C., Newton, A. C., Carver, B. S., and Trotman, L. C. (2011) *Cancer Cell* **20**, 173-186

32. Mikula, M., Schreiber, M., Husak, Z., Kucerova, L., Ruth, J., Wieser, R., Zatloukal, K., Beug, H., Wagner, E. F., and Baccarini, M. (2001) *The EMBO journal* **20**, 1952-1962

33. Warfel, N. A., Niederst, M., Stevens, M. W., Brennan, P. M., Frame, M. C., and Newton, A. C. (2011) *J Biol Chem* **286**, 19777-19788

34. Castillo, S. S., Brognard, J., Petukhov, P. A., Zhang, C., Tsurutani, J., Granville, C. A., Li, M., Jung, M., West, K. A., Gills, J. G., Kozikowski, A. P., and Dennis, P. A. (2004) *Cancer Res* **64**, 2782-2792

35. Winzell, M. S., and Ahren, B. (2004) *Diabetes* **53 Suppl 3**, S215-219

36. Saavedra, A., Garcia-Martinez, J. M., Xifro, X., Giralt, A., Torres-Peraza, J. F., Canals, J. M., Diaz-Hernandez, M., Lucas, J. J., Alberch, J., and Perez-Navarro, E. (2009) *Cell Death Differ* **17**, 324-335

37. Albrecht, U., and Eichele, G. (2003) *Curr Opin Genet Dev* **13**, 271-277

38. Panda, S., Antoch, M. P., Miller, B. H., Su, A. I., Schook, A. B., Straume, M., Schultz, P. G., Kay, S. A., Takahashi, J. S., and Hogenesch, J. B. (2002) *Cell* **109**, 307-320

39. Carver, B. S., Chapinski, C., Wongvipat, J., Hieronymus, H., Chen, Y., Chandarlapaty, S., Arora, V. K., Le, C., Koutcher, J., Scher, H., Scardino, P. T., Rosen, N., and Sawyers, C. L. (2011) *Cancer Cell* **19**, 575-586

40. Mulholland, D. J., Tran, L. M., Li, Y., Cai, H., Morim, A., Wang, S., Plaisier, S., Garraway, I. P., Huang, J., Graeber, T. G., and Wu, H. (2011) *Cancer Cell* **19**, 792-804

41. Pei, H., Li, L., Fridley, B. L., Jenkins, G. D., Kalari, K. R., Lingle, W., Petersen, G., Lou, Z., and Wang, L. (2009) *Cancer Cell* **16**, 259-266

42. Bernal-Mizrachi, E., Fatrai, S., Johnson, J. D., Ohsugi, M., Otani, K., Han, Z., Polonsky, K. S., and Permutt, M. A. (2004) *The Journal of clinical investigation* **114**, 928-936

43. Stanger, B. Z., Stiles, B., Lauwers, G. Y., Bardeesy, N., Mendoza, M., Wang, Y., Greenwood, A., Cheng, K. H., McLaughlin, M., Brown, D., Depinho, R. A., Wu, H., Melton, D. A., and Dor, Y. (2005) *Cancer Cell* **8**, 185-195

44. Berger, A. H., Knudson, A. G., and Pandolfi, P. P. (2011) *Nature* **476**, 163-169

45. Leal, J. F., Fominaya, J., Cascon, A., Guijarro, M. V., Blanco-Aparicio, C., Lleonart, M., Castro, M. E., Ramon, Y. C. S., Robledo, M., Beach, D. H., and Carnero, A. (2008) *Oncogene* **27**, 1961-1970

46. Denhardt, D. T., Edwards, D. R., McLeod, M., Norton, G., Parfett, C. L., and Zimmer, M. (1991) *Experimental cell research* **192**, 128-136

47. Todaro, G. J., and Green, H. (1963) *The Journal of cell biology* **17**, 299-313

48. Masubuchi, S., Gao, T., O'Neill, A., Eckel-Mahan, K., Newton, A. C., and Sassone-Corsi, P. (2010) *Proc Natl Acad Sci U S A* **107**, 1642-1647

49. Patterson, S. J., Han, J. M., Garcia, R., Assi, K., Gao, T., O'Neill, A., Newton, A. C., and Levings, M. K. (2011) *J Immunol* **186**, 5533-5537

Chapter 3:

PKCα promotes cell migration through a PDZ-dependent interaction with its novel substrate Discs Large homolog (DLG) 1

Abstract

Protein scaffolds maintain precision in kinase signaling by coordinating kinases with components of specific signaling pathways. Such spatial segregation is particularly important in allowing specificity of signaling mediated by the 10 member family of protein kinase C (PKC) isozymes. Here we identified a novel interaction between PKCα and the Discs large homolog (DLG) family of scaffolds that is mediated by a class I C-terminal PDZ (PSD-95, disheveled, and ZO1) ligand unique to this PKC isozyme. Specifically, use of a proteomic array containing 96 purified PDZ domains identified the third PDZ domains of DLG1/SAP97 and DLG4/PSD95 as interaction partners for the PDZ-binding motif of PKCα. Co-immunoprecipitation experiments verified that PKCα and DLG1 interact in cells by a mechanism dependent on an intact PDZ ligand. Functional assays revealed that the interaction of PKCα with DLG1 promotes wound healing; scratch assays using cells depleted of PKCα and/or DLG1 have impaired cellular migration that is no longer sensitive to PKC inhibition, and the ability of exogenous PKCα to rescue cellular migration is dependent on the presence of its PDZ ligand. Furthermore, we identified T656 as a novel phosphorylation site in the SH3 (Src homology 3)-Hook region of DLG1 that acts as a marker for PKCα activity at this scaffold. Increased phosphorylation of T656 is correlated with increased invasiveness in non-small cell lung cancer (NSCLC) lines from the NCI-60, consistent with this phosphorylation site serving as a marker of PKCα-mediated invasion. Taken together, these data establish the requirement of scaffolding to DLG1 for PKCα to promote cellular migration.

Introduction

Targeting of signaling proteins to specific intracellular locations via scaffolding proteins allows signals to be efficiently and selectively integrated, propagated, and regulated (1). Scaffolds

serve a particularly important function in the organization of signaling by protein kinases, because kinase substrate selectivity is determined by not only consensus motifs but also availability of substrates near the active site (2).

The PKC branch of the AGC kinase family tree has 10 family members that are regulated not only by phosphorylation and binding to lipid second messengers but also by interaction with binding partners. PKC isozymes are grouped into the following three classes based upon their cofactor dependence: the conventional PKC (cPKC) isozymes α, the alternatively spliced βI and βII, and γ, which depend on diacylglycerol and Ca^{2+} for their activity; the novel PKCs δ, ε, η, and θ, which depend on diacylglycerol; and the atypical PKCs ζ and λ/ι, which rely mainly on protein-protein interactions for activation (3). While the stimuli governing PKC activation have been extensively characterized, assigning specific biological roles to PKC isozymes has proved more difficult, partially owing to the divergent roles of the different family members in various cellular processes (4). However, ever since the discovery that PKCs act as receptors for tumor-promoting phorbol esters (5), these enzymes have been hypothesized to positively regulate tumor progression and metastasis. Indeed, there is an increasing body of evidence implicating PKCα, in particular, in cancer cell survival and migration (6-10). In this regard, an antisense molecule targeting PKCα has been shown to have preclinical efficacy in various cancer models, including advanced non-small cell lung cancer (11,12). Note, however, that the effects of PKCα signaling are complex, because several types of cancer cells, including those generated in mouse models of colon cancer, show dramatically reduced levels of PKCα (13). Cell type-dependent differences in PKCα signaling are likely accounted for by differential interactions with key regulatory proteins, notably scaffold proteins.

PKC protein scaffolds have long been known to play essential roles in PKC function. Mochly-Rosen and coworkers first described the role of protein scaffolds in directing the cellular function of PKC with the identification of proteins they named Receptors for Activated C-Kinase or RACKs (14). Since then, numerous PKC-binding proteins have been identified and shown to

regulate PKC in many ways, including 1) relieving PKC autoinhibition, 2) mediating PKC's association with the actin cytoskeleton, 3) controlling the availability of upstream regulators of PKC, and 4) mediating PKC's interaction with receptors, small GTPases, and other signaling proteins (10,15,16). These interactions play important roles in regulating PKC function, notably the transmission of signals from sites of cell-cell or cell-matrix contact to the cytoskeleton, with resulting effects on cell spreading and migration (2,16). The key role of scaffolding in PKC signaling is epitomized by an elegant study by Zuker and coworkers showing that the PDZ (PSD-95, disheveled, and ZO1) domain-containing protein encoded by the *inaD* gene, which scaffolds PKC, is required for light-induced PKC signaling in the fly eye (17). The binding of *Drosophila* eye PKC to this scaffold is mediated by binding of a C-terminal PDZ ligand, which has the amino acid sequence ITII (17,18). PDZ ligand-based interactions are powerful coordinators of cell signaling (19), yet their roles in signaling by mammalian PKC isozymes are relatively unexplored.

Of the 8 diacylglycerol-regulated PKC isozymes, only PKCα contains a C-terminal PDZ ligand motif. The last four amino acids of this isozyme (QSAV) encode a class I PDZ ligand. PDZ ligands bind PDZ domains, which are relatively small globular domains (~90 amino acid) that are abundant in the mammalian proteome; their canonical role is to bind short C-terminal peptide motifs (20). The only identified partner for the PDZ ligand of mammalian PKCα is the PDZ scaffold PICK1 (protein that interacts with C kinase 1) (21). PKCα's PDZ ligand has been shown to be necessary and sufficient for long-term depression in cerebellar cultures (22). *In vitro*, peptides containing this motif bind numerous murine PDZ domains, including the third PDZ domain of all four members of the membrane-associated guanylate kinase (MAGUK) protein scaffold family. In rat brain extracts, PKCα has been shown to co-immunoprecipitate with the MAGUKs SAP-102 (synapse-associated protein 102; also known as Discs large homolog 3) and PSD-95, with these interactions hypothesized to be mediated by the first and second PDZ domains of the MAGUKs (23). In addition, PKC has been shown to exist in a complex with protein kinase A, A-kinase anchoring protein 150, and PSD-95 or SAP-97 (synapse-associated protein

97; also known as DLG1 or Discs large homolog 1) (23,24). Although the direct binding of the PDZ ligand of PKCα to these MAGUK proteins was not explored, and no functional studies were performed to address the physiological importance of PKCα/MAGUK associations, these data suggest the possibility that PDZ interactions may coordinate the signaling of PKCα.

In this study, we used a PDZ domain array to identify the third PDZ domains of DLG1/SAP-97 and DLG4/PSD95 as binding partners for the PDZ ligand of PKCα. Biochemical studies validated the interaction in cells, established that PKCα phosphorylates DLG1 on a novel site, T656, and showed that both PKCα's PDZ ligand and DLG1 are required for PKCα to promote cellular migration. Our data are consistent with a model in which DLG1 acts as a scaffold for PKCα to control PKC-dependent regulation of cellular migration.

Materials and Methods

Materials and Antibodies – Mitomycin C, Gö6983, Gö6976, PMA, and calyculin A were purchased from Calbiochem. A control siRNA SmartPool and a siRNA SmartPool targeting human DLG1 were purchased from Dharmacon; the latter included the following sequences: 1) CCAAAAUGUAUAGAUCGUU; 2) CGAUGAGGUCGGAGUGAUU; 3) CCAGGAACAUAAAUUCAUU; 4) CCCACAAGUAUGUAUAUGA. A second siRNA (referred to as "DLG1 siRNA #2") used to validate the effect of DLG1 depletion on wound healing was purchased from Sigma-Aldrich, along with a universal negative control siRNA, and had the targeting sequence CAGAGAAGAACUUAUCAGA. Two shRNAs against human PKCα and a non-targeting control lentivirus were obtained from Sigma-Aldrich. Sequences of the shRNAs were as follows (with target sequences underlined): PKCα #1, CCGGCAUGGAACUCAGGCAGAAAUUCUCGAGAAUUUCUGCC; PKCα #2, CCGGCGAGCTATTTCAGTCTATCATCTCGAGATGATAGACTGAAATAGCTCGTTTTT; non-targeting control, CCGGCAACAAGAUGAAGAGCACCAACUCGAG. PKCα shRNA #1 was used in all experiments except where otherwise noted. Primers used for PCR-based cloning were from IDT. All restriction enzymes were from NEB. Antibodies and dilutions used were: mouse anti-Myc

(1:1,000, 9E10; Covance), rat anti-HA (1:2,000; Roche Diagnostics), rabbit anti-GST (1:1,000; Sigma), mouse anti-SAP97/DLG1 (1:500 for Western blot, 1:200 for immunofluorescence (IF) staining; Stressgen), rabbit anti-PKCα (1:1,000 for Western blot, 1:200 for IF staining; Santa Cruz), mouse anti-ß-actin (1:1,000; Sigma), and mouse anti-hsp70 (1:1000; BD Biosciences). Secondary antibodies used for immunofluorescence were: goat anti-mouse-Alexa 568, goat anti-rabbit-Alexa 488, goat anti-mouse-Alexa 488, and goat anti-rabbit-Alexa 568, all from Invitrogen. The pT656 antibody was raised by immunizing rabbits with an Ac-CKERARLK-T(PO_3H_2)-VKFN-NH_2 peptide that was conjugated to KLH and was affinity purified using the phospho-peptide antigen (NeoMPS). This antibody was used at 1:5,000 for Western blot. All other materials were reagent grade.

Construction of plasmids – A cDNA fragment encoding the last 25 amino acids of bovine PKCα was ligated into pGEX-6-P3 (Amersham) to generate a GST-fusion peptide (GST-PDZα). Sequences for bovine PKCα and PKCα lacking the last three amino acids (PKCαΔPDZ) were cloned into pcDNA3-HA by PCR, generating HA-PKCα and HA-PKCαΔPDZ. CFP-tagged DLG1/SAP97 (i3) was a generous gift from M. Dell'Acqua, and Myc-DLG1 was a generous gift from C. Garner. All mutagenesis was performed using a QuikChange kit (Stratagene) according to the manufacturer's instructions.

Purification of GST-tagged proteins – The GST-PDZα construct was transformed into BL21 (DE3) cells, which were grown at 37 °C until their A_{600} reached 0.6 and then induced with 1 mM IPTG for four h at 25 °C. Cells were pelleted and homogenized in a buffer containing 50 mM Tris (pH 7.5), 1 mM EDTA, 1 mM DTT, 300 nM PMSF, 500 nM benzamidine, 500 ng/ml leupeptin, and 1 mg/ml lysozyme. The lysates were rocked for 30 minutes at 4 °C and briefly sonicated before treatment with DNAse (100 µg/ml) and centrifugation at 14,000 x g for 30 minutes at 4 °C. The fusion peptide was purified from the filtered supernatant using the Profinia Protein Purification System (BioRad) according to the manufacturer's specifications. The eluted pure protein was dialyzed against 20 mM HEPES (pH 7.5)/50 mM NaCl.

Peptide overlay array – An array of 96 PDZ domains was spotted onto membranes as described previously (25). Purified GST-PDZα (0.5 mg/ml) was overlaid onto the array and detected using a far Western blot approach, as previously described (26).

Dot blot validation of pT656 antibody – To analyze the specificity of the pT656 antibody, phosphorylated (Ac-CKERARLK-T(PO_3H_2)-VKFN-NH_2) and unphosphorylated (Ac-CKERARLK-TVKFN-NH_2) peptides were synthesized by NeoMPS and spotted onto nitrocellulose membranes. Dot blots were incubated with various concentrations of the pT656 antibody and analyzed by Western blot.

Cell culture, PMA stimulation experiments, and Western blotting – Unless otherwise noted, cells were maintained in DMEM (Cellgro) supplemented with 10% fetal bovine serum (FBS, Hyclone) and 1% penicillin/streptomycin (P/S), except for SNB-19, NCI-H322M, NCI-H23, A549, and HOP62 cells, which were cultured in RPMI 1640 (Cellgro) with 10% FBS and 1% P/S. Immortalized PKCα +/+ and -/- mouse embryonic fibroblasts (MEFs) were a generous gift from M. Leitges, primary astrocytes were isolated as described below, H1703 and SNB-19 cells were purchased from ATCC, and NCI-H322M, NCI-H23, A549, and HOP62 cells were gifts from the NCI. Cells were incubated at 37 °C/5% CO_2. For PMA stimulation experiments, cells were treated for the indicated times at 37 °C with PMA (200 nM), Gö6976 (500 nM), Gö6983 (250 nM), and/or calyculin A (100 nM). Unless otherwise noted, all stock solutions used were in DMSO, and a corresponding amount of DMSO was used as a control. The final concentration of DMSO in the culture media did not exceed 0.4% (vol/vol). For immunoblotting, primary astrocytes and H1703 cells were lysed in 1X Laemmli sample buffer, and the NCI-60 NSCLC lines and PKCα +/+ and -/- MEFs were lysed in a buffer consisting of 50 mM Tris [pH 7.4], 150 mM NaCl, 1% Triton, 0.5% sodium deoxycholate, 0.1% SDS, 30 mM sodium pyrophosphate, 0.1 mM sodium vanadate, 200 mM benzamidine, 40 mg/ml leupeptin, and 1 mM PMSF. MEF and NSCLC lysate protein concentrations were quantified using a BCA protein assay kit (Thermo Scientific) and normalized. Levels of total and phosphorylated proteins were analyzed by SDS-PAGE and Western blotting.

Immunoprecipitations – HA-PKCα or HA-PKCαΔPDZ and Myc-DLG1 were transfected into HEK293T cells using Effectene (Qiagen) according to the manufacturer's instructions. Approximately 24 hours later, cells were lysed in IP buffer (50 mM Tris [pH 7.5], 10 mM sodium pyrophosphate, 50 mM NaF, 5 mM EDTA, 1% Triton, 1 mM DTT, 200 mM benzamidine, 40 mg/ml leupeptin, and 1 mM PMSF); the lysates were then cleared by centrifugation at 16,000 x g for 5 min at 22 °C and incubated with a anti-HA antibody (Covance; monoclonal; 1:450) overnight at 4 °C with rocking. In the morning, Ultra-Link Protein A/G beads (Thermo Scientific) were added to the immune complexes and incubated for 1 h at 4 °C with rocking. Beads were then washed with IP buffer followed by IP buffer containing 50 mM NaCl, and analyzed by SDS-PAGE and Western blotting.

Primary astrocyte isolation – Following isolation as described in (27), adherent astrocytes were washed twice with PBS, trypsinized, and plated at approximately 3 X 10^5 cells per ml on lysine-coated six-well dishes. All astrocyte preparations that were subjected to wound healing analysis had at least 80% glial fibrillary acidic protein-positive cells by immunofluorescence, and experiments were performed on cells derived from three different preparations.

Wound healing assay – Primary murine astrocytes, SNB-19 GBM cells, and H1703 NSCLC cells were plated on lysine-coated six-well dishes at consistent cell densities. Approximately 48 h after plating, confluent monolayers were treated with mitomycin C (10 μg/ml, stock solution dissolved in PBS) in serum-free DMEM or RPMI for one hour to inhibit cell proliferation and then washed twice with PBS. Fresh DMEM or RPMI containing 10% FBS and either DMSO or Gö6976 (500 nM) was added to the cells. After 20 minutes of pretreatment, monolayers were scratched once with a 10 μl pipet tip, and pictures of the central region of the scratch were taken immediately and at various time points after scratch with a 5X objective lens. During the assay, cells were maintained at 37 °C/5% CO_2. The wound area at the various time points was quantified using ImageJ (NIH).

Immunofluorescence – Primary murine astrocytes were prepared and scratched as

described above, except that they were plated on lysine-coated glass cover slips. Four hours after being scratched, cells were washed twice in cold PBS, fixed with 3% paraformaldehyde and 2% sucrose in PBS (pH 8.0) for 20 min, quenched in 50 mM NH_4Cl in 10 mM PIPES (pH 6.8), 150 mM NaCl, 5 mM EGTA, 5 mM glucose, and 5 mM $MgCl_2$ for 15 min, and blocked in blocking buffer (10% goat serum in PBS, 0.1% Triton) for 1 hour prior to overnight incubation at 4 °C with primary antibodies diluted in blocking buffer. After washing, the indicated secondary antibodies were added at a dilution of 1:600 in PBS, 0.1% Tween for 1 hour at 4 °C. Washed slides were mounted using Vectashield and photographed on a Zeiss Axiovert microscope (Carl Zeiss Microimaging, Inc.) using a MicroMax digital camera (Roper-Princeton Instruments) controlled by MetaFluor software (Universal Imaging, Corp.). Optical filters were obtained from Chroma Technologies. PKCα/DLG1 colocalization was assessed in a blinded fashion for at least 30 cells per condition per experiment (n=5 experiments using three different astrocyte preparations).

Lentiviral shRNA production and infection – A shRNA targeting human PKCα was packaged into recombinant lentiviruses using the Invitrogen ViraPower™ Lentiviral Expression System according to the manufacturer's protocol. A non-targeting lentiviral RNAi (NT shRNA) that recognizes no human genes was used as a negative control. For lentiviral shRNA infection, H1703 cells were seeded in 100-mm plates and grown to 70–80% confluency. The culture medium was removed from the cells, and three ml of complete culture media containing polybrene (6 mg/ml) was added. After 5 min at 22 °C, 400 ml (multiplicity of infection ~3) of viral supernatant was added. Following a 24 h incubation at 37 °C, cells were washed and grown for 24 h in 10 ml of fresh culture medium. Populations of stably infected cells were selected in 5 mg/ml puromycin.

Re-expression of PKCα in stable PKCα knockdown cells – HA-tagged bovine PKCα constructs, which are resistant to knockdown by our shRNA construct targeted against human PKCα, were transfected into NT shRNA- or PKCα shRNA-expressing H1703 cells as follows. Cells were plated into 24-well plates and, three hours after plating, transfected with eGFP

(enhanced green fluorescent protein) alone or with HA-PKCα (wild type; 0.25 μg per well) or HA-PKCαΔPDZ (0.2 μg per well) using Jetprime transfection reagent (Polyplus) according to the manufacturer's instructions. Fresh culture media was added 4 h after transfection, and cells were incubated overnight before being re-plated onto lysine-coated 6-well plates at consistent cell densities. Wound healing assays were performed approximately 12 hours after re-plating. At least 70% of cells were transfected (as marked by GFP fluorescence at the time of scratch), and cells were lysed in 1X Laemmli buffer immediately after scratch for validation of PKCα expression.

Transient siRNA transfection – H1703 cells were transiently transfected with control or DLG1 siRNA (50 nM) and subjected to wound healing analysis as described previously (28), with minor modifications. Briefly, cells were transfected using Lipofectamine 2000 (Invitrogen) in DMEM without FBS and penicillin/streptomycin three h after plating and incubated overnight before addition of fresh media with 10% FBS and penicillin/streptomycin. At 48 h after transfection, cells were re-plated onto lysine-coated 6-well dishes at consistent cell densities. Wound healing assays were performed starting at approximately 72 hours after transfection, and cells were lysed in 1X Laemmli sample buffer immediately upon completion of the assay for verification of DLG1 knockdown by Western blot.

Identification and alignment of PKCα phosphorylation site – A consensus PKCα/ß/γ phosphorylation site in DLG1 was identified using Scansite (scansite.mit.edu), and comparison of amino acid motifs in the human DLG family and in DLG1 isoforms from various species was performed using MegAlign.

Statistical analyses – Differences among groups were analyzed using Student's t-test or ANOVA, with significance set at $p<0.05$. For multiple comparisons, a post-hoc Tukey test was applied after the ANOVA.

Results

The PDZ ligand of PKCα mediates binding to DLG1 – To identify potential binding partners for the PDZ ligand of PKCα, we generated a GST-fusion of the last 25 amino acids of

bovine PKCα and overlaid it onto a PDZ domain array containing 96 PDZ domains (mostly Type I PDZ domains) from various proteins (Figure 3.1B). Far Western blotting for GST revealed that the C-terminal peptide of PKCα bound strongly to the third (but not first and second) PDZ domain of PSD-95 (also known as DLG4) (Figure 3.1A B8). In addition, we identified weaker, but readily detectable, binding to the third (but not first and second) PDZ domain of DLG1 (SAP97) (Figure 3.1A, C3), ß2-syntrophin (E8), PAPIN 1 (E11), and PTPN13 (F9). In contrast to PKCα, the last 25 amino acids of PKCζ, the only other PKC isozyme that contains a PDZ ligand motif, failed to bind to any of the PDZ domains on the array (M.T. Kunkel and R.A. Hall, unpublished data). Because PKCζ's PDZ ligand (EESV) is predicted to bind only Type III PDZ domains (20), this finding was not unexpected and points to a specific PDZ-based interaction of PKCα with DLG scaffolds. The binding of PKCα's PDZ ligand to the third PDZ domain of two DLG scaffolds prompted us to focus on this interaction. To validate the PKCα/DLG1 interaction, we overexpressed HA-tagged bovine PKCα and Myc-tagged rat DLG1 in HEK293T cells and asked if DLG1 was present in immunoprecipitates of PKCα. Figure 3.1C shows that Myc-DLG1 was present in HA-PKCα immunoprecipitates (lane 2) but not control immunoprecipitates (lane 1). This interaction depended on the PDZ ligand of PKCα: DLG1 did not co-immunoprecipitate with a construct of PKCα lacking the last three amino acids (PKCαΔPDZ; lane 3). Similar results were obtained for the interaction between PKCα and PSD95 (data not shown). These results reveal that the PDZ ligand of PKCα mediates the binding of PKCα to the third PDZ domain of DLG1/SAP97 and DLG4/PSD95.

PKCα and DLG1 colocalize at the leading edge of migrating cells – Given the scaffolding interaction between PKCα and DLG1, we asked whether these two proteins colocalize in cells. Specifically, we examined the distribution of the two proteins in primary murine astrocytes in a wound healing assay (as described in (28)). Detection of endogenous PKCα or DLG1 by immunofluorescence revealed that the two proteins codistributed at the leading edge in approximately 30% of migrating primary astrocytes four h after scratch (Figure 3.2A, middle row),

but not at the membranes of unscratched cells (Figure 3.2A, top row). This scratch-induced codistribution depended on PKC activity because pretreatment with the cPKC inhibitor Gö6976 decreased codistribution (Figure 3.2A, bottom row). Blinded scoring of DLG1 and PKCα colocalization in >30 cells over three different astrocyte preparations (n=5 experiments) revealed that treatment with Gö6976 results in a ~60% decrease in colocalization of the two proteins (Figure 3.2B). These data indicate that PKCα and DLG1 codistribute at the leading edge of migrating cells and that this colocalization depends on cPKC activity.

PKCα positively regulates wound healing – Given the codistribution of PKCα and DLG1 at the leading edge of migrating cells, we next asked whether the activity of PKC enhances wound healing. Using the same wound healing paradigm described above, we examined the effect of inhibition of cPKC activity by pretreatment with Gö6976 on the rate of migration of primary astrocytes (Figure 3.2C), SNB-19 GBM cells (Figure 3.2D), or H1703 NSCLC cells (Figure 3.2E). In all three cell types, Gö6976 (squares) reduced the rate of cellular migration by approximately 25-40% compared to vehicle treatment (circles). To determine whether the Gö6976 sensitivity reflected exclusively inhibition of PKCα, H1703 cells were stably transfected with a non-targeting (NT) shRNA (open symbols) or an shRNA targeting PKCα (filled symbols), and the sensitivity of cellular migration to Gö6976 was tested in wound healing assays. Importantly, PKCα knockdown and Gö6976 treatment did not have an additive effect on the inhibition of cellular migration (Figure 3.2E, filled squares). Furthermore, the rate of migration of control cells treated with the PKC inhibitor (open squares) was the same as that of cells depleted of PKCα (filled circles). Western blot analysis of lysates revealed that PKCα was knocked down by 70±10% (Figure 3.2F). To further validate the specific role of PKCα in wound healing, we depleted H1703 cells of PKCα using a second shRNA, resulting in 60±10% inhibition of PKCα expression and a 70% decrease in wound healing (Figure 3.3). The inability of Gö6976 to further inhibit migration in PKCα-depleted cells reveals that PKCα is the major cPKC promoting cell migration.

PKCα's PDZ ligand is necessary for its ability to promote wound healing – We next

attempted to rescue the effects of PKCα knockdown on wound healing by expressing a shRNA-resistant bovine form of PKCα in PKCα-depleted H1703 cells (Figure 3.4). Re-expression of wild type PKCα at a level close to that of control cells (Figure 3.4, compare lanes 1 and 3) resulted in a complete rescue of wound healing (Figure 3.4, filled squares), whereas expression of a PKCα mutant lacking the last three amino acids (PKCαΔPDZ) only slightly increased the rate of wound healing (Figure 3.4, filled diamonds). These data support the conclusion that PKCα's PDZ ligand, which mediates its interaction with DLG1, is required for a large portion of PKCα's positive effects on cellular migration.

DLG1 depletion blocks the ability of PKCα to promote cellular migration – We next asked whether DLG1 is necessary for PKCα to promote cell migration by examining the effect of inhibiting conventional PKC activity on cell migration in control cells, cells lacking PKCα, or cells lacking PKCα and DLG1. Specifically, stably transfected NT or PKCα shRNA-expressing H1703 cells were transiently transfected with a control siRNA (ctrl siRNA; Figure 3.5, circles) or a siRNA targeting human DLG1 (DLG1 siRNA; Figure 3.5, squares), and cell migration was measured in wound healing assays. DLG1 siRNA transfection resulted in an ~50% reduction in DLG1 levels (n=3; Figure 3.5, upper panel); these cells displayed a reduction in migration that was similar to that observed in cells depleted of PKCα (Figure 3.5, lower panel). To further validate the specific role of DLG1 in wound healing, we depleted H1703 cells of DLG1 using a second siRNA sequence, resulting in 64±7% inhibition of DLG1 expression and a 20% decrease in wound healing, similar to that observed with the original siRNA (Figure 3.6). Strikingly, no further reduction in migration was observed in cells depleted of both DLG1 and PKCα (Figure 3.5, filled squares). These data suggest that the regulation of cellular migration by PKCα depends on DLG1.

PKCα phosphorylates DLG1 at T656 – Analysis of the sequence of full-length DLG for predicted phosphorylation sites (ScanSite) revealed the presence of a putative cPKC phosphorylation site at T656. This residue lies between the SH3 and Hook domains of DLG1

(Figure 3.7A). Alignment of DLG isoforms and MAGI-3 (Figure 3.7B) revealed that this phosphorylation site is conserved in all of these proteins except PSD-95, which has an Ala at the potential phospho-acceptor site. Furthermore, this potential phosphorylation site is conserved among species, including *Drosophila*. To identify whether this site is phosphorylated in cells, we generated a phospho-specific antibody using a phosphorylated peptide corresponding to the region surrounding T656. Figure 3.7C shows that this antibody (pT656) recognizes the phosphorylated peptide with almost 100-fold selectivity compared to the unphosphorylated peptide.

We next tested whether T656 is phosphorylated in cells. Primary astrocytes, chosen because of their high level of expression of DLG1, were treated with: 1) phorbol myristate acetate (PMA), which acutely stimulates PKC activity; 2) Gö6983, which inhibits conventional and novel PKC isoforms; and 3) Gö6976, which inhibits only the conventional PKC isoforms. Western blot analysis of astrocyte lysates in Figure 3.8A shows that an antibody for total DLG1 recognized a doublet that likely corresponds to splice variants of DLG1 (29). These bands were strongly labeled by the pT656 antibody in lysates from cells treated with PMA (lane 2) but not vehicle alone (lane 1). Importantly, pT656 labeling was abolished in cells pre-treated with the PKC inhibitors Gö6976 (lane 3) or Gö6983 (lane 4) prior to PMA stimulation.

To determine whether PKCα is the primary kinase that phosphorylates DLG1 at T656, we examined the phosphorylation state of this residue in MEFs lacking the gene for PKCα (PKCα -/-) compared to that in their wild type counterparts (PKCα +/+). MEFs were treated with PMA to promote PKC-catalyzed phosphorylation and the PP1/PP2A inhibitor calyculin A to stabilize the phosphorylated state or pretreated with the PKC inhibitors Gö6983 and Gö6976 and then treated with PMA and calyculin A. The Western blot in Figure 3.8B shows that DLG1 migrated as a doublet in the MEFs, similar to what we observed for DLG1 in astrocytes. The bands were only weakly labeled with the pT656 antibody, but immunoreactivity increased upon PMA treatment, and cotreatment with calyculin A further enhanced labeling with this antibody. This PMA/calyculin

A-stimulated phosphorylation of DLG1 was abolished in cells treated with Gö6983 and significantly reduced in cells treated with Gö6976, as shown by quantitation of the data from 8 separate experiments, presented in Figure 3.8D. Both basal and phorbol ester-stimulated phosphorylation of T656 were significantly reduced in PKCα -/- MEFs: quantitation of 8 independent experiments (Figure 3.8D) revealed that basal phosphorylation was reduced approximately 50%, with no significant increase following phorbol ester treatment. Calyculin A treatment unmasked a very modest increase in phosphorylation of T656, which was not significantly affected by PKC inhibitors, suggesting that inhibition of phosphatases allowed slight phosphorylation of this site by other kinases. These data reveal that PKCα is the predominant kinase catalyzing the phosphorylation of T656 in MEFs.

We also examined whether DLG1 is phosphorylated by PKCα in H1703 NSCLC cells, which were used to examine the effects of PKCα and DLG1 on migration. Because of the low basal level of endogenous DLG1 phosphorylation in these cells, we overexpressed a CFP-tagged form of DLG1 in H1703 cells expressing a non-targeting shRNA or a PKCα shRNA and examined phosphorylation of T656 under conditions of PKC activation and inhibition. The results (Figure 3.8C) were very similar to those observed in the PKCα +/+ and -/- MEFs; depletion of PKCα (by 60±10%) impaired DLG1 phosphorylation stimulated by treatment with PMA and calyculin A (compare lanes 3 and 8), as did pretreatment with Gö6976 (lane 4) or Gö6983 (lane 5). Quantitation of n=7 experiments (Figure 3.8E) showed that interference with PKCα expression or activity significantly decreased T656 phosphorylation in H1703 cells, establishing PKCα as the primary kinase for this site in this NSCLC cell line.

PKCα activity at the DLG1 scaffold is increased in highly invasive cells – Given that PKCα mediates phosphorylation of DLG1 at T656, we next examined whether DLG1-associated PKCα activity (as read out by T656 phosphorylation) is correlated with invasiveness in human lung cancers. Taking advantage of a study profiling invasion by the 9 NSCLC lines in the NCI-60 (30), we chose two cell lines with a non-invasive phenotype (NCI-H322M and NCI-23; invasion

scores of less than 1000) and two more highly invasive cell lines (A549 and HOP62; invasion scores of ~4000) and examined PKCα expression and DLG1 phosphorylation. Similar to H1703 cells, these cell lines have very low basal levels of endogenous DLG1 phosphorylation, so we examined PKCα signaling at the DLG1 scaffold by overexpressing CFP-DLG1 and treating with PMA and calyculin A, with or without pretreatment with the cPKC inhibitor Gö6976. Overall PKCα expression was significantly increased (2.5- to 3-fold) in A549 and HOP62 cells compared to H322M and H23 cells (Figure 3.8A and B), in accordance with data from reverse phase protein array profiling of the NCI-60 (31), which establish relative PKCα protein levels in these four cell lines as 1.0 (H322M), 1.3 (H23), 4.7 (A549) and 4.6 (HOP62). To read out PKCα activity at the scaffold, we examined the component of PMA-stimulated DLG1 phosphorylation that was reversed by Gö6976 treatment, corresponding to cPKC-mediated phosphorylation. This parameter was increased in the more highly invasive cell lines (Figure 3.8A); quantitation of 8 separate experiments revealed increases of 1.7±0.5-fold and 3±1-fold in Gö6976-reversible T656 phosphorylation in A549 and HOP62 cells, respectively, compared to H322M, though only the difference between the H322M and HOP62 cells was significant. As expected, the difference between H322M and H23 cells was negligible (Figure 3.8C). These results show that DLG1-associated PKCα activity is correlated with invasion across several human lung cancer cell lines.

Discussion

In this study, we have identified the PDZ domain-containing scaffold DLG1 as a binding partner and substrate for PKCα that is required for PKCα to promote cell migration. Specifically, we show that the PDZ ligand of PKCα binds the third PDZ domain of DLG1, coordinating the phosphorylation at T656 on DLG1. These two proteins colocalize at the leading edge of migrating cells, a dynamic region controlled by cytoskeletal interactions, where they promote scratch-induced migration in several different cell types. Key to our study was the finding that PKCα inhibition did not affect wound healing when DLG1 was depleted. Taken together, our results are consistent with a model in which the DLG1 scaffold coordinates signaling by PKCα to regulate

cellular migration in 2D culture and in which phosphorylation of DLG1 at T656 marks PKCα activity at this scaffold.

Many studies have shown that PKCα plays roles in cell motility *in vitro* and *in vivo* (6); phorbol esters, which activate PKC, enhance cellular migration and have well-characterized effects on the actin cytoskeleton (10), and PKCα-specific inhibitors and siRNA attenuate cell spreading, wound healing, metalloprotease activation, and metastasis in several models (32-39). Recently, microRNA (miR) profiling revealed that the presence of brain metastasis in NSCLC patients could be predicted in part by the expression of a miR whose forced expression results in upregulation of PKCα levels, suggesting that PKCα plays an important role in metastasis in human lung cancer (40). Such effects on motility have been suggested to be mediated by several PKC binding proteins/substrates, including α6-tubulin (32), RhoGDP-dissociation inhibitor and syndecan-4 (34-36), ADAM (a disintegrin and metalloprotease)-10 (38), and fascin (33). However, the majority of these studies do not address the question of whether the PKCα-mediated effects on cellular migration are dependent on the presence of the substrate in question. Our results demonstrate a PKCα-DLG1 signaling pathway that positively affects migration and could play a pro-oncogenic role. Although DLG1 has historically been characterized as a tumor suppressor (41,42), it varies in expression among malignancies (43) and is known to play different and sometimes opposing roles in various processes involved in tumor progression, including differentiation, cytokinesis, proliferation, cell migration, and control of the tumor microenvironment (42,44). Moreover, a DLG1 mutant mouse in which the gene is disrupted starting after the third PDZ domain shows no increase in tumor development but does demonstrate a cleft palate phenotype that is consistent with failure of cell migration (45).

Previous studies have demonstrated a role for DLG1 in scratch-induced migration in primary astrocytes. Specifically, atypical PKC activity regulates the leading edge localization of DLG1, where it controls the localization of adenomatous polyposis coli (APC) and polarization of microtubules. Furthermore, DLG1 interacts with guanylate kinase anchoring protein (GKAP) and

dynein intermediate chain along the microtubules to contribute to proper microtubule dynamics, which allow the cell to properly position the centrosome, establish cell polarity, and migrate into the scratch wound (46-48). These observations point to a critical role for DLG1 in astrocyte migration, and highlight the importance of the guanylate kinase (GK) homology domain in carrying out this function of DLG1.

The C-terminal moiety of DLG1 is composed of an SH3 domain and a GK homology domain separated by a Hook (hinge) region. In the fly, SH3-Hook mutants or mutations that otherwise disrupt SH3-GK binding phenocopy DLG null mutants (49,50); thus, this region is critical for the function of this scaffolding protein. The Hook domain of DLG1 cooperates with the SH3 domain to bind the GK domain inter- and intramolecularly and regulate the accessibility of this domain to binding partners (50,51). Thus, phosphorylation at T656, which is situated between the SH3 and Hook regions, could alter the interaction of DLG1 with partners whose binding site has been mapped to the SH3-GK region, including the previously mentioned GKAP and ADAM-10, which bind to DLG1's SH3 domain and also to PKCα (38,52). Importantly, a GK deletion mutant is unable to rescue the microtubule polarization defects upon DLG1 knockdown in migrating astrocytes (47), so this region is critical to DLG1's function in astrocyte migration. Despite the critical functions of this region, and despite our finding that PKCα and DLG1 cooperate in regulating wound healing, mutation of the phospho-acceptor site had no effect on wound healing (data not shown). It is possible that DLG1 overexpression can compensate for mutation of this PKCα phosphorylation site. An alternative hypothesis is that DLG1 scaffolds PKCα to other substrates that are important for PKCα's effects on wound healing, and therefore phosphorylation of DLG1 at T656 serves as a marker for PKCα activity at the scaffold but is not itself required to mediate the pro-migratory effects of PKCα. For example, the membrane-associated protein 4.1, which participates in membrane reorganization in multiple cell types, binds to DLG1 through 4.1's conserved N-terminal FERM (four.one protein, ezrin, radixin, moesin) domain (53) and is phosphorylated by PKCα at a conserved (54) serine that is important for

spectrin-actin association (55,56). DLG1 may promote PKCα-mediated phosphorylation of 4.1 to promote membrane destabilization and allow cellular migration. Thus, although the specific functional consequences of T656 phosphorylation remain to be elucidated, this phosphorylation event is correlated with increased invasiveness in four NSCLC cell lines, supporting a critical role for DLG1-associated PKCα activity in cancer cell motility.

In this study we connect PKCα, which is known to positively regulate cellular migration, with the scaffold DLG1, which acts to enable migration via interactions with numerous proteins involved in motility. Specifically, we identify a novel PDZ ligand interaction of PKCα that is necessary for it to facilitate cell migration.

Acknowledgments

I thank Dr. C. Garner for the Myc-DLG1 plasmid, Dr. M. Dell'Acqua for the CFP-DLG1 plasmid, the NCI for the NSCLC cell lines, and members of the laboratories of Dr. Newton and Dr. J. Brugge for helpful discussions.

The text of Chapter 3 is, in part, a reprint of the material as it appears in the Journal of Biological Chemistry, 2011, by O'Neill AK, Gallegos LL, Justilien V, Garcia EL, Leitges M, Fields AP, Hall RA, and Newton AC. I was the co-primary author and researcher.

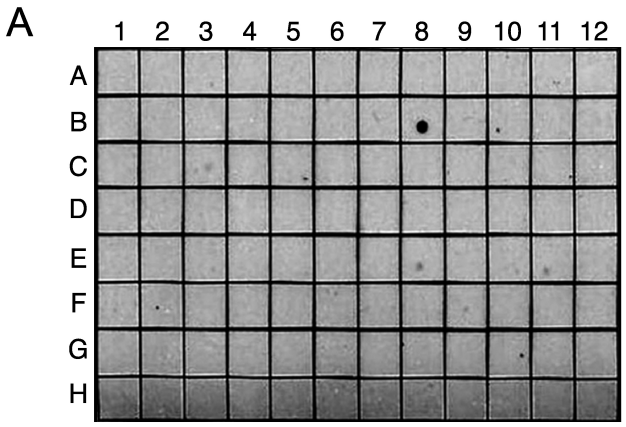

B

Bin	PDZ Domain	Bin	PDZ Domain
A1	MAGI-1 PDZ1	E1	RHOPHILIN-2
A2	MAGI-1 PDZ2	E2	HARMONIN PDZ1
A3	MAGI-1 PDZ3	E3	HARMONIN PDZ2
A4	MAGI-1 PDZ 4+5	E4	NEURABIN PDZ
A5	MAGI-2 PDZ1	E5	SPINOPHILIN PDZ
A6	MAGI-2 PDZ2	E6	α1-SYNTROPHIN
A7	MAGI-2 PDZ3	E7	β1-SYNTROPHIN
A8	MAGI-2 PDZ4	E8	β2-SYNTROPHIN
A9	MAGI-2 PDZ 5	E9	γ1-SYNTROPHIN
A10	MAGI-3 PDZ1	E10	γ2-SYNTROPHIN
A11	MAGI-3 PDZ2	E11	PAPIN 1
A12	MAGI-3 PDZ3	E12	MUPP1 PDZ1
B1	MAGI-3 PDZ4	F1	MUPP1 PDZ6
B2	MAGI-3 PDZ5	F2	MUPP1 PDZ7
B3	NHERF-1 PDZ1	F3	MUPP1 PDZ8
B4	NHERF-1 PDZ2	F4	MUPP1 PDZ 10
B5	NHERF-2 PDZ1	F5	MUPP1 PDZ12
B6	NHERF-2 PDZ2	F6	MUPP1 PDZ13
B7	PSD-95 PDZ1+2	F7	PTPN13 PDZ1
B8	PSD-95 PDZ3	F8	PTPN13 PDZ3
B9	PDZ-GEF1 PDZ	F9	PTPN13 PDZ4+5
B10	CAL PDZ	F10	PDZK1 PDZ1
B11	nNOS PDZ	F11	PDZK1 PDZ2
B12	INADL PDZ5	F12	PDZK1 PDZ3
C1	INADL PDZ6	G1	PDZK1 PDZ4
C2	DLG1 PDZ1+2	G2	PDZK2 PDZ1
C3	DLG1 PDZ3	G3	PDZK2 PDZ2
C4	SAP102 PDZ1+2	G4	PDZK2 PDZ3
C5	SAP102 PDZ3	G5	PDZK2 PDZ4
C6	CHAP110 PDZ1+2	G6	LNX1 PDZ1
C7	CHAP110 PDZ3	G7	LNX1 PDZ2
C8	E6TP1 PDZ	G8	LNX1 PDZ3
C9	ERBIN PDZ	G9	LNX1 PDZ4
C10	ZO-1 PDZ1	G10	LNX2 PDZ1
C11	ZO-1 PDZ2	G11	LNX2 PDZ2
C12	ZO-1 PDZ3	G12	LNX2 PDZ4
D1	ZO-2 PDZ1	H1	PTPN4 PDZ
D2	ZO-2 PDZ2	H2	RHO-GEF PDZ
D3	ZO-2 PDZ3	H3	RA-GEF PDZ
D4	ZO-3 PDZ1	H4	ENIGMA PDZ
D5	ZO-3 PDZ2	H5	LARG PDZ
D6	ZO-3 PDZ3	H6	MAST205 PDZ
D7	C2PA PDZ	H7	PTPN3 PDZ
D8	GIPC PDZ	H8	SHANK1 PDZ
D9	MALS-1 PDZ	H9	TAMALIN PDZ
D10	MALS-3 PDZ	H10	PAR-3 PDZ1
D11	DENSIN-180	H11	PAR-3 PDZ2
D12	RHOPHILIN-1	H12	PAR-3 PDZ3

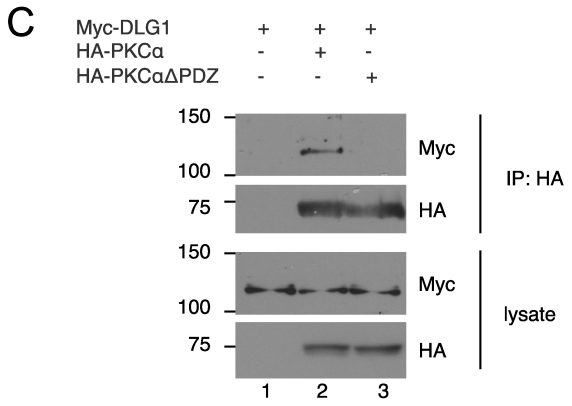

Figure 3.1: PKCα interacts via its PDZ ligand with the PDZ domain scaffold DLG1/SAP97.
A. PDZ domain array overlay. The last 25 amino acids of PKCα were tagged with GST and overlaid on an array of 96 PDZ domains. B. List of PDZ domains in the array shown in (A), with two positive interactions boxed. C. Co-immunoprecipitation of PKCα and DLG1. Myc-tagged DLG1 was expressed alone (lane 1) or in combination with HA-tagged PKCα (lane 2) or HA-tagged PKCα lacking the last three amino acids (HA-PKCαΔPDZ; lane 3) in HEK293T cells, PKCα was immunoprecipitated using the HA tag, and immunoprecipitates were probed for Myc-DLG1 or HA-PKCα.

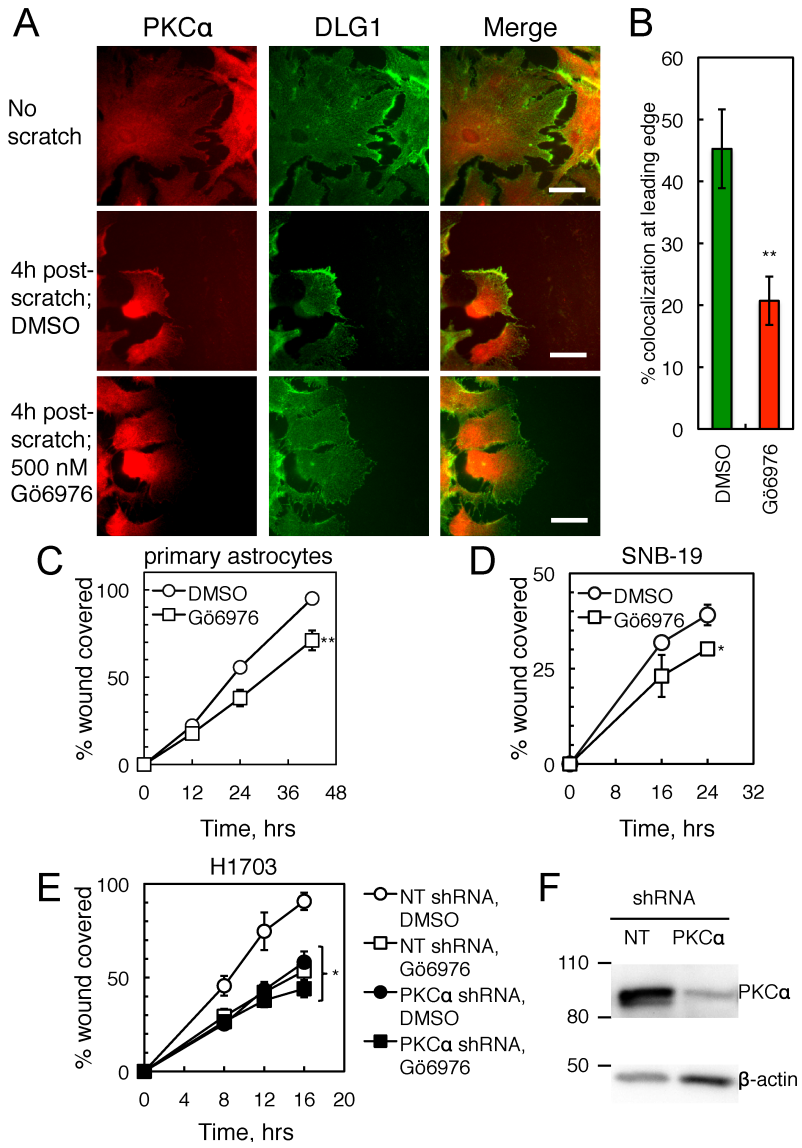

Figure 3.2: PKCα promotes cell migration in wound healing assays.
A. PKCα and DLG1 colocalization at the leading edge of migrating astrocytes. Primary murine astrocytes were pretreated with Gö6976 (500 nM; bottom row) or a corresponding amount of DMSO (middle row), scratched with a 10-uL pipet tip, fixed four hours after scratch, and stained for endogenous PKCα and DLG1. Scale bars: 50 nm. B. Quantification of the percent of cells with colocalization of PKCα and DLG1 at the leading edge of migrating cells (n=5 experiments with >30 cells per condition in each experiment). C, D, and E. Effect of cPKC inhibition on wound healing. Primary astrocytes (C), SNB-19 GBM cells (D), and stable non-targeting shRNA expressing (NT; open symbols) or PKCα shRNA-expressing (filled symbols) cell lines derived from H1703 NSCLC cells (E) were pre-treated with mitomycin C (to inhibit proliferation) followed by DMSO (circles) or Gö6976 (squares), scratched with a pipet tip, and followed over 12-42,16-24, or 8-16 hours, respectively. The area covered by migrating cells was quantified using ImageJ; data points represent the mean ± SEM of at least three experiments. F. Western blot showing PKCα knockdown efficiency for a representative experiment as in (E). After completion of the scratch assay, cells were lysed and lysates probed for PKCα and the loading control β-actin. *, significantly different from control DMSO-treated cells, $p<0.05$; **, $p<0.01$.

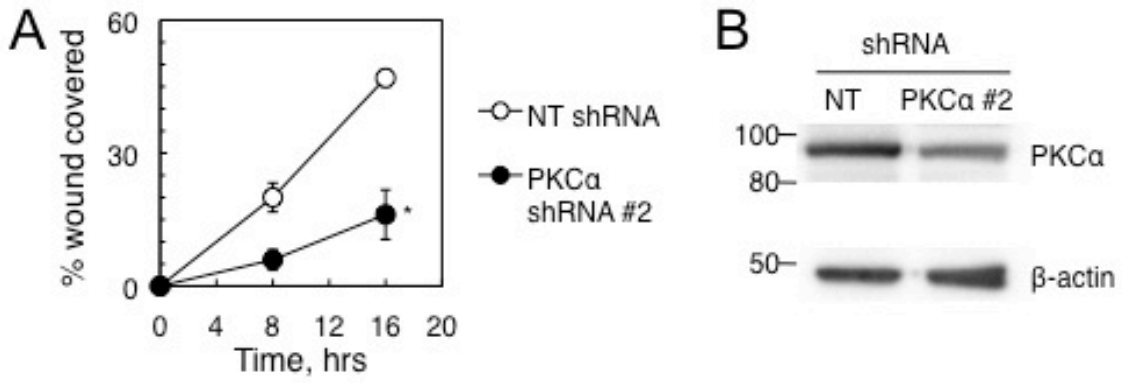

Figure 3.3: A second shRNA construct targeting PKCα also inhibits wound healing.
A. NT (open circles) or PKCα shRNA #2-expressing (filled circles) cell lines derived from H1703 NSCLC cells were subjected to a wound healing assay as described for Figure 3. Results reflect the means±SEM of three experiments. B. Western blot showing PKCα knockdown efficiency for a representative experiment as in (A). *, significantly different from NT shRNA-expressing cells, $p<0.05$.

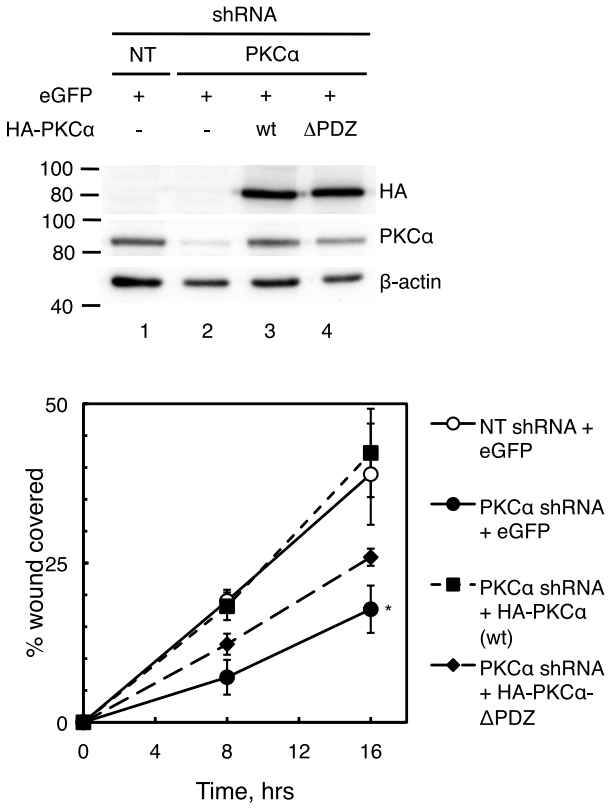

Figure 3.4: Wild type PKCα but not PKCα lacking the last three amino acids rescues wound healing in PKCα-depleted H1703 cells.
Upper panel: Western blot showing re-expression of bovine wild type (wt) HA-tagged PKCα or PKCα lacking the last three amino acids (ΔPDZ) in H1703 cells stably expressing NT or PKCα shRNA in a wound healing assay as described below. After completion of the scratch assay, cells were lysed and lysates probed for PKCα, HA, and ß-actin. Lower panel: effect of PKCα rescue on wound healing. The indicated H1703 cells were transiently transfected with eGFP (as a marker for transfection) with or without HA-PKCα or HA-PKCα-ΔPDZ. Cells were plated at equal densities and then pre-treated with mitomycin C (to inhibit proliferation), scratched with a pipet tip, and their migration monitored over 8-16 hours. The area covered by migrating cells was quantified using ImageJ, and data points represent the mean ± SEM of four experiments. *significantly different from the NT shRNA + eGFP condition, $p<0.05$.

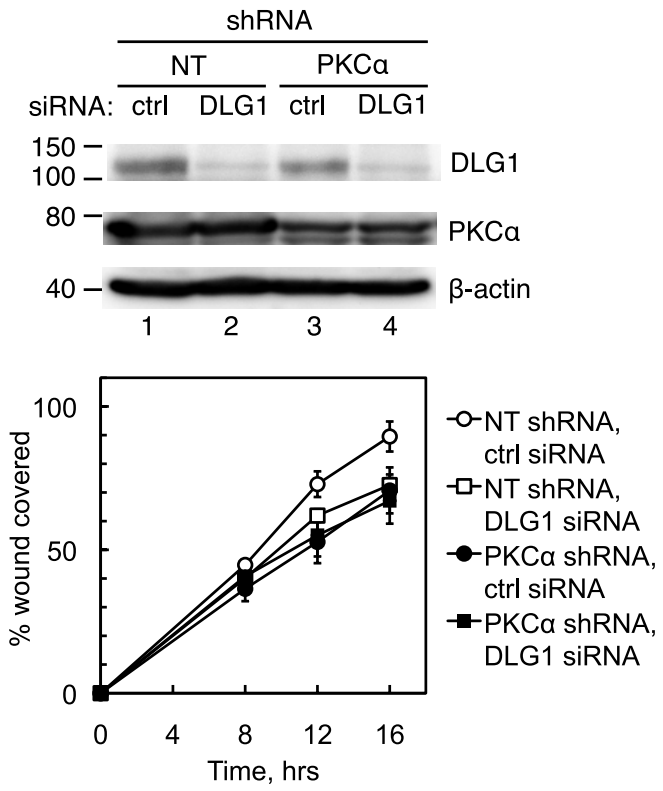

Figure 3.5: Interfering with DLG1 blocks the effects of PKCα knockdown on wound healing. Upper panel: Western blot showing DLG1 and PKCα knockdown efficiencies for a representative wound healing experiment as described below. After completion of the scratch assay, cells were lysed and lysates probed for PKCα, DLG1, and actin. Lower panel: effect of combined PKCα and DLG1 knockdown on wound healing. H1703 NSCLC cells stably expressing a non-targeting (NT) or a PKCα shRNA were transiently transfected with a scrambled siRNA pool (ctrl) or a siRNA pool targeting DLG1, re-plated, and subjected to a wound healing assay as described for Figure 3. Results reflect the means±SEM of three experiments.

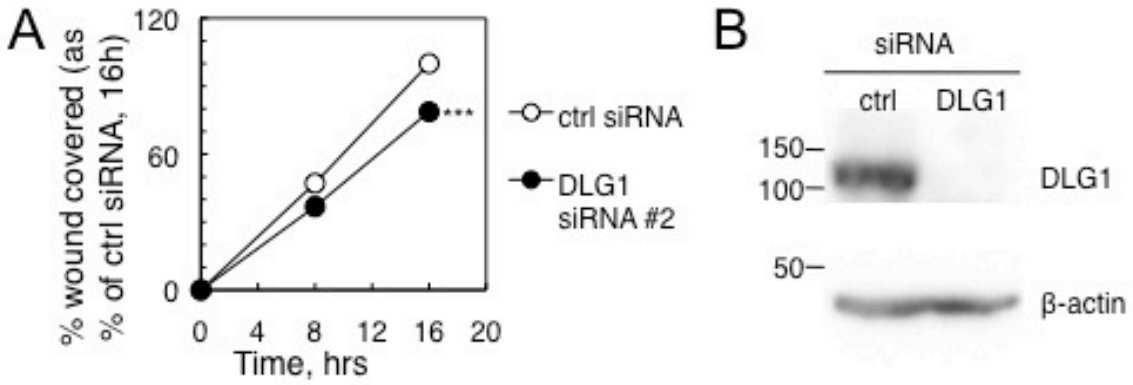

Figure 3.6: A second siRNA targeting DLG1 also inhibits wound healing.
A. H1703 cells transfected with a negative control siRNA (ctrl siRNA, open circles) or siRNA targeting DLG1 (DLG1 #2 siRNA, filled circles) were re-plated and subjected to a wound healing assay as described for Figure 3. Results were normalized to the values for the control cells and reflect the means±SEM of 8 experiments. B. Western blot showing DLG1 knockdown efficiency for a representative experiment as in (A). ***, significantly different from control cells, $p<0.001$.

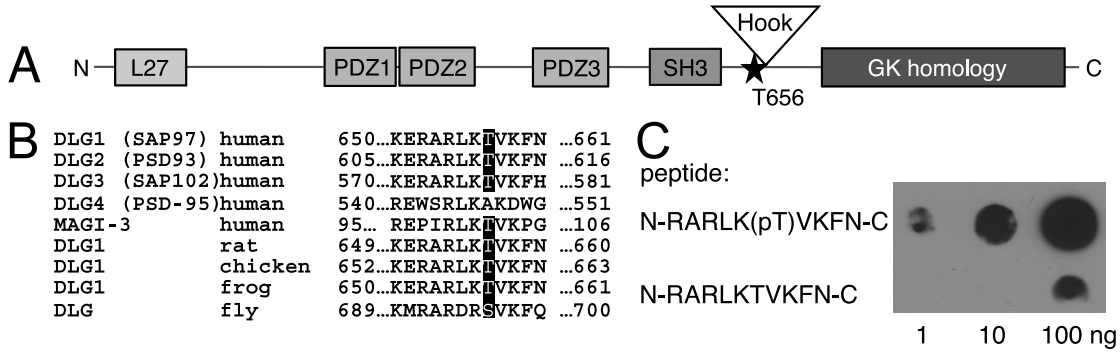

Figure 3.7: DLG1 contains a conserved conventional PKC phosphorylation site.
A. Domain architecture of rat DLG1/SAP97, showing the location of a putative PKC phosphorylation site, identified using Scansite, at threonine 656. B. Alignment showing conservation of the PKC phosphorylation site in three out of four human DLG isoforms and DLG isoforms from lower organisms. C. Generation of an antibody specific for DLG1 phosphorylated at T656. Various amounts of phospho- and de-phospho peptides corresponding to residues 649-661 of human DLG1 were spotted onto nitrocellulose and overlaid with the phospho-specific (pT656) antibody.

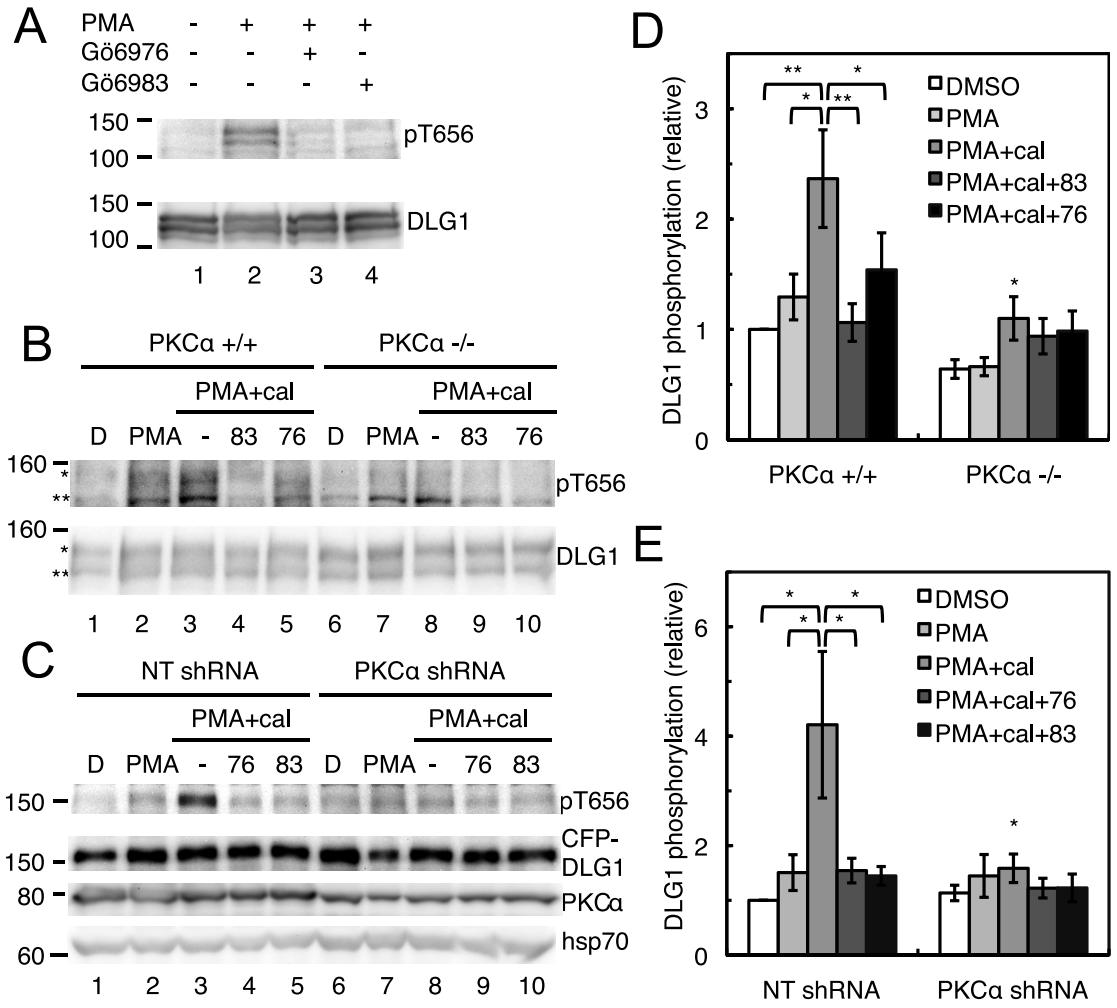

Figure 3.8: PKCα phosphorylates DLG1 at T656.
A. cPKC-dependent phosphorylation of DLG1. Primary murine astrocytes were treated for 30 minutes with vehicle or PMA (lanes 2-4) and Gö6976 (lane 3), or Gö6983 (lane 4). Cells were lysed and lysates probed for levels of phospho- and total DLG1. B. DLG1 phosphorylation in the presence and absence of PKCα. Immortalized wild type MEFs (PKCα +/+) or MEFs lacking the gene for PKCα (PKCα -/-) were pretreated with DMSO (denoted by "D"), Gö6983 (83), or Gö6976 (76) for 10 minutes prior to the addition of PMA for 20 minutes and the phosphatase inhibitor calyculin A (cal) for the last two minutes of PMA treatment. Cells were lysed and lysates probed for DLG1 phosphorylated at T656 (pT656; relevant bands marked with asterisks) and total DLG1 levels. C. Changes in DLG1 phosphorylation upon PKCα knockdown. H1703 NSCLC cells stably expressing a non-targeting (NT) or a PKCα shRNA were transfected with CFP-tagged DLG1 and treated as described in B; lysates were probed for pT656, DLG1, PKCα, and the loading control heat shock protein 90 (hsp90). D. Bar graph representing the mean ± SEM of 8 experiments as described in B. E. Bar graph representing the mean ± SEM of 7 experiments as described in C. Significantly different from control PMA+cal-treated cells, *, $p<0.05$; **, $p<0.01$.

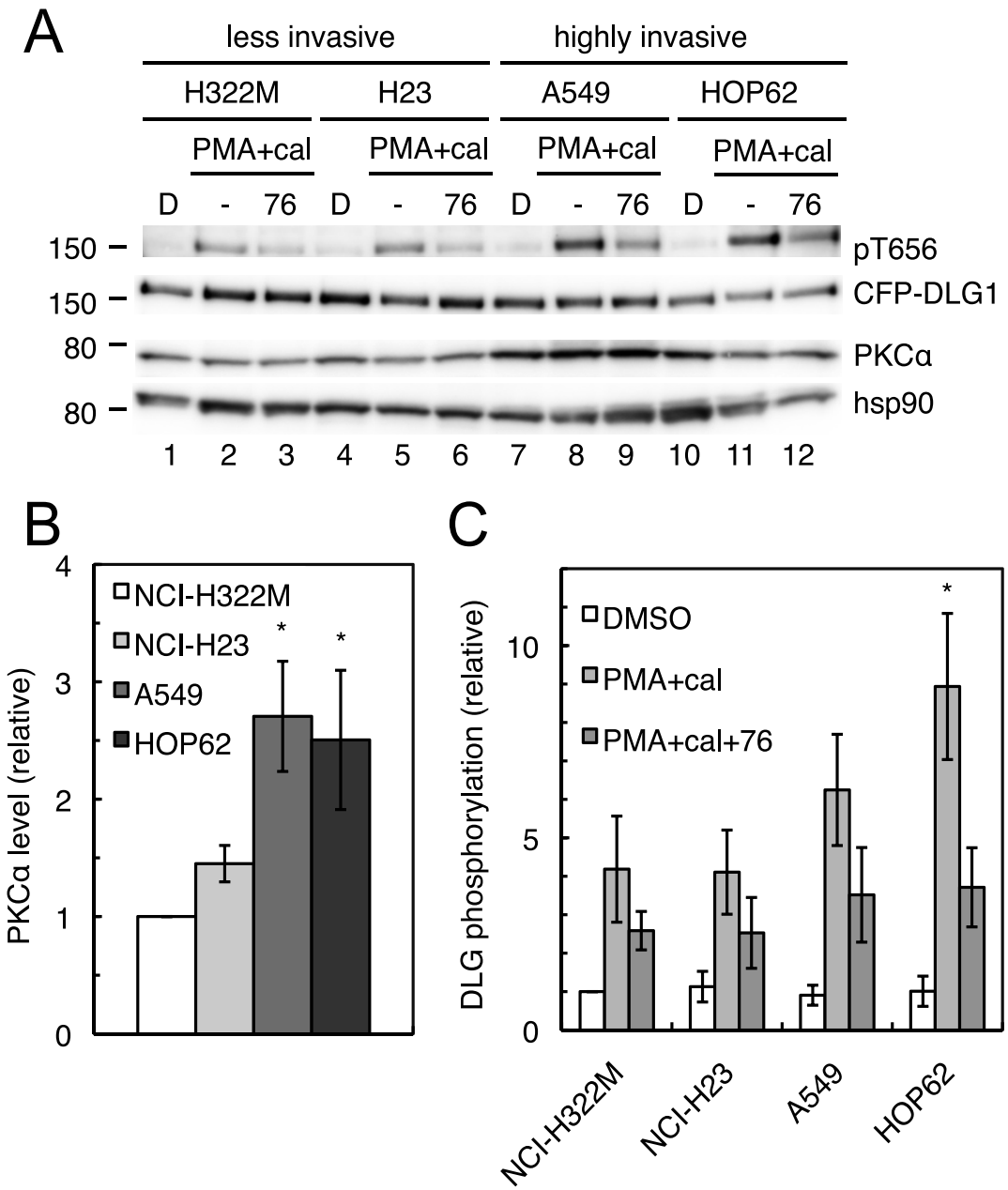

Figure 3.9: PKCα signaling at the DLG1 scaffold is increased in highly invasive NSCLC lines relative to their less invasive counterparts.

A. PKCα expression and phosphorylation of DLG1 at T656 in NSCLC lines. NCI-H322M, NCI-H23, A549, and HOP62 cells were transiently transfected with CFP-DLG1 and pretreated with DMSO (denoted by "D") or the PKC inhibitor Gö6976 (76) for 10 minutes prior to the addition of PMA for 20 minutes and the phosphatase inhibitor calyculin A (cal) for the last 10 minutes of PMA treatment. Cells were lysed and the lysates probed for pT656, DLG1, PKCα, and the loading control hsp90. B and C. Bar graphs representing the mean ± SEM of PKCα expression (B) and DLG1 phosphorylation at T656 (C) in 8 experiments as described in A. Gö6976-reversible phosphorylation was calculated by subtracting the relative phosphorylation in the PMA+cal+76 condition from the relative phosphorylation in the PMA+cal condition. Significantly different from H322M cells, *, $p<0.05$.

References

1. Pawson, C. T., and Scott, J. D. (2010) *Nature structural & molecular biology* **17**, 653-658

2. Rosse, C., Linch, M., Kermorgant, S., Cameron, A. J., Boeckeler, K., and Parker, P. J. (2010) *Nat Rev Mol Cell Biol* **11**, 103-112

3. Newton, A. C. (2010) *Am J Physiol Endocrinol Metab* **298**, E395-402

4. Dempsey, E. C., Newton, A. C., Mochly-Rosen, D., Fields, A. P., Reyland, M. E., Insel, P. A., and Messing, R. O. (2000) *Am J Physiol Lung Cell Mol Physiol* **279**, L429-438

5. Castagna, M., Takai, Y., Kaibuchi, K., Sano, K., Kikkawa, U., and Nishizuka, Y. (1982) *J Biol Chem* **257**, 7847-7851

6. Konopatskaya, O., and Poole, A. W. (2010) *Trends Pharmacol Sci* **31**, 8-14

7. Fan, Q. W., Cheng, C., Knight, Z. A., Haas-Kogan, D., Stokoe, D., James, C. D., McCormick, F., Shokat, K. M., and Weiss, W. A. (2009) *Sci Signal* **2**, ra4

8. Guo, J., Ibaragi, S., Zhu, T., Luo, L. Y., Hu, G. F., Huppi, P. S., and Chen, C. Y. (2008) *Cancer Res* **68**, 8473-8481

9. Holinstat, M., Mehta, D., Kozasa, T., Minshall, R. D., and Malik, A. B. (2003) *J Biol Chem* **278**, 28793-28798

10. Larsson, C. (2006) *Cell Signal* **18**, 276-284

11. Dean, N., McKay, R., Miraglia, L., Howard, R., Cooper, S., Giddings, J., Nicklin, P., Meister, L., Ziel, R., Geiger, T., Muller, M., and Fabbro, D. (1996) *Cancer Res* **56**, 3499-3507

12. Paz-Ares, L., Douillard, J. Y., Koralewski, P., Manegold, C., Smit, E. F., Reyes, J. M., Chang, G. C., John, W. J., Peterson, P. M., Obasaju, C. K., Lahn, M., and Gandara, D. R. (2006) *J Clin Oncol* **24**, 1428-1434

13. Fields, A. P., and Murray, N. R. (2008) *Adv Enzyme Regul* **48**, 166-178

14. Mochly-Rosen, D., Khaner, H., and Lopez, J. (1991) *Proc Natl Acad Sci U S A* **88**, 3997-4000

15. Mochly-Rosen, D., and Gordon, A. S. (1998) *FASEB J* **12**, 35-42

16. Poole, A. W., Pula, G., Hers, I., Crosby, D., and Jones, M. L. (2004) *Trends Pharmacol Sci* **25**, 528-535

17. Tsunoda, S., Sierralta, J., Sun, Y., Bodner, R., Suzuki, E., Becker, A., Socolich, M., and Zuker, C. S. (1997) *Nature* **388**, 243-249

18. Adamski, F. M., Zhu, M. Y., Bahiraei, F., and Shieh, B. H. (1998) *J Biol Chem* **273**, 17713-17719

19. van Ham, M., and Hendriks, W. (2003) *Mol Biol Rep* **30**, 69-82

20. Lee, H. J., and Zheng, J. J. (2010) *Cell Commun Signal* **8**, 8

21. Staudinger, J., Lu, J., and Olson, E. N. (1997) *J Biol Chem* **272**, 32019-32024

22. Leitges, M., Kovac, J., Plomann, M., and Linden, D. J. (2004) *Neuron* **44**, 585-594

23. Lim, I. A., Hall, D. D., and Hell, J. W. (2002) *J Biol Chem* **277**, 21697-21711

24. Colledge, M., Dean, R. A., Scott, G. K., Langeberg, L. K., Huganir, R. L., and Scott, J. D. (2000) *Neuron* **27**, 107-119

25. Kunkel, M. T., Garcia, E. L., Kajimoto, T., Hall, R. A., and Newton, A. C. (2009) *J Biol Chem* **284**, 24653-24661

26. Lau, A. G., and Hall, R. A. (2001) *Biochemistry* **40**, 8572-8580

27. Citro, S., Malik, S., Oestreich, E. A., Radeff-Huang, J., Kelley, G. G., Smrcka, A. V., and Brown, J. H. (2007) *Proc Natl Acad Sci U S A* **104**, 15543-15548

28. Valster, A., Tran, N. L., Nakada, M., Berens, M. E., Chan, A. Y., and Symons, M. (2005) *Methods* **37**, 208-215

29. Roberts, S., Calautti, E., Vanderweil, S., Nguyen, H. O., Foley, A., Baden, H. P., and Viel, A. (2007) *Exp Cell Res* **313**, 2521-2530

30. Hsu, Y. C., Yuan, S., Chen, H. Y., Yu, S. L., Liu, C. H., Hsu, P. Y., Wu, G., Lin, C. H., Chang, G. C., Li, K. C., and Yang, P. C. (2009) *Clin Cancer Res* **15**, 7309-7315

31. Park, E. S., Rabinovsky, R., Carey, M., Hennessy, B. T., Agarwal, R., Liu, W., Ju, Z., Deng, W., Lu, Y., Woo, H. G., Kim, S. B., Cheong, J. H., Garraway, L. A., Weinstein, J. N., Mills, G. B., Lee, J. S., and Davies, M. A. (2010) *Mol Cancer Ther* **9**, 257-267

32. Abeyweera, T. P., Chen, X., and Rotenberg, S. A. (2009) *J Biol Chem* **284**, 17648-17656

33. Anilkumar, N., Parsons, M., Monk, R., Ng, T., and Adams, J. C. (2003) *EMBO J* **22**, 5390-5402

34. Bass, M. D., Roach, K. A., Morgan, M. R., Mostafavi-Pour, Z., Schoen, T., Muramatsu, T., Mayer, U., Ballestrem, C., Spatz, J. P., and Humphries, M. J. (2007) *J Cell Biol* **177**, 527-538

35. Elfenbein, A., Rhodes, J. M., Meller, J., Schwartz, M. A., Matsuda, M., and Simons, M. (2009) *J Cell Biol* **186**, 75-83

36. Horowitz, A., Tkachenko, E., and Simons, M. (2002) *J Cell Biol* **157**, 715-725

37. Kim, J., Thorne, S. H., Sun, L., Huang, B., and Mochly-Rosen, D. (2011) *Oncogene* **30**, 323-333

38. Kohutek, Z. A., diPierro, C. G., Redpath, G. T., and Hussaini, I. M. (2009) *J Neurosci* **29**, 4605-4615

39. Lin, C. W., Shen, S. C., Chien, C. C., Yang, L. Y., Shia, L. T., and Chen, Y. C. (2010) *J Cell Physiol* **225**, 472-481

40. Arora, S., Ranade, A. R., Tran, N. L., Nasser, S., Sridhar, S., Korn, R. L., Ross, J. T., Dhruv, H., Foss, K. M., Sibenaller, Z., Ryken, T., Gotway, M. B., Kim, S., and Weiss, G. J. (2011) *Int J Cancer* **10.1002/ijc.25939**

41. Bilder, D. (2004) *Genes Dev* **18**, 1909-1925

42. Humbert, P. O., Grzeschik, N. A., Brumby, A. M., Galea, R., Elsum, I., and Richardson, H. E. (2008) *Oncogene* **27**, 6888-6907

43. Cavatorta, A. L., Fumero, G., Chouhy, D., Aguirre, R., Nocito, A. L., Giri, A. A., Banks, L., and Gardiol, D. (2004) *Int J Cancer* **111**, 373-380

44. Unno, K., Hanada, T., and Chishti, A. H. (2008) *Experimental cell research* **314**, 3118-3129

45. Caruana, G., and Bernstein, A. (2001) *Mol Cell Biol* **21**, 1475-1483

46. Etienne-Manneville, S., Manneville, J. B., Nicholls, S., Ferenczi, M. A., and Hall, A. (2005) *J Cell Biol* **170**, 895-901

47. Manneville, J. B., Jehanno, M., and Etienne-Manneville, S. (2010) *J Cell Biol* **191**, 585-598

48. Dujardin, D. L., and Vallee, R. B. (2002) *Curr Opin Cell Biol* **14**, 44-49

49. Hough, C. D., Woods, D. F., Park, S., and Bryant, P. J. (1997) *Genes Dev* **11**, 3242-3253

50. Newman, R. A., and Prehoda, K. E. (2009) *J Biol Chem* **284**, 12924-12932

51. Funke, L., Dakoji, S., and Bredt, D. S. (2005) *Annu Rev Biochem* **74**, 219-245

52. Marcello, E., Gardoni, F., Mauceri, D., Romorini, S., Jeromin, A., Epis, R., Borroni, B., Cattabeni, F., Sala, C., Padovani, A., and Di Luca, M. (2007) *J Neurosci* **27**, 1682-1691

53. Lue, R. A., Marfatia, S. M., Branton, D., and Chishti, A. H. (1994) *Proc Natl Acad Sci U S A* **91**, 9818-9822

54. Parra, M., Gascard, P., Walensky, L. D., Gimm, J. A., Blackshaw, S., Chan, N., Takakuwa, Y., Berger, T., Lee, G., Chasis, J. A., Snyder, S. H., Mohandas, N., and Conboy, J. G. (2000) *J Biol Chem* **275**, 3247-3255

55. Diakowski, W., Grzybek, M., and Sikorski, A. F. (2006) *Folia Histochem Cytobiol* **44**, 231-248

56. Manno, S., Takakuwa, Y., and Mohandas, N. (2005) *J Biol Chem* **280**, 7581-7587

Chapter 4:

Summary and Conclusions

With the recent explosion of studies examining mechanisms of cellular signal transduction has come the realization that the concept of signaling as a linear, orderly process connecting stimulus to response is a gross oversimplification. Rather, signaling is mediated through complex networks of protein-protein interactions (involving not only enzymes and small molecule second messengers but also scaffolds and other proteins) that display considerable amounts of redundancy, auto-regulation (through feedback loops), and spatiotemporal constraint. Completely mapping these systems will require not only biochemical techniques but also genetic manipulations that enable examination of the effect of depleting or deleting a specific member of the network. These types of perturbations, along with reliable measures of specific cellular outputs, allow researchers to determine which signaling components are essential for a given output and, crucially, which components act in the same genetic pathways to regulate cellular behaviors. In this thesis, I have employed genetic techniques to determine that 1) the phosphatase PHLPP1 is dispensable for normal development but is necessary under conditions requiring tight control of Akt signaling, and 2) the kinase PKCα and the scaffold DLG1 cooperate to promote cellular migration in lung cancer cells (Figure 4.1).

Mice lacking PHLPP1 develop normally and do not display increases in insulin signaling – As shown in Chapter 2, PHLPP1-null mice are born at the expected Mendelian ratios, develop normally, and demonstrate no obvious abnormalities apart from a slight decrease in size. Unexpectedly, I did not observe any changes in the levels or phosphorylation of the targets of PHLPP (Akt, PKC isozymes, and the EGF receptor) in tissues and primary MEFs from these mice. Also, both insulin secretion and sensitivity were intact in PHLPP1-null mice fed a normal chow diet, and subjecting the mice to a high fat diet revealed no differences in overall glucose tolerance and only a slight decrease (i.e., the opposite of the expected effect) in insulin sensitivity. Taken together, these data suggest that PHLPP1 is not necessary for Akt or PKC

dephosphorylation in the intact mouse, despite being expressed in every tissue examined, albeit at varying levels. One possible explanation for these results (discussed in more detail below) is that PHLPP2, which is also ubiquitously expressed, can compensate for the loss of PHLPP1 in most normal situations, and that PHLPP1 is required to provide an additional level of control only when certain physiological systems or other regulators of the Akt pathway are perturbed.

PKCα and DLG1 cooperate to allow directed cellular migration – A screen to identify binding partners for the PDZ ligand of PKCα resulted in the discovery of a PDZ-dependent interaction between PKCα and the MAGUK family scaffold DLG1. These proteins colocalize at several sites of actin dynamics, including invadopodia and the leading edge of migrating astrocytes. Though I determined that DLG1 is dispensable for invadopodia formation and maintenance, I found that DLG1 and PKCα are both required for efficient cellular migration in a wound healing assay. Notably, these two proteins act in the same genetic pathway, and PKCα's PDZ ligand is required for its effects on wound healing, suggesting that the interaction between them is critical for their effects on migration. One consequence of this interaction is the phosphorylation of DLG1 at a conserved threonine by PKCα; though mutation of this phosphorylation site is without effect on wound healing (and invadopodia formation), it is located in a region of the protein that is important for intramolecular interactions and could be important for other functions of DLG1, as discussed in more detail below. Also, phosphorylation of this site might serve as a marker of invasiveness in human lung cancer, because a highly invasive subset of lung cancer cell lines from the NCI-60 have increased DLG1 phosphorylation relative to their less invasive counterparts. Altogether, the studies presented in Chapter 3 provide a possible mechanistic explanation for the well-known role of PKCα in cytoskeletal dynamics, namely that this isozyme, by virtue of its unique PDZ ligand, can specifically control and be controlled by PDZ domain-containing scaffolds such as DLG1.

Therapeutic implications

The lack of a dramatic phenotype in the PHLPP1-null mouse has several implications for possible therapies based on modulating signaling through the PI3K/Akt pathway. First, as suggested by Chen and colleagues (1), inactivation of another negative regulator of the system (such as PTEN or PHLPP2) in addition to PHLPP1 may be necessary to promote full-blown prostate carcinogenesis *in vivo*. Studies in PHLPP1-null MEFs support this hypothesis: given the lack of upregulation of growth factor signaling in primary MEFs as compared to immortalized MEFs (Figure 2.7), it is logical to conclude that additional genetic alterations as necessary to permit oncogenic signaling in cells lacking PHLPP1. Recent work by Georgescu and colleagues in GBM has also led to the conclusion that PHLPP1 acts as an "extra layer of inhibition" of Akt signaling: in samples from patients with GBM, PHLPP1 and PTEN protein levels are frequently co-downregulated, and in LN229 GBM cells, PHLPP1 levels are only negatively correlated with Akt phosphorylation when PTEN is deleted (2). Taken together, these results imply that loss of PHLPP1 alone may not initiate increased Akt signaling and carcinogenesis but may instead be a secondary event that allows cancer progression. In particular, co-deletion of PHLPP1 and PTEN could turn out to be a strong predictor of advanced disease, though this idea remains to be fully tested.

Interpreting the results of the PHLPP1 deletion studies with respect to treatment of human cancer is difficult; the lack of a dramatic effect of loss of PHLPP1 could mean that Akt (and PHLPP's other targets) are not very sensitive to overall gene dosage and thus may not be affected by treatments seeking to upregulate PHLPP's activity. However, reconstituting PHLPP1β in immortalized PHLPP1-null MEFs rescues at least some of the effects of PHLPP1 deletion (M. Niederst, G. Reyes-Cava, M.T. Kunkel, J. Brognard, J. Enserink, and A.C. Newton, manuscript in preparation), implying that upregulation of overall PHLPP activity may be a valid strategy in the treatment of cancers that have lost PHLPP1. Also noteworthy is the fact that PHLPP2 seems able to compensate for the loss of PHLPP1, even in tissues that have high levels of Akt2 (the canonical target of PHLPP1), such as white adipose tissue and skeletal muscle ((3); see Figures

2.3 and 2.7). Under conditions of transient knockdown in human lung cancer cells, PHLPP1 and PHLPP2 have non-redundant functions in dephosphorylating specific Akt isozymes; in the whole-body knockout mouse, this does not appear to be the case. This implies that therapeutic strategies that increase the activity of either PHLPP will cause decreases in the phosphorylation of all three Akt isozymes, a finding which should be taken into account in diseases such as breast cancer, where activation of Akt1 versus Akt2 have opposing effects on cancer development (4). Ultimately, further research into the other substrates of PHLPP, as well as determination of the physiological effects of deleting and/or upregulating both PHLPPs, will be necessary before PHLPP activation can be used as a therapeutic strategy.

The finding that both PKCα and its binding partner DLG1 are essential for directed motility in lung cancer cells raises the possibility that interfering with either of these proteins, or with their interaction, could reduce metastasis in human lung cancer. DLG1 is highly expressed in normal lung and in lung cancer, while PKCα staining is low or absent in normal lung but expressed in at least 20% of stage I/II non-small cell lung cancers (5,6). Thus, either protein could be a viable target in lung cancer, especially with treatment targeted towards cancers expressing PKCα. An antisense oligonucleotide directed against PKCα yielded positive results in phase I/II clinical trials in lung cancer but failed to meet standards in phase III trials (7,8). This disappointing lack of effect could be due to several factors, including 1) failure to stratify potential subjects based on PKCα expression and 2) effects of PKCα inhibition on cellular behaviors other than metastasis.

Our results implicating DLG1 in the control of motility driven by PKCα suggest that interfering with the interaction between the two proteins could be a novel way to specifically repress invasion by lung cancer cells. The idea that PDZ-driven protein-protein interactions can be abolished using small molecules that mimic PDZ ligands is not new (for review, see (9)); indeed, such a molecule has recently been used to disrupt the interaction between the PDZ scaffold PICK1 and its ligand GluR2, blocking the expression of long-term depression and long-

term potentiation in hippocampal slices (10). Theoretically, a peptide corresponding to the PDZ ligand of PKCα could be used to block PKCα's interaction with DLG1 and/or other PDZ scaffolds, leading to decreased lung cancer cell motility and metastasis *in vivo*, though much work clearly remains to be done before the efficacy of this approach can be tested.

Another possible applications of the studies presented in Chapter 3 relates to the use of DLG1 phosphorylation as a biomarker. Because PKCα activity at DLG1 is important for cell motility, we hypothesized that phosphorylation of DLG1 at T656 would correlate with increased metastasis *in vivo*. Though we have not fully tested this theory in metastatic versus non-metastatic patient samples, our work in highly invasive versus non-invasive lung cancer cell lines strongly supports the use of T656 phosphorylation as a marker of invasive capability. Ideally, lung cancer patients in whom PKCα levels are upregulated would also be tested for increased DLG1 phosphorylation at this site, which might help predict their metastatic risk.

Unanswered questions and future directions

An obvious question raised by this work is why deletion of the gene for PHLPP1, which has been shown to be essential for efficient dephosphorylation of the hydrophobic motif of Akt (among other targets), does not result in changes in Akt phosphorylation in normal mouse tissues or in the derangement of processes that critically depend on regulation of Akt, such as growth and insulin signaling. An attractive hypothesis is that PHLPP2 can compensate for the loss of PHLPP1 *in vivo*; attempts to generate a PHLPP2-null mouse are ongoing and will eventually provide a definitive answer to this question. Another possibility is that PHLPP1 is only required in situations where particularly tight control of Akt is called for (e.g., in regulatory T cells) or where other factors restraining Akt signaling (e.g., PTEN) are lost. This theory is compatible with the results of studies comparing primary and immortalized MEFs lacking PHLPP1, which showed that immortalized PHLPP1-null cells have increases in growth factor signaling and oncogenic properties such as resistance to apoptosis relative to primary PHLPP1-null cells. It seems clear that the immortalized cells acquired additional modifications during the immortalization process

that allow for upregulated phosphorylation of Akt and other targets of PHLPP1. The identity of these modifications is unknown, but studies in the prostate tissue of mice lacking PHLPP1 suggest that mutation of p53 cooperates with loss of PHLPP1 to promote carcinogenesis, making p53 an attractive candidate. Functional loss of this protein would allow cells to escape senescence, which is critical for extended proliferation in culture. Future studies examining the effect of mutated p53 in PHLPP1-deleted or PHLPP1-depleted cells could shed more light on this possibility.

Our data also shows that DLG1 specifically scaffolds PKCα, allowing it to positively regulate cellular migration. However, the mechanisms underlying this effect are unclear. Though phosphorylation of DLG1 at T656 does not appear to affect migration, it is possible that our overexpression system did not adequately capture the role of endogenous DLG1 phosphorylation, or that DLG1 is phosphorylated by PKCα at other sites, allowing regulation of migration. More likely, however, given DLG1's scaffolding functions, is the hypothesis that DLG1 scaffolds PKCα near a substrate protein that is critical for migration. One candidate is protein 4.1, a protein involved in spectrin-actin association that has been shown to bind DLG1's PDZ domains in vitro. (This association does not appear to be driven by a canonical PDZ ligand-based interaction, because the N-terminal region of 4.1 also binds DLG1's PDZ domains.) (11) Interestingly, 4.1 not only colocalizes with DLG1 at cell-cell junctions (11) but is also phosphorylated by PKC at a conserved serine (12), prompting spectrin to dissociate from actin and allowing a decrease in membrane stability (13). It would be interesting to determine if a form of PKCα that cannot bind DLG1 has the same effects on 4.1 phosphorylation and membrane stability, or if DLG1 is required for PKCα to exert its effects. Another PKC substrate that binds DLG1 is ADAM-10, which cleaves N-cadherin, resulting in increased cell motility and metastasis. PKCα appears to be essential for ADAM-10's ability to translocate to the membrane, where it cleaves N-cadherin (14). DLG1 has been shown to interact with ADAM-10 in neurons, where it may act to cleave Aβ; interestingly, a peptide that blocks the interaction between ADAM-10 and

DLG1 reduces Aβ cleavage, raising the possibility that DLG1 may promote cleavage of N-cadherin via a similar mechanism (15). Experiments using this peptide could help determine whether DLG1 binding is required for PKCα to promote ADAM-10's translocation and activity towards N-cadherin. Another possibility is that PKCα could help regulate DLG1's interactions with previously characterized binding partners involved in cellular migration. For example, DLG1 is known to bind GKAP and through it dynein intermediate chain, and these interactions seem to be important for the proper organization of microtubules during migration (16,17). It would be interesting to determine whether PKCα activity is necessary for these interactions to occur, or if PKCα phosphorylates any of the members of this complex. PKCα has recently been shown to phosphorylate α6-tubulin (18), but the manner in which it is targeted to this substrate has not been explored and may depend on scaffolding by DLG1. Finally, the mechanisms by which DLG1 regulates migration are understudied, but it appears that DLG1 is required for proper microtubule organizing center (MTOC) reorientation and the establishment of cell polarity during migration via interactions with adenomatous polyposis coli (APC) (16). If inhibition of cPKC activity were found to mimic the effects of disrupting the APC-DLG1 interaction (which results in a lack of polarization of MTOCs in the desired direction of cell movement), it might indicate that PKCα exerts its effects on migration by promoting proper cell polarization through DLG1.

A related question concerns the mechanism of DLG1 and PKCα localization at the leading edge of migrating astrocytes. It seems likely that movement along actin or microtubule filaments is involved, although preferential sequestration of these two proteins (by actin-binding factors, for instance) could also play a role. Actin, myosin, and microtubules are all involved in lamellipodial extension and collective cell migration, though actin seems to play a dominant role in driving membrane protrusions (19). Determining which structural proteins are necessary for PKCα/DLG1 colocalization would provide a starting place for examination of the mechanisms that are necessary for enrichment of these two proteins at the leading edge and might also suggest ways that cPKC signaling could contribute to this enrichment.

In this work we discovered a novel PKC phosphorylation site in the Hook region of DLG1; though mutating this site had little effect on wound healing in our system, it might affect other uninvestigated functions of the scaffold. In particular, it might affect DLG1's ability to bind itself in *cis* and *trans*. The interaction between the SH3 and GK has been shown to be important for receptor clustering mediated by DLG1's close relative PSD-95 (20), and the SH3-GK interaction in DLG1 is important for the development of cell polarity in *Drosophila* (21) and for proper MTOC reorientation in migrating astrocytes (17). The crystal structure of this region of PSD-95 has been solved; though PSD-95 lacks the PKC substrate motif found in DLG1, it does suggest that the area in which it lies is important for facilitating the interaction between the SH3 and GK domains (22). It would be interesting, therefore, to generate mutants of the DLG1 SH3-Hook domain in which the T656 phosphorylation site was absent and to compare the binding of the mutant domain to the GK domain with that of the wild type region. Another, broader approach to determining the effects of phosphorylation at this site might involve a proteomic screen to determine binding partners for wild type DLG1 versus DLG1-T656A; preliminary results from such a study indicate that the T656A mutant may preferentially bind myosin and myosin-associated proteins (data not shown). Experiments such as these could reveal the molecular functions and suggest possible downstream consequences of phosphorylation at this site.

In this thesis, I have investigated signaling through both PKCα and its negative regulator PHLPP1 with an eye to the redundancy and specificity present in the pathways of which these proteins are members. Studies in PHLPP1-null mice demonstrated that PHLPP1 is dispensable for normal development and for insulin signaling, suggesting a compensatory role for PHLPP2 or other repressors of the PI3K/Akt pathway. Investigation of the oncogenic properties of PHLPP1-null MEFs revealed that PHLPP1 becomes more critical for restraining growth factor signaling in immortalized cells and that PHLPP1 loss may cooperate with other mutations in promoting cancer *in vivo*. I also investigated specificity in PKC signaling mediated by the PDZ ligand unique to PKCα, which mediated binding of this isozyme to the scaffolding protein DLG1. This interaction

proved critical for the ability of PKCα to support directed migration in NSCLC cells, and PKCα activity at this scaffold (read out as phosphorylation of a conserved threonine residue on DLG1) served as a marker for invasiveness in a panel of NSCLC lines. These results have implications for the use of PHLPP activators and PKCα inhibitors to block the growth and metastasis of various cancers, though a full understanding of the mechanisms of signaling by these enzymes will require much more investigation.

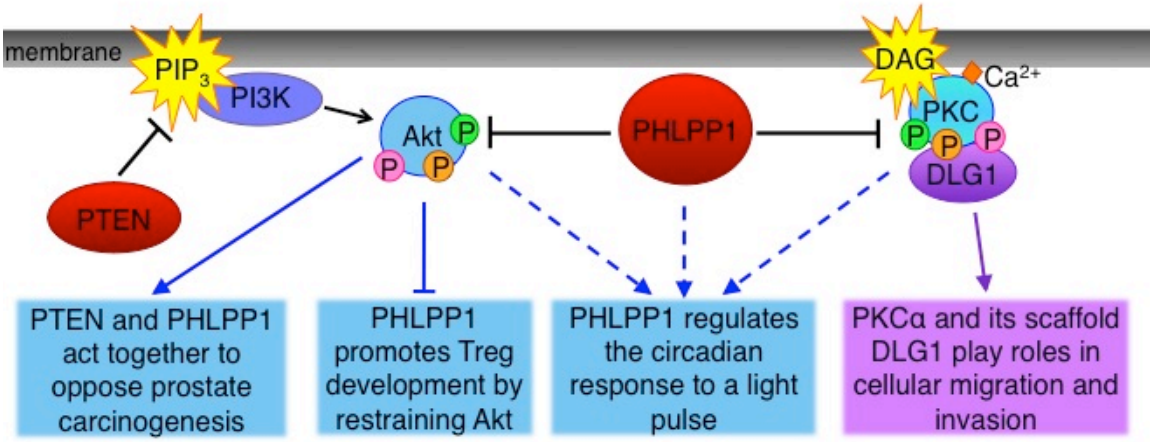

Figure 4.1: Conclusions.
1) PHLPP1, though dispensable for normal development, helps regulate several biological processes in vivo. It acts together with PTEN to oppose Akt signaling during the development of prostate cancer and also restrains Akt signaling in regulatory T cells (Tregs). PHLPP1 also regulates changes in circadian rhythm prompted by a light pulse, via unknown mechanisms (dashed lines). 2) PKCα binds the scaffolding protein DLG1 via a novel PDZ-driven interaction. Both proteins are necessary for the efficient migration of lung cancer cells, and PKCα activity at the scaffold is a marker for invasive potential.

References

1. Chen, M., Pratt, C. P., Zeeman, M. E., Schultz, N., Taylor, B. S., O'Neill, A., Castillo-Martin, M., Nowak, D. G., Naguib, A., Grace, D. M., Murn, J., Navin, N., Atwal, G. S., Sander, C., Gerald, W. L., Cordon-Cardo, C., Newton, A. C., Carver, B. S., and Trotman, L. C. (2011) *Cancer Cell* **20**, 173-186

2. Molina, J. R., Agarwal, N. K., Morales, F. C., Hayashi, Y., Aldape, K. D., Cote, G., and Georgescu, M. M. (2011) *Oncogene*

3. Yang, Z. Z., Tschopp, O., Hemmings-Mieszczak, M., Feng, J., Brodbeck, D., Perentes, E., and Hemmings, B. A. (2003) *J Biol Chem* **278**, 32124-32131

4. Maroulakou, I. G., Oemler, W., Naber, S. P., and Tsichlis, P. N. (2007) *Cancer Res* **67**, 167-177

5. Lahn, M., Su, C., Li, S., Chedid, M., Hanna, K. R., Graff, J. R., Sandusky, G. E., Ma, D., Niyikiza, C., Sundell, K. L., John, W. J., Giordano, T. J., Beer, D. G., Paterson, B. M., Su, E. W., and Bumol, T. F. (2004) *Clinical lung cancer* **6**, 184-189

6. Uhlen, M., Oksvold, P., Fagerberg, L., Lundberg, E., Jonasson, K., Forsberg, M., Zwahlen, M., Kampf, C., Wester, K., Hober, S., Wernerus, H., Bjorling, L., and Ponten, F. (2010) *Nature biotechnology* **28**, 1248-1250

7. Konopatskaya, O., and Poole, A. W. (2010) *Trends Pharmacol Sci* **31**, 8-14

8. Paz-Ares, L., Douillard, J. Y., Koralewski, P., Manegold, C., Smit, E. F., Reyes, J. M., Chang, G. C., John, W. J., Peterson, P. M., Obasaju, C. K., Lahn, M., and Gandara, D. R. (2006) *J Clin Oncol* **24**, 1428-1434

9. Blazer, L. L., and Neubig, R. R. (2009) *Neuropsychopharmacology : official publication of the American College of Neuropsychopharmacology* **34**, 126-141

10. Thorsen, T. S., Madsen, K. L., Rebola, N., Rathje, M., Anggono, V., Bach, A., Moreira, I. S., Stuhr-Hansen, N., Dyhring, T., Peters, D., Beuming, T., Huganir, R., Weinstein, H., Mulle, C., Stromgaard, K., Ronn, L. C., and Gether, U. (2010) *Proceedings of the National Academy of Sciences of the United States of America* **107**, 413-418

11. Lue, R. A., Marfatia, S. M., Branton, D., and Chishti, A. H. (1994) *Proc Natl Acad Sci U S A* **91**, 9818-9822

12. Parra, M., Gascard, P., Walensky, L. D., Gimm, J. A., Blackshaw, S., Chan, N., Takakuwa, Y., Berger, T., Lee, G., Chasis, J. A., Snyder, S. H., Mohandas, N., and Conboy, J. G. (2000) *J Biol Chem* **275**, 3247-3255

13. Manno, S., Takakuwa, Y., and Mohandas, N. (2005) *J Biol Chem* **280**, 7581-7587

14. Kohutek, Z. A., diPierro, C. G., Redpath, G. T., and Hussaini, I. M. (2009) *J Neurosci* **29**, 4605-4615

15. Marcello, E., Gardoni, F., Mauceri, D., Romorini, S., Jeromin, A., Epis, R., Borroni, B., Cattabeni, F., Sala, C., Padovani, A., and Di Luca, M. (2007) *J Neurosci* **27**, 1682-1691

16. Etienne-Manneville, S., Manneville, J. B., Nicholls, S., Ferenczi, M. A., and Hall, A. (2005) *J Cell Biol* **170**, 895-901

17. Manneville, J. B., Jehanno, M., and Etienne-Manneville, S. (2010) *J Cell Biol* **191**, 585-598

18. Abeyweera, T. P., Chen, X., and Rotenberg, S. A. (2009) *J Biol Chem* **284**, 17648-17656

19. Ridley, A. J. (2011) *Cell* **145**, 1012-1022

20. Shin, H., Hsueh, Y. P., Yang, F. C., Kim, E., and Sheng, M. (2000) *J Neurosci* **20**, 3580-3587

21. Newman, R. A., and Prehoda, K. E. (2009) *J Biol Chem* **284**, 12924-12932

22. McGee, A. W., Dakoji, S. R., Olsen, O., Bredt, D. S., Lim, W. A., and Prehoda, K. E. (2001) *Molecular cell* **8**, 1291-1301

Appendix A:

PKCα signaling in invadopodia

Abstract

Among PKC's known roles in cytoskeletal dynamics is the maintenance of invadopodia or podosomes, dynamic actin-based structures that mediate adhesion to the extracellular matrix and matrix degradation. In cancer cells, invadopodia mediate mesenchymal-type motility and invasion and may be crucial for metastasis. Building on an initial observation that PKCα and DLG1 colocalize at invadopodia-like structures in fibroblast-like cos7 cells, I investigated the roles of these two proteins in Src-transformed fibroblasts, which have well-defined invadopodia. I found that both proteins localize at these structures and that conventional PKC signaling is necessary but not sufficient for invadopodia formation. However, neither DLG1 localization at invadopodia nor DLG1 expression is necessary for invadopodia formation or stability, suggesting that PKCα regulates invadopodia formation by other mechanisms.

Introduction

Podosomes and invadopodia are actin-based structures that mediate adhesion to the extracellular matrix (ECM) and, critically, matrix degradation (1,2). The current convention in the podosome/invadopodia field is to use "podosomes" to refer to structures found in normal cells (such as macrophages, osteoclasts, and smooth muscle cells) and "invadopodia" to refer to structures found in transformed and carcinoma cells (3). Podosomes and invadopodia share common features: they are composed of an actin-rich core surrounded by a ring of actin-binding proteins and signaling factors, are found at the ventral (matrix-binding) surface of cells, and require formation of branched and unbranched actin filaments. Most importantly, they are involved in processes that require matrix remodeling, whether they are bone remodeling and monocyte extravasation (in normal cells) or invasion and metastasis (in cancer cells). However, there are some important differences between podosomes and invadopdodia. First, podosomes are generally ring-like in appearance (with a three-dimensional diameter of 0.5-2 μm), whereas

invadopodia are usually punctate; though their width is roughly equivalent to that of podosomes, they tend to protrude farther into the matrix. Also, microtubules are required for the formation and elongation of podosomes but only for the elongation of invadopodia, implying that the two structures have different modes of formation. Similarly, invadopodia have relatively long half-lives (on the order of hours), whereas podosomes turn over rapidly (within minutes), and the actin molecules within them turn over even faster (1,3). (Notably, invadopodia/podosomes were first characterized in Src-transformed fibroblasts; in these cells, they have characteristics of both podosomes (ring-like structure, rapid turnover) and invadopodia (larger size, transformed cell type). In keeping with the current convention, I will refer to the structures present on these cells as "invadopodia" (3).) Actin dynamics mediated by the actin nucleation complex Arp2/3 and the formins mDia 1-3 are critical for the formation of both invadopodia and podosomes (2,4).

In addition to actin and microtubules, many other structural and signaling proteins are required for invadopodia/podosome formation [reviewed in (3,5)]. These include integrins, which link the cytoskeleton to the ECM and participate in ECM-induced signaling (6); cortactin, which supports actin nucleation and inhibits actin de-branching, leading to the assembly of new actin networks (7,8); Rho GTPases, particularly Cdc42 (4); the actin polymerization factor N-WASP (Neural Wiskott-Aldrich syndrome protein), which acts downstream of Cdc42 (7); adaptor proteins including Tks5 (tyrosine kinase substrate with five SH3 domains)(9) and AFAP (actin filament associated protein) 110 (10); and proteases such as MT1-MMP (membrane type 1-matrix metalloprotease) (11) and ADAM-15, which are critical for ECM degradation. Invadopodia/podosomes are major sites of tyrosine phosphorylation, so it is unsurprising that several tyrosine kinases and phosphatases are present at these structures. Of these, the best characterized is Src, which stimulates actin nucleation and phosphorylates a number of invadopodium components, including cortactin, Tks5, AFAP-110, N-WASP, and integrins (3,12). PKC is also involved in signaling at invadopodia; phorbol esters have been shown to promote podosome formation in a number of cell types, including human umbilical vein endothelial cells

(13), osteoclasts (14), and smooth muscle cells (15). PKC phosphorylates AFAP-110, N-WASP, β1-integrin, and fascin (an actin bundling protein required for invadopodia stability) and is thought to mediate invadopodia maintenance. Thus, PKC and Src have overlapping sets of substrates and may synergize to promote invadopodia formation and stabilization (12).

Though PKC signaling is important for invadopodia, it is unclear which isozymes mediate the effects of phorbol esters in this context and how PKC-mediated phosphorylation events control invadopodia formation. (See the discussion for a detailed description of the available data on PKC signaling in invadopodia.) The studies in this chapter were prompted by the finding that when cos7 cells overexpressing fluorescently tagged PKCα and DLG1 are treated with phorbol esters, the fluorescent proteins assemble into rings that strongly resemble podosomes (L.L. Gallegos, unpublished observations). This result suggested the hypothesis that PKCα and DLG1 act to promote podosome/invadopodia formation; thus, the objective of these studies was to investigate the roles of these two proteins in invadopodia formation and maintenance in Src-transformed fibroblasts, with particular focus on the function of DLG1 phosphorylation at T656. The results of these experiments confirm that 1) endogenous PKCα and DLG1 colocalize at invadopodia; 2) cPKC activity is indeed necessary for invadopodia formation and maintenance in these cells (though phorbol ester treatment does not increase invadopodia formation); and 3) DLG1 knockdown has no effect on invadopodia formation, suggesting that the effects of PKCα are mediated by other substrates and/or scaffolding proteins.

Materials and Methods

Materials – Phorbol myristate acetate (PMA), UO126, PP2, and Gö6976 were purchased from Calbiochem and used at the concentrations indicated below. Electrophoresis reagents were from Bio-Rad Laboratories, Inc. Src-transformed fibroblasts were a generous gift from S. Courtneidge. All other reagents and chemicals were reagent-grade.

Antibodies – Antibodies and dilutions used were: mouse anti-Myc (1:1,000, 9E10; Covance), mouse anti-DLG1 (1:500 for Western blot, 1:200 for immunofluorescence (IF) staining;

Stressgen), rabbit anti-PKCα (1:1000 for Western blot, 1:200 for IF staining; Santa Cruz), rabbit anti-Tks5 (1:1,000; a generous gift of Sara Courtneidge), rabbit anti-GFP (1:1,000; Cell signaling), and mouse anti-actin (1:1,000; Sigma). Secondary antibodies for immunofluorescence were: goat anti-mouse-Alexa 568, goat anti-rabbit-Alexa 488, goat anti-mouse-Alexa 488, and goat anti-rabbit-Alexa 568, all from Invitrogen. Actin was stained in fixed cells using phalloidin-Alexa 647 or phalloidin-Alexa 546 (1:500; Invitrogen).

Plasmids, siRNA, and transfection – Myc-tagged DLG1 was a gift from C. Garner; mutagenesis of T656 was performed using a QuikChange site-directed mutagenesis kit according to the manufacturer's protocol (Stratagene, Inc.). DLG1 constructs were transfected into Src3T3 cells using Jetprime (Polyplus, Inc.) according to the manufacturer's instructions, and cells were fixed for examination by immunofluoresence (IF) on the day after transfection. A pool of three siRNAs directed against mouse DLG1 was obtained from Santa Cruz (catalog number sc-36453), along with a non-targeting control siRNA (catalog number sc-37007); both siRNA reagents were used at a final concentration of 50 nM. Src3T3 cells were transfected with the indicated siRNA reagent using Lipofectamine 2000 (Invitrogen) according to the manufacturer's instructions; 24 hours later, they were re-plated onto 6-well tissue culture plates for Western blotting and to cover slips for IF analysis. Cells were lysed (for Western blotting) or fixed (for IF) 24 hours after re-plating (48 hours after transfection).

Cell culture, drug treatment, and Western blotting – Src3T3 cells were maintained in DMEM (Cellgro) supplemented with 10% fetal bovine serum (FBS, Hyclone) and 1% penicillin/streptomycin (P/S) and treated for the indicated times at 37 °C with PMA (200 nM), Gö6976 (500 nM), UO126 (25 μM), and/or PP2 (10 μM). All stock solutions used were in DMSO, and a corresponding amount of DMSO was used as a control. For the invadopodia re-formation assay, the PP2-containing media was applied to cells for 30 minutes, after which the cells were washed twice with PBS and then incubated in new media containing DMSO or Gö6976. For immunoblotting, cells were lysed in RIPA buffer (consisting of 50 mM Tris [pH 7.4], 150 mM NaCl,

1% Triton, 0.1% sodium dodecyl sulfate (SDS), 0.5% sodium deoxycholate, 0.1% SDS, 30 mM sodium pyrophosphate, 0.1 mM sodium vanadate, 200 mM benzamidine, 40 mg/ml leupeptin, and 1 mM PMSF). Protein levels were analyzed by SDS-PAGE and Western blotting.

Immunofluorescence (IF) analysis – Cells plated onto cover slips were rinsed twice in ice-cold PBS, fixed in 4% paraformaldehyde for 15 min, rinsed twice with ice-cold PBS, incubated in quenching buffer (50 mM NH_4Cl, 10 mM PIPES [pH 6.8], 150 mM NaCl, 5 mM EGTA, 5 mM glucose, and 5 mM $MgCl_2$) for 15 minutes, rinsed twice with cold PBS, permeabilized with 0.5% Triton in PBS for 15 minutes, blocked for one hour in 1% goat serum in PBS and incubated overnight in primary antibody diluted in 1% goat serum in PBS. All of the preceding steps were performed at 4°C. The next day, the cover slips were washed three times in PBS containing 0.1% Triton and incubated for one hour at room temperature in PBS containing the following: 1% goat serum; diluted, Alexa-conjugated phalloidin; and (when applicable) diluted, Alexa-conjugated secondary antibodies. The cover slips were then washed twice in PBS containing 1% Triton and once in quenching buffer, air-dried, and mounted onto slides using Vectashield mounting media (Vector Labs) containing 4',6-diamidino-2-phenylindole (DAPI) for staining of the nuclei. Slides were visualized and photographed using a Zeiss Axiovert microscope (Carl Zeiss Microimaging, Inc.) with a MicroMax digital camera (Roper-Princeton Instruments) controlled by MetaFluor software (Universal Imaging, Corp.). Photographs were acquired using a 10% neutral density filter and the following setups: for DAPI images, a 420/20-nm excitation filter, a 450-nm dichroic mirror, and a 475/40-nm emission filter were used; for Alexa 568 images, a 560/25-nm excitation filter, a 593-nm dichroic mirror, and a 629/53-nm emission filter were used; for Alexa 488 images, a 480/30-nm excitation filter, a 505-nm dichroic mirror, and a 535/45-nm emission filter were used; and for Alexa 647 images, a 635/20-nm excitation filter, a 660-nm dichroic mirror, and a 680/30-nm emission filter were used. Excitation and emission filters were switched in filter wheels (Lambda 10–2, Sutter). Photographs were taken and analyzed by an observer who was blinded to the treatment conditions. Cells were analyzed for the presence of at least one actin-based ring

or “rosette” corresponding to an invadopodium (as described in (16)). For the DLG1 localization experiments, cells with rosettes were analyzed for the association of DLG1 staining with an actin-based ring. At least 30 cells were counted per experimental point, and all experiments were repeated at least twice. For presentation, images were pseudo-colored and merged using ImageJ (NIH).

Results

PKCα and DLG1 colocalize at invadopodia in Src-trasformed fibroblasts – NIH3T3 fibroblasts transformed by v-Src (henceforth referred to as Src3T3 cells) are characterized by the presence of large, ring-shaped invadopodia that stain positive for actin and numerous other invadopodia markers, including cortactin and Tks5 (3,9). We examined the distribution of PKCα and DLG1 in these cells by immunofluorescence staining and found that both proteins co-localize with Tks5 at actin rosettes/invadopodia (Figure A.1). Neither protein was restricted to invadopodia, however, consistent with the known effects of PKCα and DLG1 in other cellular regions.

Inhibition of cPKC activity opposes invadopodia formation – To determine whether PKC activity is necessary for the formation and/or maintenance of invadopodia, I treated Src3T3 cells with the conventional PKC inhibitor Gö6976, stained them for actin, and examined the number of cells containing one or more actin-based rosettes in a blinded fashion (Figure A.2A-B). As a positive control, I treated a separate set of cells with the MEK (mitogen-activated protein kinase kinase) inhibitor U1026 for 6 hours; in these cells, prolonged treatment with UO126 results in inhibition of ERK5, which is necessary for invadopodia maintenance (16). Treatment with Gö6976 resulted in a 30±10% decrease in the number of cells with invadopodia, which was comparable to that observed with the positive control UO126 (40±20%); these data indicate that cPKC signaling is necessary to maintain the steady state levels of invadopodia. I next investigated whether cPKC activity was necessary for the efficient formation of these structures using an invadopodia re-formation assay (Figure A.2C). In Src3T3 cells, the maintenance of invadopodia is heavily

dependent on Src activity, and treatment with the Src inhibitor PP2 for 30 minutes results in the complete abolition of these structures (data not shown). However, these actin-based structures turn over rapidly (1); once the PP2-containing media is washed out and replaced with normal media, invadopodia re-form within 5 minutes, and the number of cells containing rosettes returns to a normal level of approximately 30% within 60 minutes. Therefore, I examined the effect of Gö6976 on invadopodia levels during the first 30 minutes after PP2 washout and found that the rate of invadopodia formation was decreased by approximately 30% (Figure A.2D), implying that cPKC activity is necessary for invadopodia formation.

Increasing PKC activity is not sufficient to increase the number of cells with invadopodia – Stimulation of PKC activity with phorbol esters such as PMA is known to stimulate podosome formation in several normal cell types (13,15); to test whether PKC stimulation had a similar effect in Src3T3 cells, I treated the cells with PMA for 20 minutes and examined the number of cells with invadopodia. Contrary to my hypothesis, I observed no change in the percentage of cells with invadopodia after treatment with PMA (Figure A.3A-B).

DLG1 localization at invadopodia requires cPKC activity but not phosphorylation of T656 – I began to examine possible mechanisms underlying the effects of PKC on invadopodia by assessing the localization of DLG1 at these structures under conditions of PKC inhibition. Treatment of Src3T3 cells with Gö6976 resulted in not only a reduction in the number of cells with invadopodia (see Figure A.2A-B) but also reduced the invadopodial localization of DLG1 in cells that still had invadopodia (Figure A.4A-B). I also tested the localization of exogenous, Myc-tagged DLG1 phosphorylation mutants after Gö6976 treatment by immunofluorescent staining for Myc and found slightly higher localization of the overexpressed wild type DLG1 at invadopodia (compared to the endogenous protein). However, mutation of the phospho-acceptor site to a non-phosphorylatable residue (T656A) or a phospho-mimetic (T656E) had no significant effect on the localization of DLG1, nor did it alter the Gö6976-induced change in localization. These data

suggest that the effects of cPKC activity on invadopodia and on DLG1 localization are not driven by PKCα-mediated phosphorylation of DLG1 at T656.

DLG1 is not necessary for invadopodia integrity – To determine if scaffolding by DLG1 played a role in PKC's effects on invadopodia, I first tested if DLG1 was necessary for invadopodia formation by depleting DLG1 from Src3T3 cells (Figure A.5A) and examining the percentage of cells with invadopodia. Inhibiting DLG1 production by approximately 50% had no effect on invadopodia maintenance (Figure A.5B) or formation (in the invadopodia re-formation assay described in Figure A.2C; data not shown).

Discussion

In this appendix, I have presented data showing that PKCα and DLG1 co-localize at invadopodia in Src3T3 cells and that cPKC activity is required for invadopodia formation. These results suggest that PKC is an initiating as well as a stabilizing factor for invadopodia in these cells, contrary to the hypothesis that Src is solely responsible for invadopodia formation. However, because invadopodia formation in these cells is so heavily dependent on Src activity, teasing out the exact contribution of these two enzymes may prove difficult. Previous studies support the idea that cooperation between PKC and Src is necessary for the formation of these structures. Quintavalle et al. (17) implicate crosstalk between PKCε and Src in PDGF-induced podosome formation in A7r5 smooth muscle cells; PKCα may also play a role in podosome formation in these cells, as PdBu induces the formation of PKCα-containing podosomes in a cPKC-dependent manner (15). Thus, the role of PKC and the specific PKC isozyme involved may vary depending on the stimulus used to promote podosome formation. In Src3T3 cells, PKC stimulation with PMA did not further increase the number of cells with invadopodia (Figure A.3). In these experiments, I treated cells with PMA for 20 minutes, which may not have been long enough to see effects on invadopodia stability. However, given the rapid turnover of these structures and given that cPKC inhibition has effects within 20 minutes of treatment (Figure A.2), it seems unlikely that this length of treatment (which results in maximal PKC activation) was

insufficient. Another possibility is that PKC activation, though necessary, is not rate limiting for invadopodia formation in this cell type.

The mechanisms by which PKC activity supports invadopodia formation are still unknown. Conventional PKC inhibition promotes the translocation of DLG1 away from invadopodia (Figure A.4), but at least some of the cells without DLG1 at the invadopodia are able to maintain these structures, implying that DLG1 is not necessary for invadopodia maintenance. This conclusion is confirmed by studies showing that depletion of DLG1 has no effect on invadopodia in Src3T3 cells (Figure A.5). Apart for DLG1, there are a number of other PKC-binding proteins that may be involved in invadopodia/podosome formation and stability. The PKC substrate and scaffold SSeCKS (Src-suppressed C kinase substrate) seems to act to repress invadopodia formation in prostate cancer cells by inhibiting PKC and MEK (18). Also, the PKC substrate fascin is required for the stability of invadopodia and for invasion of mesenchymal-type melanoma cells in a 3D matrix; however, a non-phosphorylatable form of fascin (S39A) also promotes invadopodia formation, suggesting that PKC may negatively regulate invadopodia in these cells (19). Finally, in a cell system similar to that used in this chapter (SYF fibroblasts re-expressing c-Src), Myr-PKCα promotes podosome formation in a manner that seems to depend on the actin cross-linking protein and PKC substrate AFAP-110, which scaffolds PKCα and Src, resulting in Src activation (10,20). Thus, PKC binding to scaffolds promotes invadopodia formation in several different ways, including cooperation with other kinases (MEK and Src) and direct effects on actin. The data presented in this chapter unveil a previously unknown role for conventional PKC signaling in invadopodia in Src3T3 cells and indicate that PKC specifically acts to promote invadopodia formation in these cells.

Acknowledgements

I thank Dr. Lisa Gallegos (currently at Harvard Medical School) for initial data concerning the formation of invadopodia-like structures in cos7 cells and staining of DLG1 and PKCα in Src3T3 cells, Dr. Sara Courtneidge (Sanford Burnham Medical Research Institute) for the gifts of

Src3T3 cells and the Tks5 antibody, and Dr. Craig Garner (Stanford University) for the gift of the Myc-DLG1 construct.

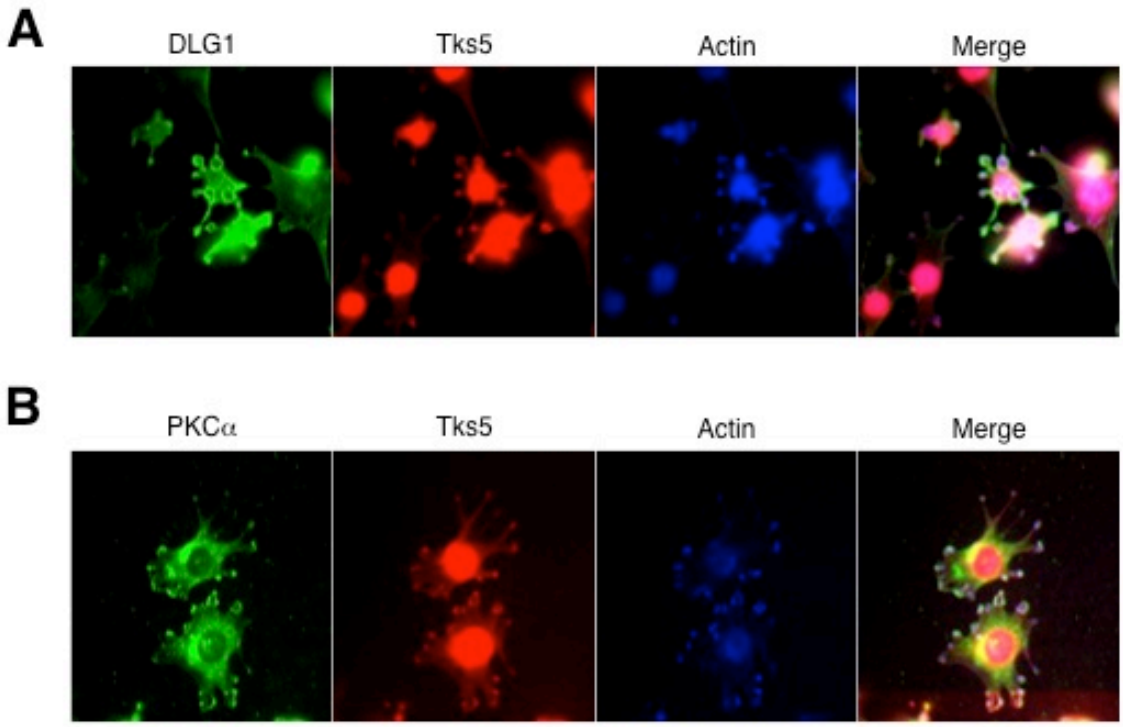

Figure A.1: DLG1 and PKCα are both present at invadopodia in Src-transformed 3T3 fibroblasts. The images depict Src3T3 cells co-stained with phalloidin (to mark actin; blue), and antibodies against the invadopodia marker Tks5 (red) and DLG1 (panel A, green) or PKCα (panel B, green). Merged images are also shown.

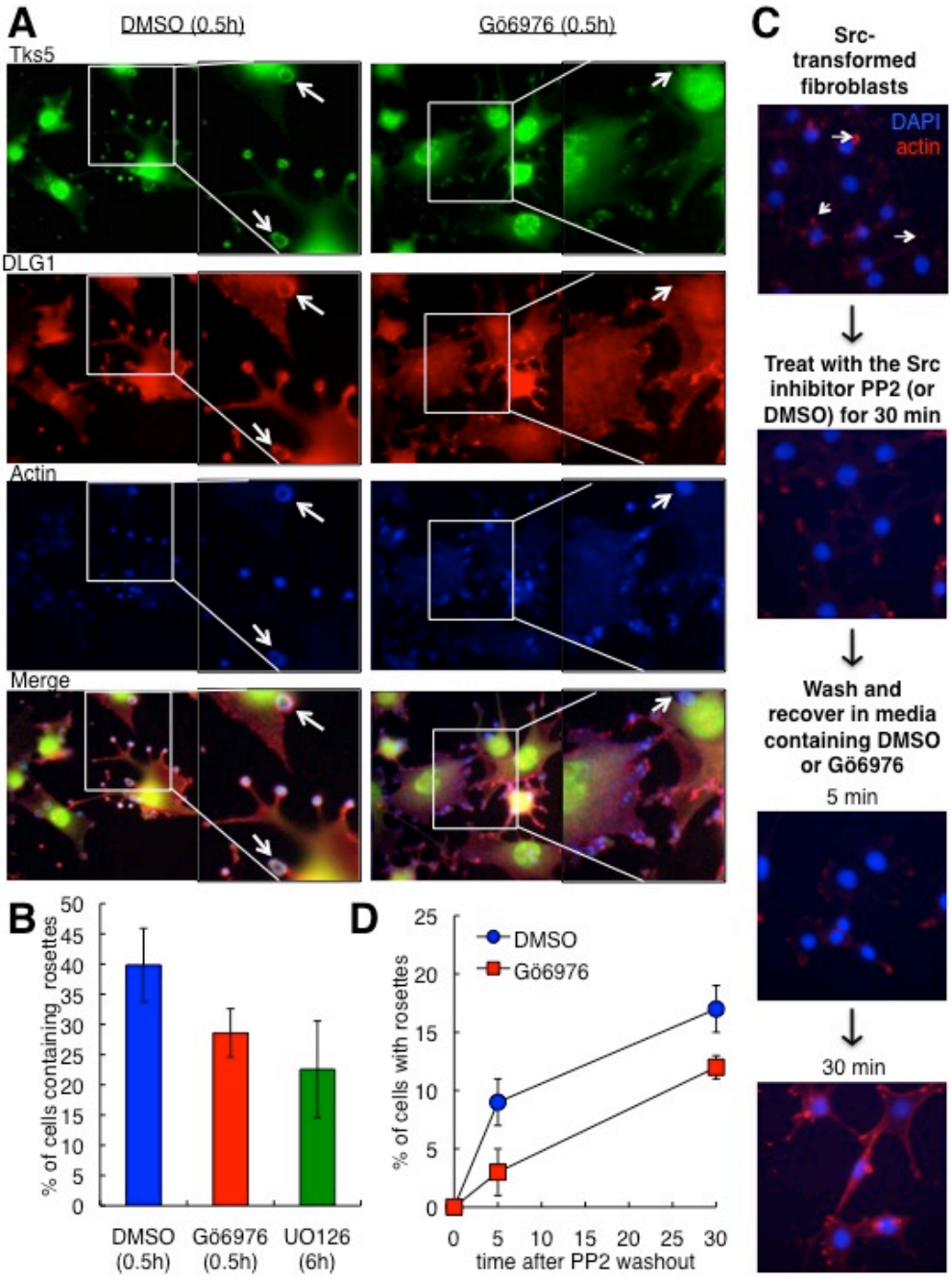

Figure A.2: Conventional PKC activity is necessary for the maintenance and formation of invadopodia in Src-trasformed 3T3 fibroblasts.

A. Staining of Src3T3 cells treated with DMSO or the cPKC inhibitor Gö6976 for 30 minutes and stained for Tks5, DLG1, and actin. The arrows in the insets mark actin-based rings or “rosettes”, corresponding to invadopodia. B. Quantification of the number of cells containing one or more actin-based rosettes after treatment with DMSO, Gö6976, or the positive control UO126 (n=5 experiments as in A). C. Invadopodia re-formation assay. Images of cells (stained with DAPI to label nuclei and phalloidin to label actin) show abolition of invadopodia rosettes upon treatment with PP2 and recovery of rosettes at 5 and 30 minutes after PP2 washout. D. Quantification of the number of cells containing one or more actin-based rosettes after treatment with PP2 followed by washout and treatment with DMSO or Gö6976 (n=3 experiments as in C).

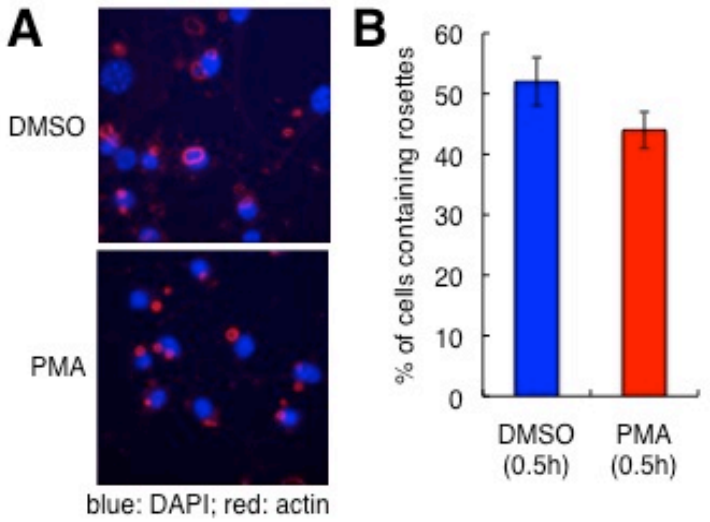

Figure A.3: Stimulation of PKC activity is not sufficient to increase invadopodia formation in Src-transformed fibroblasts.
A. Src3T3 cells treated with DMSO or PMA and stained with DAPI (blue) to label nuclei and phalloidin (red) to label actin. B. Quantification of the number of cells containing one or more actin-based rosettes after treatment with DMSO or PMA in three experiments as in A.

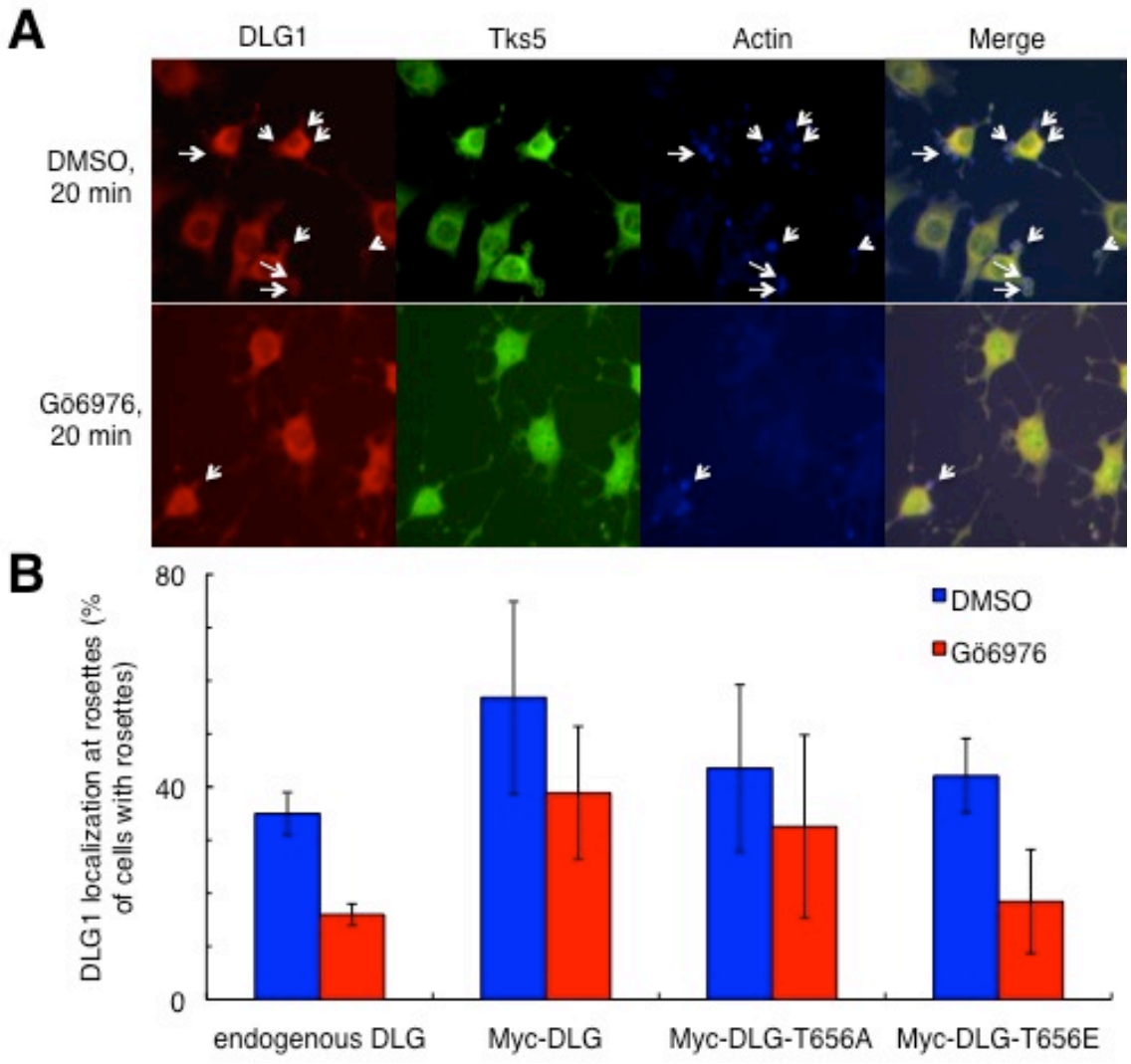

Figure A.4: DLG1 localization at invadopodia is dependent on cPKC activity but not presence of the phosphoacceptor at position T656.
A. Staining of Src3T3 cells treated with DMSO or Gö6976 for 20 minutes and stained for Tks5, DLG1, and actin. The arrows mark actin-based rings or "rosettes", corresponding to invadopodia. B. Untransfected Src3T3 cells ("endogenous DLG") or cells transfected with Myc-tagged DLG1 mutants were treated with DMSO or Gö6976 for 20 minutes and stained for DLG1 and actin. Cells containing invadopodia rosettes were scored for the presence of DLG1 staining at the rosettes, and the data represent the means±SEM of at least three experiments.

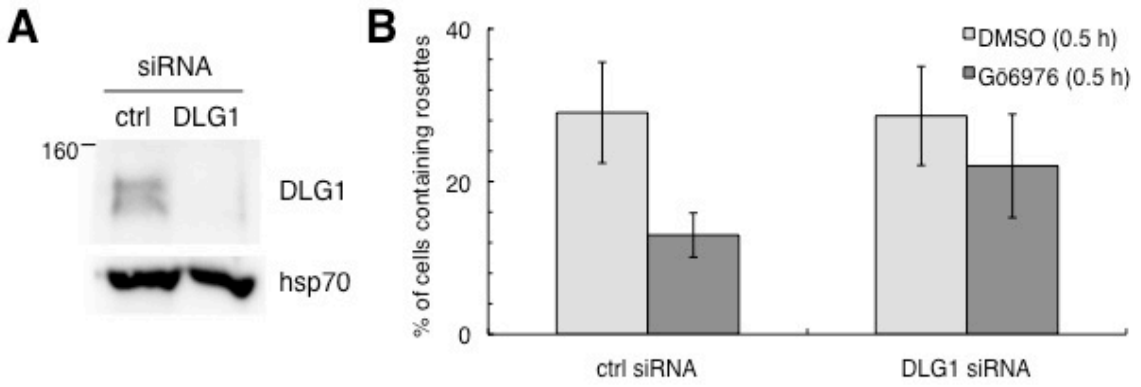

Figure A.5: DLG1 is not necessary for maintenance of invadopodia in Src-transformed fibroblasts. A. Src3T3 cells were transfected with non-targeting siRNA (ctrl) or siRNA targeting DLG1 and re-plated for Western blot and immunofluorescence using phalloidin to stain actin as described for Figure A.3. B. Quantification of the number of cells containing one or more actin-based rosettes after siRNA transfection and treatment with DMSO or Gö6976 in three experiments as in A.

References

1. Linder, S. (2007) *Trends in cell biology* **17**, 107-117

2. Ridley, A. J. (2011) *Cell* **145**, 1012-1022

3. Murphy, D. A., and Courtneidge, S. A. (2011) *Nature reviews. Molecular cell biology* **12**, 413-426

4. Yamaguchi, H., Lorenz, M., Kempiak, S., Sarmiento, C., Coniglio, S., Symons, M., Segall, J., Eddy, R., Miki, H., Takenawa, T., and Condeelis, J. (2005) *The Journal of cell biology* **168**, 441-452

5. Stylli, S. S., Kaye, A. H., and Lock, P. (2008) *Journal of clinical neuroscience : official journal of the Neurosurgical Society of Australasia* **15**, 725-737

6. Destaing, O., Planus, E., Bouvard, D., Oddou, C., Badowski, C., Bossy, V., Raducanu, A., Fourcade, B., Albiges-Rizo, C., and Block, M. R. (2010) *Molecular biology of the cell* **21**, 4108-4119

7. Desmarais, V., Yamaguchi, H., Oser, M., Soon, L., Mouneimne, G., Sarmiento, C., Eddy, R., and Condeelis, J. (2009) *Cell motility and the cytoskeleton* **66**, 303-316

8. Oser, M., Yamaguchi, H., Mader, C. C., Bravo-Cordero, J. J., Arias, M., Chen, X., Desmarais, V., van Rheenen, J., Koleske, A. J., and Condeelis, J. (2009) *The Journal of cell biology* **186**, 571-587

9. Buschman, M. D., Bromann, P. A., Cejudo-Martin, P., Wen, F., Pass, I., and Courtneidge, S. A. (2009) *Molecular biology of the cell* **20**, 1302-1311

10. Gatesman, A., Walker, V. G., Baisden, J. M., Weed, S. A., and Flynn, D. C. (2004) *Molecular and cellular biology* **24**, 7578-7597

11. Artym, V. V., Zhang, Y., Seillier-Moiseiwitsch, F., Yamada, K. M., and Mueller, S. C. (2006) *Cancer research* **66**, 3034-3043

12. Destaing, O., Block, M. R., Planus, E., and Albiges-Rizo, C. (2011) *Current opinion in cell biology* **23**, 597-606

13. Tatin, F., Varon, C., Genot, E., and Moreau, V. (2006) *Journal of cell science* **119**, 769-781

14. Teti, A., Colucci, S., Grano, M., Argentino, L., and Zambonin Zallone, A. (1992) *The American journal of physiology* **263**, C130-139

15. Hai, C. M., Hahne, P., Harrington, E. O., and Gimona, M. (2002) *Experimental cell research* **280**, 64-74

16. Schramp, M., Ying, O., Kim, T. Y., and Martin, G. S. (2008) *The Journal of cell biology* **181**, 1195-1210

17. Quintavalle, M., Elia, L., Condorelli, G., and Courtneidge, S. A. (2010) *The Journal of cell biology* **189**, 13-22

18. Su, B., Bu, Y., Engelberg, D., and Gelman, I. H. (2010) *The Journal of biological chemistry* **285**, 4578-4586

19. Li, A., Dawson, J. C., Forero-Vargas, M., Spence, H. J., Yu, X., Konig, I., Anderson, K., and Machesky, L. M. (2010) *Current biology : CB* **20**, 339-345

20. Dorfleutner, A., Cho, Y., Vincent, D., Cunnick, J., Lin, H., Weed, S. A., Stehlik, C., and Flynn, D. C. (2008) *Journal of cell science* **121**, 2394-2405